ANTICANCER NATURAL PRODUCTS: EVOLUTION AND THEIR BIOSYNTHETIC SITE-SELECTIVE CONJUGATION TO ANTIBODIES

By STEPHANIE VANNER, B.Arts Sc.

A Thesis Submitted to the School of Graduate Studies in Partial Fulfillment of the

Requirements for the Degree Master of Science

McMaster University Master of Science (2014) Hamilton, Ontario (Chemical Biology)

TITLE: Anticancer Natural Products: Evolution and their Biosynthetic Site-Selective Conjugation to Antibodies. AUTHOR: Stephanie Vanner, B.Arts Sc. (McMaster University), SUPERVISOR: Asst. Professor Nathan A. Magarvey. NUMBER OF PAGES: xvii,158.

Abstract

Natural products are an important resource for cancer therapy, with highly potent and diverse anticancer activities. Natural product biosynthesis is well comprehended, however the evolutionary principles governing the alteration of enzymatic assembly lines to yield molecules with activity toward distinct various cellular targets are not understood. This gap in knowledge hinders efforts to synthetically combinatorialize assembly lines to yield "unnatural" natural products with important or hybrid activity toward up-regulated targets in cancer. Furthermore, natural products did not evolve in the context of mammalian systems and would benefit from a delivery mechanism to cancerous cells to improve their ability to generate successful clinical outcomes. Consequently, natural products were linked to antibodies targeted to cell surface proteins up-regulated on cancer cells, generating antibody-drug conjugates (ADC). The conjugation methodology is problematic by yielding ADCs with varying numbers of drugs loaded per antibody. This lack of batch-to-batch standardization limits our ability to completely evaluate the safety profiles and efficacy of ADCs and determine proper dosages for patients. In this research, light was shed on biosynthetic evolutionary changes through the study of the antimycin-type family of depsipeptides, specifically demonstrating that modular insertions or deletions lead to natural product structural diversification. Additionally, a novel biosynthetic enzymatic method was established to site-selectively conjugate natural products to antibodies in order to facilitate the development of more sophisticated cancer therapies.

Acknowledgments

I would like to thank my supervisor Nathan Magarvey for all of his guidance throughout this process. His creativity and innovative ideas have allowed me to explore some truly exciting areas of science. Additionally, he has provided many significant and unique opportunities that have undoubtedly helped me to achieve success in this degree and in future endeavours.

I would also like to acknowledge my committee members Fred Capretta and Eric Brown for providing their counsel and support, in addition to advancing my scientific inquiries during committee meetings.

I would like to recognize my collaborators from the Sidhu lab at the University of Toronto, particularly Sachdev Sidhu and Shane Miersch, who have made a lot of this work possible and generously volunteered their time and facilities.

The members of the Magarvey lab have also been very influential during my time at McMaster. In particular, I would like to thank Morgan Wyatt and Chad Johnston for their friendship and all of the time and thought they dedicated toward helping me, which has contributed to my development as a scientist.

I would also like to extend a big thank you to my friends and family for their care and support over the past two years. I would specifically like to mention Leslie Flynn, Stephen Vanner, Robert Vanner, Catherine Vanner and David Macintosh – without their encouragement, love, advice, and strength I would not be where I am today.

Table of Contents

List of Tables

Chapter 2

Chapter 3

Chapter 4

List of Figures

Chapter 1

Chapter 2

Chapter 3

Chapter 4

Abbreviations

A	adenylation
ACP	acyl carrier protein
Ala	alanine
AMP	adenosine monophosphate
anti-SMASH	antibiotics & Secondary Metabolite Analysis Shell
Arg	arginine
Asn	asparagine
AT	acyltransferase
ADC	antibody-drug conjugate
BAX	Bcl-2-associated protein X
Bcl-xL	B-cell lymphoma-extra large
BH3	Bcl-2 homology domain 3
BLAST	Basic Local Alignment Search Tool
C	condensation
cBID	cleaved BH3-interacting domain death agonist
CD	cluster of differentiation
CMCB	Centre for Microbial Chemical Biology
CoA	coenzyme A
COSY	correlation spectroscopy
DAR	drug-to-antibody ratio
DNA	deoxyribonucleic acid

DR5	death receptor 5
DTNB	5,5'-dithiobis-(2-nitrobenzoic acid)
DTT	dithiothreitol
ECD	extracellular domain
EGFR	epidermal growth factor receptor
ELISA	enzyme-linked immunosorbent assay
ESI	electrospray ionization
Fab	fragment antigen-binding region
FPLC	fast protein liquid chromatography
Fc	fragment crystallizable region
FDA	Food and Drug Administration
HDAC	histone deacetylase
HER2	human epidermal growth factor receptor 2
HIC-HPLC	hydrophobic interaction chromatography-high performance liquid chromatography
HIF-1	hypoxia-inducible factor 1
HMBC	heteronuclear multiple-bond correlation
HMQC	heteronuclear multiple quantum correlation
HPLC	high performance liquid chromatography
Hsp90	heat shock protein 90
IgG	immunoglobulin G
IPTG	isopropyl β-D-1-thiogalactopyranoside

KR	ketoreductase
KS	ketosynthase
LB	Luria-Bertani
Leu	leucine
LC-MS	liquid chromatography-mass spectrometry
Lys	lysine
mAb	monoclonal antibody
MALDI-TOF	matrix-assisted laser desportion/ionization- time-of-flight
MS	mass spectrometry
MT	methyltransferase
MWCO	molecular weight cut-off
NADH	nicotinamide adenine dinucleotide
NCI	National Cancer Institute
NMR	nuclear magnetic resonance
NOESY	nuclear Overhauser effect spectroscopy
NRP	nonribosomal peptide
NRP-PK	nonribosomal peptide-polyketide
NRPS	nonribosomal peptide synthetase
NRPS-PKS	nonribosomal peptide synthetase-polyketide synthase
*p*AMF	para-azidomethyl-L-phenylalanine
PCR	polymerase chain reaction
PK	polyketide

PKS	polyketide synthase
PMPI	*p*-maleimidophenyl isocyanate
PMSF	phenylmethylsulfonyl fluoride
RNA	ribonucleic acid
SAR	structure-activity relationship
SDS	sodium dodecyl sulfate
Ser	serine
T	thiolation
TCEP	Tris(2-carboxyethyl) phosphate
TDC	THIOMAB-drug conjugate
T-DM1	trastuzumab emtansine
Thr	threonine
TLC	thin layer chromatography
TRAIL	TNF-related apoptosis-inducing ligand
tRNA	transfer ribonucleic acid

Declaration of Academic Achievement

Chapter 2 of this thesis is published work and Chapter 3 is prepared in paper format for publication. The details regarding each research contribution are described within each chapter preface.

Chapter 1. Introduction

1.1 Thesis Context

Cancer is now the leading cause of death in Canada.[1] It is one of the most elusive diseases in terms of understanding its biological mechanisms and tumor cell heterogeneity, which consequently challenges treatment efforts. Nature has consistently served as a prolific source of chemically rich chemotherapeutic agents with diverse anticancer activities.[2-6] The biosynthetic pathways and enzymatic assembly lines present in plants, bacteria and fungi, are highly evolved to generate small molecules with potent activities towards a variety of eukaryotic biological targets that play critical roles in disease.[7] Comprehensive study of these pathways led to an extensive understanding of the chemistry and biology behind nature's assemblies and the development of streamlined approaches to biosynthetic pathway characterization and anticancer natural product discovery.[8-10] Significant inquiry into determining natural products' specific cellular targets in cancer and defining their structural interactions also proved valuable, facilitating synthetic, semisynthetic or chemoenzymatic generation of analogues with superior activity toward anticancer targets.[5,11-13] We know how chemotherapeutic natural products hit a diverse set of cellular targets, their biosynthetic origins and thus routes to improve them. It is not known, however, how nature *itself* varies molecules to alter their activities, making them attuned to selective anticancer targets over others (Fig. 1.1). With insight into how nature directs structural combinatorializations, it may be possible to artificially revise biosynthetic pathways, thereby altering or fusing natural products to hit unique or multiple targets in cancerous cells.

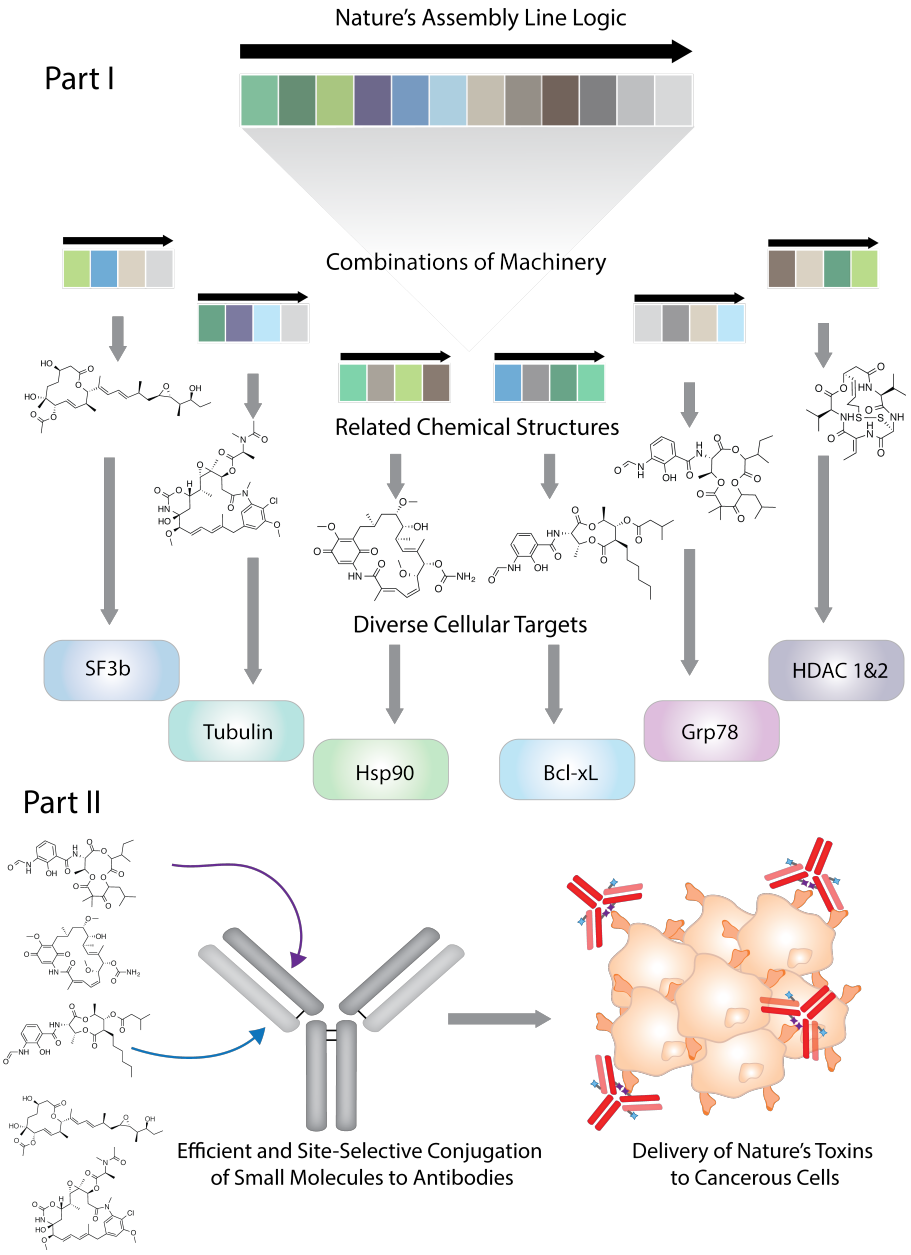

Fig. 1.1 *Common problems in natural product evolution and chemotherapeutic targeting. Specifically, a depiction of the unexplored and unanswered questions that are addressed in this thesis regarding the evolutionary diversification of biosynthetic assembly lines to yield natural products with activities toward*

unique cellular targets in cancer and the delivery of these molecules to the sites of disease. There is a thorough comprehension of nature's assembly line logic – the unique enzymatic components (depicted in blocks of colour) and how they function together to generate these complex natural chemistries.[7] *Basic components must be combined in different patterns and iterations to yield molecules that in many cases share structural similarities. Interestingly, natural products often have activity toward distinct up-regulated or overactive cellular targets in cancer despite their chemical resemblance. For example, from left to right, pladeinolide B inhibits tumor cell splicing by inhibiting the splicing factor SF3b, maytansine binds to tubulin inhibiting microtubule assembly, geldanamycin binds to the heat shock protein 90 (Hsp90), antimycin inhibits anti-apoptotic protein-protein interactions by inhibiting Bcl-xL, JBIR-06 down-regulates GRP78 which is a molecular chaperone involved in the unfolded protein response, and romidepsin inhibits histone deacetylases (HDACs).*[14-19] *It is currently unclear, however, how nature actually targets these specific yet disparate cellular programs. Despite understanding the stand-alone logic, we do not have an appreciation of the evolutionary principles and biosynthetic alterations that result in nature's combinatorial chemistry experimentation. Part I of this thesis aims to shed light on this matter. To enhance nature's evolution toward cellular targets and target cancer in a more sophisticated manner, a delivery mechanism is required to take these molecules to the site of disease. Antibodies, specific for cell surface membrane proteins up-regulated in cancer, provide a honing mechanism. However, there is a need for methods to site-selectively and efficiently load anticancer natural products onto antibodies. Part II of this thesis seeks to explore a technique to effectively and site-selectively load one or two diverse natural products onto antibodies to affect multiple cellular targets and therefore deliver more potent hits to cancerous cells.*

Another important area of natural chemical biology for cancer therapy is selective targeting. Although natural chemicals are effective at destroying cancerous cells, often they also impact healthy cells, causing serious negative side effects and dose-limiting toxicity. Thus, in order to access the full therapeutic and clinical potential of

chemotherapeutic natural products and thereby improve current cancer treatment methods, a delivery mechanism is required. Consequently, there is a new addition to the field of immunotherapies, antibody-drug conjugates (ADC), which pairs the targeting ability of monoclonal antibodies with the cytotoxicity of natural products. This combination provides a direct means for the targeting and cellular internalization of a toxic payload to cancerous cells, leading to cell death. This selective approach decreases the negative side effects experienced with typical general chemotherapies, allows for the introduction of more potent cancer-killing natural products, and has the potential to target forms of cancer that were previously untreatable.[20-22]

The main challenge for ADCs to date has been the methodology used for linking drugs to antibodies. Synthetic chemistry was traditionally used, however, antibodies are extremely complex proteins with many different functionalities that can bind to small molecules in these reactions. Therefore, synthetic techniques result in heterogeneous mixtures of ADCs. Drug variability can cause serious issues downstream in terms of separation and purification, but more importantly for the health of the patient as lack of standardization can lead to improper dosages.[23-25] To overcome these problems, several alternative techniques have been developed that integrate a "defined" conjugation site into the antibody in order to generate homogeneous ADCs. These techniques for improved site-selectivity still face numerous challenges and there remains a need for novel linking technologies that eliminate ADC heterogeneity. Additionally, these methods only allow for the "site-specific" loading of *one* small molecule species, limiting the potential efficacy of these drugs.[23,26,27] It would be beneficial to have a technique to

site-specifically load *multiple* uniquely functioning small molecules onto an antibody to generate a polytherapy ADC, targeting various pathological pathways in cancer (Fig. 1.1).[28]

My thesis aims first to understand how nature diversifies molecules toward different eukaryotic targets in cancer and second to optimize the delivery tools used to take them to the site of disease (Fig. 1.1). This introduction serves first to outline the catalogue of natural products that have potent activity towards targets that are overactive or up-regulated in cancerous cells and highlight why they have been a valuable source of drugs. Next, it is illustrated how they are assembled in nature, the exploitation of this knowledge to advance their role as anticancer therapeutics, and most importantly how certain areas of biosynthetic assembly have been overlooked. Subsequently, the drawbacks that have limited natural products clinical success to date and the generation of ADCs in response to this need are explained. Additionally, the considerations challenging ADC research, which are key to the future of their therapeutic success, are featured. Finally, the need for a novel site-specific ADC generation technique is emphasized and the aims of this thesis to answer these natural product biosynthetic and delivery mechanism questions are outlined.

1.2 Chemotherapeutic Natural Products and their Assembly in Nature

1.2.1 The Institution of Chemotherapy

The birth of clinical chemotherapy occurred with the recognition by Louis Goodman and Alfred Gilman that nitrogen mustard caused tumor regression.[29-32] The inadvertent discovery in the late 1950's and 60's that the *Vinca* alkaloids vinblastine and

vincristine stop the proliferation of cancerous cells by inhibiting microtubule polymerization offered a new mode of therapeutic action toward cancer, and opened up an entirely new and untapped resource of chemotherapeutic options – small molecules from nature (Fig. 1.2A).[33-35]

1.2.2 Anticancer Natural Products

Targeted antitumour screens performed by the National Cancer Institute (NCI) and discoveries by pharmaceutical companies and academics led to the assembly of a vast library of anticancer natural products over the past 50 years.[2] This catalogue consists of structurally and functionally unique scaffolds including terpenes, alkaloids, nonribosomal peptides, and polyketides.[36] Antimitotic agents in particular stunt division and proliferation rates of cancerous cells and are a mainstay of cancer therapy. Traditionally this antimitotic class was defined by their mode of action with respect to tubulin.[3] Paclitaxel (Taxol) and the epothilones are prime examples of microtubule stabilizing agents.[37,38,39] Paclitaxel exhibits strong efficacy towards breast and ovarian cancers and has become a blockbuster drug that is widely used in a clinical setting (Fig. 1.2B).[2,40,41] Additionally, a semisynthetic analogue of epothilone, ixabepilone is used to treat patients with metastatic or locally advanced taxane resistant breast (Fig. 1.2B).[42] Alternatively, vincristine, vinblastine and halichondrin B bind to tubulin, inhibiting the occurrence of microtubule polymerization. Vincristine and vinblastine are used in the clinic to treat lymphoma and a synthetic derivative of halichondrin B, eribulin, is currently used to treat metastatic breast cancer (Fig. 1.2A).[3,43] Together these show that microtubule targeted natural products are a valuable source of chemotherapies and play a significant role in the

clinic as cancer treatment options.

Other important non-tubulin interfering antimitotic natural product agents include topoisomerase (type I and II) inhibitors. DNA topoisomerases create breaks in DNA and re-ligate strands during the cell cycle. Inhibition of topoisomerase II prevents the re-ligation of DNA, causing the accumulation of DNA strand breaks leading to apoptosis.[44] Etoposide is a semisynthetic derivative of the lignan natural product podophyllotoxin. It forms a complex between DNA and topoisomerase II and is a first-line treatment for small and large cell lung cancers, myeloid leukemia and testicular cancer.[45] Daunorubicin and doxorubicin are polyketides isolated from *Streptomyces* sp. that are a part of the anthracycline antibiotic class and inhibit the action of topoisomerase II by intercalating DNA.[46,47,48] Daunorubicin is used to treat acute lymphocytic and acute myeloid leukemia and doxorubicin is used in the treatment of soft tissue sarcoma and breast cancer (Fig. 1.2C).[49-51]

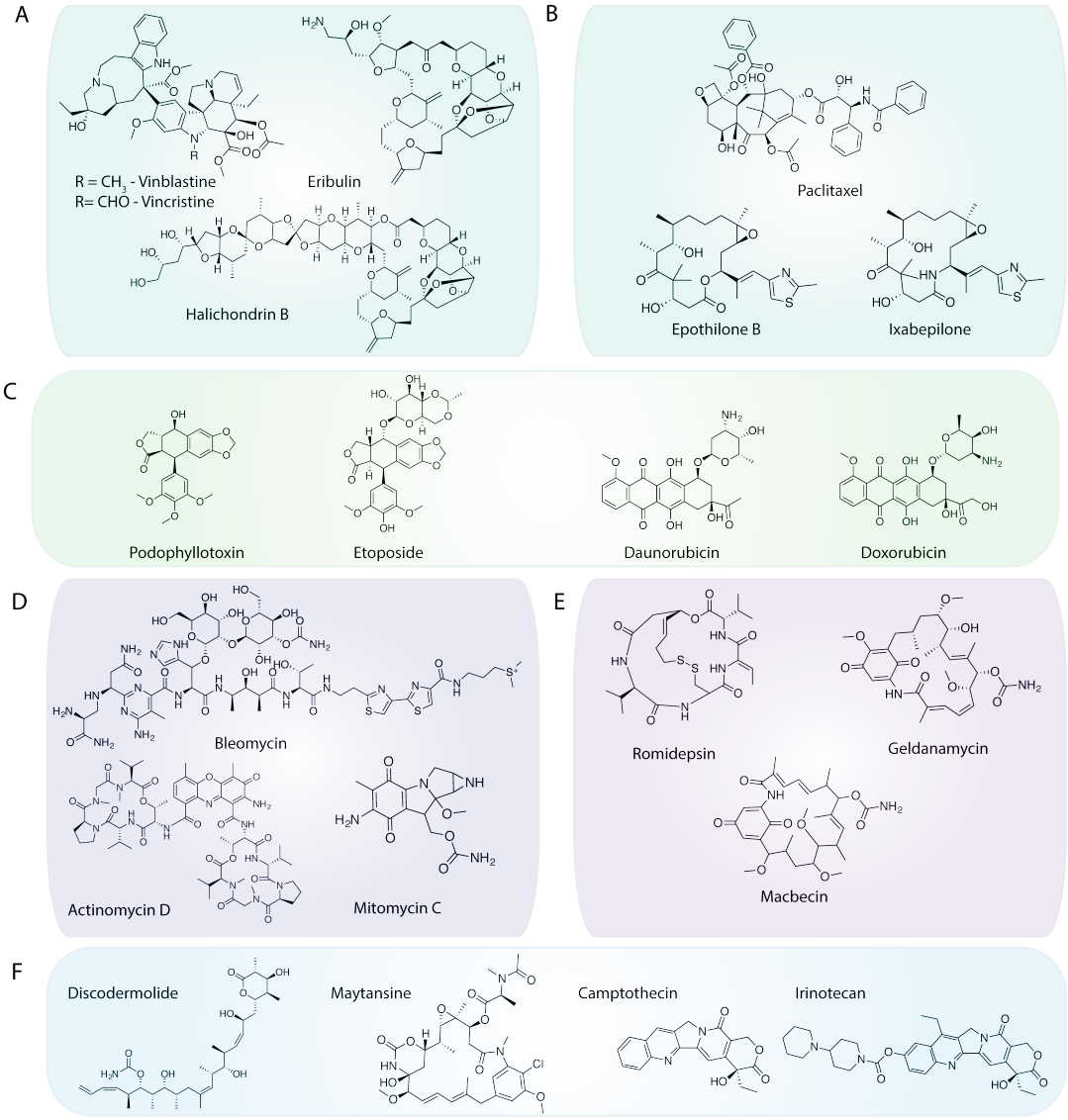

Fig. 1.2 *Anticancer natural products grouped according to cellular target or activity.* ***(A)*** *Microtubule destabilizing agents.* ***(B)*** *Microtubule stabilizing agents.* ***(C)*** *Topoisomerase inhibitors.* ***(D)*** *DNA-breaking antimicrobial (doxorubicin and daunorubucin may be cross-listed in this category).* ***(E)*** *Natural products that hit targets involved in apoptosis.* ***(F)*** *Natural products that failed clinical trials due to adverse side effects or faced clinical setbacks.*

Another important group of anticancer natural products are DNA-breaking antimicrobial natural products isolated from soil dwelling *Streptomyces* species. Bleomycin induces DNA strand scission, generating free radicals that damage DNA.[52,53] It is used in the treatment of squamous cell carcinoma and lymphomas.[54,55] Actinomycin D inhibits transcription of DNA and RNA elongation for the treatment of Wilms' tumor and metastasized testicular cancer.[56,57] Mitomycin C alkylates DNA, causing DNA crosslinks, and is used to treat locally advanced or metastasized forms of gastric cancer and pancreatic adenocarcinoma (Fig 1.2D).[58,59]

In addition to the traditional antimitotic and DNA disrupting agents, there are a variety of natural products with refined selectivities that hit more discrete pathways and targets involved in apoptosis. For instance, romidepsin or FK228, is a depsipeptide isolated from the bacteria *Chromobacterium violaceum* which exhibits inhibition of class I histone deacetylases (HDAC inhibitor) that are often up-regulated in certain forms of cancer (Fig. 1.2E).[60] HDAC inhibition causes the induction of pro-apoptotic genes, encoding for proteins such as TRAIL, DR5 and Fas. Consequently, apoptotic pathways are activated leading to cell death.[19,61] Furthermore, there are numerous molecules that have been found to inhibit heat shock protein 90 (Hsp90) such as geldanamycin and macbecin which are isolated from *Actinobacteria* (Fig. 1.2E). Hsp90 is a chaperone protein that is anti-apoptotic in nature as it aids cells to survive under stress by stabilizing signal transduction proteins and growth factor receptors that are responsible for cancerous cell proliferation. Hsp90 inhibition consequently induces apoptosis.[16] There is great interest in the targeted activities of these molecules for cancer treatment.

It is clear from these examples that significant research has been done to characterize natural products' interactions with specific cellular targets as a result of the deep recognition of natural products' importance in the realm of cancer therapy. This information has provided the basis for numerous studies to improve natural products' affinity for their targets through structural modification and also combine molecules to generate more efficacious therapies that hit numerous targets in cancer cells.

1.2.3 Synergistic Combinations of Natural Product Chemotherapies

Despite some chemotherapies having potent activity as a single treatment, many do not reach their full therapeutic capacity as discrete entities. Often when synergistic chemotherapies are combined they converge to kill cancerous cells, providing a more efficacious treatment.[28] This is observed with combinations such as doxorubicin and mitomycin C, paclitaxel and doxorubicin, bleomycin and vinblastine, and etoposide and cisplatin (a synthetic DNA crosslinker).[62-70] By disrupting diverse pathways or stages of cellular growth, these therapeutic regimes deliver multiple hits to cancerous cells, consequently causing faster and broader killing effects and more effectively eradicating heterogeneous and drug resistant forms of the disease.[28] Having illustrated the success and potential of natural products to treat cancer, it is now important to appreciate the elaborate biosynthetic systems responsible for their assembly.

1.2.4 Nature's Assembly of Anticancer Toxins

Over the past 20 years the logic behind the assembly of natural products has become well understood through the study of biosynthetic gene clusters and biochemical investigations of biosynthetic enzymes (Fig. 1.3). The following two sections, 1.2.4 and

1.2.5, serve to illustrate what is known regarding the basic biochemical logic of biosynthetic assembly lines and how this knowledge has been successfully exploited to discover or generate new natural products. In addition, the modular nature of assembly lines has combinatorial potential and has inspired designed efforts to create hybrid or recombined "unnatural" natural products.[7,71,72] It is subsequently highlighted that artificial combinatorial efforts are challenged by a key aspect of biosynthetic assembly that is *not* understood: how biosynthetic components communicate and undergo molecular scission and splicing to integrate or remove enzymatic parts.

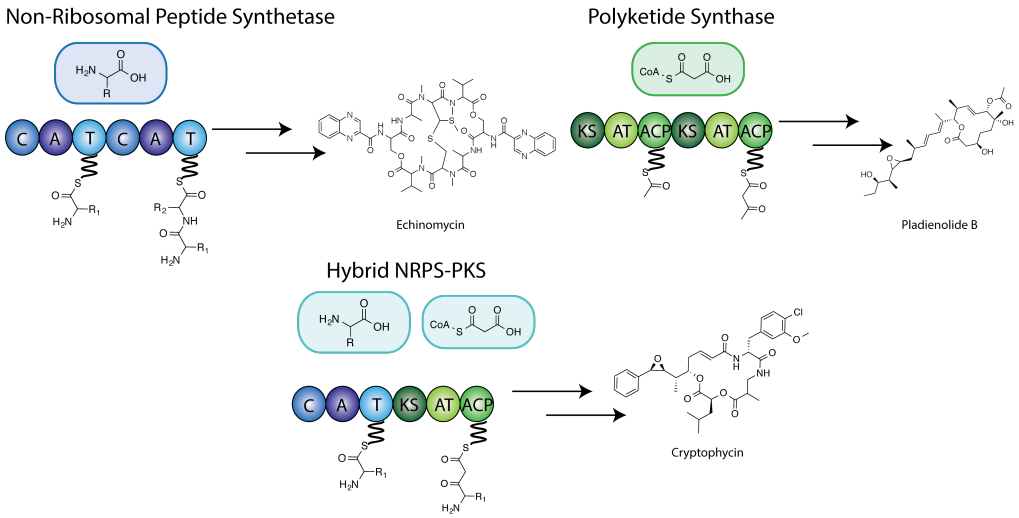

Fig. 1.3 *Assembly line logic of natural products. In blue is a nonribosomal peptide synthetase (NRPS) assembly line, the mega-enzyme responsible for nonribosomal peptide generation, with the monomer it utilizes outlined in blue, amino acids. The basic domains are C, condensation domain, A, adenylation domain, T, thiolation domain. The NRPS is shown to yield echinomycin, a nonribosomal peptide produced by Streptomyces sp. which exhibits potent anticancer activity by inhibiting hypoxia-inducible factor 1 (HIF-1) DNA binding activity.[73,74] In green is a polyketide synthase (PKS) assembly line, the mega-enzyme responsible for polyketide generation, with the monomer it incorporates outlined, malonyl-CoA or its derivatives. The basic domains are KS, ketosynthase domain, AT, acyltransferase domain, ACP, acyl*

carrier protein domain. The PKS is shown to yield pladienolide B, a polyketide produced by Streptomyces platensis which exhibits potent anticancer activity by binding to splicing factor 3b and therefore inhibiting tumor cell splicing.[14,75] *A mixed green and blue assembly line depicts a hybrid nonribosomal peptide synthetase-polyketide synthase (NRPS-PKS) assembly lines that utilize both amino acids and malonyl-CoA or derivatives thereof as monomer building blocks. The NRPS-PKS is shown to yield cryptophycin, a hybrid NRP-PK from Nostoc sp. that inhibits microtubule assembly.*[11]

Here, focus is placed on nonribosomal peptides (NRP), polyketides (PK) and hybrid NRP-PK, as many of nature's anticancer chemicals fall into these classes, including halichondrin B, epothilone B, daunorubicin, doxorubicin, bleomycin, actinomycin D, romidepsin, geldanamycin, macbecin, discodermolide, and maytansine (Fig. 1.2). [15,16,19,39,47,52,57,76-78] These molecules are generated from the elongation of a series of monomeric units, for polyketides this includes malonyl-CoA and methylmalonyl-CoA and for nonribosomal peptides this includes the twenty proteinogenic amino acids and a larger library of non-proteinogenic amino acids. Iterative and coordinated chemical steps performed by enzymes arranged in an assembly line fashion lead to the elongation of monomeric units into full-length products (Fig. 1.3). Each protein domain in the assembly line is responsible for a specific action including the selection of monomeric units, performing chemical modification of the units, and catalyzing bond formation between units. First, monomeric units are selected for loading onto the assembly line by acyltransferases (AT) in PKSs and adenylation domains (A) in NRPSs. The carboxyl group of monomer units are activated for assembly line loading with either a thioester, in the case of coenzyme A activated malonic acid, or amino acyl-

AMP in the case of amino acids.[7] Carrier proteins with flexible phosphopantetheine arms are bound to thiolation (T) and acyl carrier proteins (ACP) in both NRPS and PKS assembly lines, respectively, and have a free nucleophilic thiolate anion to attack the activated acyl groups of monomeric units. This reaction loads monomers onto the assembly line with the formation of a thioester linkage. Subsequently, ketosynthase domains (KS) in PKS or condensation domains (C) in NRPS catalyze covalent bond formation between monomeric units. Ketosynthases catalyze claisen condensation reactions. The downstream tethered (methyl)malonyl-S-T-domain undergoes decarboxylation to yield a C_2 carbanion that then attacks the thioester of the previous (methyl)malonyl-S-T-domain to form a C-C bond, transferring the growing molecule to the downstream carrier protein. Condensation domains catalyze the free amine from the downstream tethered amino acid to undergo nucleophilic attack on the thioester bond of the upstream amino acid-S-T-domain. This reaction transfers the growing molecule to the downstream carrier protein with the formation of a C-N bond. In both systems thioesterase domains catalyze chain termination through hydrolysis or intramolecular attack by a hydroxyl residue to form a cyclic structure. NRPS-PKS hybrid assembly lines work using combined PKS and NRPS logic that are compatible, with growing chains being transferred between these enzymatic systems (Fig. 1.3). There are also a series of additional enzymatic domains that are often present in NRPS or PKS assembly lines that perform chemical alterations of functional groups such as dehydrations, reductions, dehydrations, epimerization or methyl transfers, that lead to the great structural diversity of PK, NRP and NRP-PK classes.[7]

1.2.5 Exploitation of Biosynthetic Assembly Line Logic: Successes and Challenges

This knowledge and appreciation of the genetic and enzymatic systems responsible for nature's assembly of PKs, NRPs, and NRP-PKSs provides the foundation for numerous directed and productive efforts to discover novel anticancer natural products, exploit assembly line features to generate analogues, or attempts at combinatorial biosynthesis to yield novel structures with different bioactivities.[9,72,79,80] Genome sequencing has become increasingly easy and cost efficient, allowing for sequencing and assembly of a vast library of bacterial genomes. Within these genomes, biosynthetic clusters can be identified and the biosynthetic enzymes they encode characterized, by using tools such as the basic local alignment search tool (BLAST) algorithm which can perform sequence comparison analyses to identify PKS and NRPS domain motifs from large gene sequences.[81] Additionally, upon cluster characterization, the natural products they produce can be predicted, as the biological and chemical roles of NRPS and PKS enzymes have been well established and substrate selection can be deduced from adenylation domain protein sequences. This is done using streamlined web-based analysis programs such as antibiotics & Secondary Metabolite Analysis Shell (anti-SMASH) and Genes to Natural Products (GNP, developed by the Magarvey lab, personal communication, Dr. Nathan Magarvey), which can predict the core structure of the molecule produced from the biosynthetic cluster, going from DNA to RNA to protein to small molecule.[82] These advances facilitate genome mining, a more efficient and logic driven approach to the discovery of new natural products than traditional bioactivity guided methods. By probing sequenced bacterial genomes for NRPS and PKS clusters,

one can identify all possible NRP and PK chemistries from the bacteria that may not have been previously isolated or expressed. Guided laboratory manipulations of growing conditions and separation techniques can lead to the discovery of predicted molecules that were not previously known or found using bioactivity guided techniques.[8,9,72,83] These genome-mining efforts have led to the discovery of new anticancer natural products such as the thailandamides, the thailandepsins/burkholdacs and the stambomycins.[84-88] The Piel group in collaboration with the Hertwick group utilized genome mining to identify a cryptic (not expressed) biosynthetic cluster that encoded for a hybrid NRPS-PKS from *B. thailandensis* E264. Through manipulation of the bacterial quorum sensing regulation and growth conditions the NRP-PK thailandamides were expressed, characterized and found to have moderate anti-proliferative activity against human tumor lines.[86] Genome mining also revealed the same bacteria contained an additional cryptic biosynthetic cluster that resembled the romidepsin cluster. The Cheng group and Brady group independently isolated and characterized members of the thailandepsin/burkholdac family that were indeed natural analogues of romidepsin that exhibited potent anticancer activity through HDAC inhibition.[84,87,88] Furthermore, the genome of *Streptomyces ambofaciens* ATCC23877 was probed and revealed a giant cryptic PKS gene cluster. Expression of a regulatory gene within the cluster prompted the expression of the PKS cluster, leading to the isolation of the stambomycins A-D. The polyketides inhibited the proliferation of human adenocarcinoma cell lines with similar activity to the agent doxorubicin and also demonstrated significant antiproliferative activities against human breast, lung, and prostate cancer cell lines.[85] Evidently, understanding natural product assembly

enzymology and the subsequent development of technologies paired with genome mining has promoted the discovery of unique anticancer chemicals from nature.

Biosynthetic lines often exhibit flexibility, with certain adenylation and acyltransferase domains having the ability to integrate alternative substrates leading to the formation of natural product analogues. Researchers have taken advantage of this aspect, by feeding in unnatural substrates in precursor directed biosynthetic efforts to generate novel analogues that may have more potent anticancer activity.[79] For instance, Magarvey *et al.* exploited the flexibility of the biosynthetic enzymes in the cryptophycin assembly line by altering the accessible monomeric PK and NRPS starter units to generate a series of unnatural cryptophycin analogues. Interestingly, this approach allowed for the natural generation of cryptophycin 52, the potent anticancer cryptophycin agent that underwent clinical trial, which had only previously been accessible through synthetic efforts.[11] Thus, it is understood that exploiting the promiscuity of these assembly lines may open up a new library of "unnatural" natural product analogues with better anticancer activity.

Several efforts were undertaken to re-engineer natural product assemblies to generate novel natural products with unique or dual bioactivities through the combination of biosynthetic system components from different assembly lines.[71,72,80] For example, Menzella *et al.* in a proof of principle study generated 154 bimodular assembly line combinations by combining the genetic information for 14 modules from 8 PKS clusters, including those from the anticancer clusters of geldanamycin and epothilone. Combinations of the modules successfully yielded a series of structurally unique triketide lactones.[89] However, in many other cases combinatorial biosynthetic efforts were

ineffective, resulting in defective recombinant assembly lines, undesired combined products or inappreciable yields of the desired hybrid natural products.[72]

This background highlights that study to date has focused on biosynthetic enzymes' function in their native assembly line setting and how this is taken advantage of to discover new or create varied forms of the original natural products. However, in order to carry out truly meaningful combinatorial biosynthetic efforts or assembly line manipulations we need to understand how nature itself makes modifications to yield molecules with activities toward distinct targets. Specifically, natural evolutionary principles must promote successful assembly line alterations, which consequently breed natural products that hit differentiated targets. The first study of this thesis in Chapter 2 attempts to reveal this evolutionary logic, in order to provide insight into how natural product assembly lines might be synthetically combined or modified to yield molecules that hit altered or combined cellular targets in cancer and are therefore more efficacious.

1.3 Antibody-Drug Conjugates: Optimization of Natural Product Delivery Tools

1.3.1 Drawbacks of Traditional Natural Product Chemotherapy

Although there is currently a vast natural product toolkit available to target different pathways in cancer, serious challenges limit the success of these therapies. Antimitotic and DNA targeting chemotherapies exploit the fast-growing nature of cancerous cells, creating a degree of therapeutic differentiation between healthy and cancerous cells. However, a large subset of healthy cells divide rapidly and are therefore highly susceptible to these treatments.[20,90] Consequently, off-target activities generate a large number of adverse side effects including bone marrow toxicity, blood disorders,

nausea, nephrotoxicity, cardiotoxicity, hair loss, fatigue and peripheral neuropathy, all of which are extremely detrimental to a patient's mental and physical health. The dose-limiting toxicities of such chemotherapies narrow their therapeutic window and lower the overall effectiveness of these drugs in the clinic.[91-98] Even agents with more unique targets, such as HDAC inhibitors, exhibit significant toxicity profiles, with romidepsin causing thrombocytopenia, leukopenia, neutropenia, nausea/vomiting, atrial fibrillation, and asymptomatic T-wave inversion.[99,100]

In many instances, severe off-target toxicities have also precluded natural products from advancing to the clinic. For example, discodermolide is a microtubule stabilizer isolated from the sea sponge *Discodermia dissoluta* (Fig.1.2F).[101] It is more potent than taxol and effective against taxol- and multidrug-resistant cell lines.[78] However, it failed to advance past Phase I clinical trials due to off-target toxicity.[102] Maytansine, another highly potent toxin, inhibits microtubule polymerization at subnanomolar concentrations. Unfortunately, it induced systemic toxicity to the gastrointestinal and central nervous systems during clinical trials and failed to advance (Fig. 1.2F).[103,15] In other cases, entry to the clinic is significantly delayed while efforts to synthetically derivatize the chemical are undertaken in order to decrease off-target toxicities. Camptothecin, for example, is a DNA topoisomerase I inhibitor that displayed great promise in the early 1970's.[104,105] However, it caused severe bladder toxicity and consequently it was not until the early 2000's that the analogue irinotecan was approved for clinical use (Fig. 1.2F).[106]

To broaden the therapeutic windows of clinical natural product chemotherapies, a delivery mechanism is required to target these drugs specifically towards cancerous cells, while sparing healthy cells. Moreover, a delivery tool would allow the continued catalogue expansion of the highly toxic small molecules we draw upon to treat cancer. This would include those that were not clinically suitable in the past due to systemic toxicity and would decrease the need to undergo prolonged semisynthetic modification efforts. Having an increased number of agents at hand will be highly beneficial to decrease the occurrence and threat posed by drug-resistant cancers. Consequently, over the past two decades monoclonal antibodies have been employed to address this need for a delivery mechanism, which has led to a new field of immunotherapy known as antibody-drug conjugates.[21,107,108]

1.3.2 Delivering Natural Product Toxins to Cancerous Cells: Antibody-Drug Conjugates

Antibody-drug conjugates are a particularly promising new area of cancer drug development, that implement more selective means of treatment, due to their exploitation of molecular differences between cancerous and healthy cells.[107] Antibodies can be produced to specifically target biological markers that are only present, or are overexpressed on the surface of cancer cells making them ideal drug delivery candidates.[109] Cytotoxic small molecules can be linked to these antibodies, providing a direct means for targeting and cellular internalization of a toxic payload to cancerous cells, while avoiding healthy cells (Fig. 1.4A and B, Fig. 1.5A). ADCs decrease the off-target activities generated by conventional chemotherapies, allow the use of anticancer

natural products that were previously seen as too toxic, and provide potential treatments for heterogeneous cancers that may not have been susceptible to general antimitotic chemotherapies alone.[107,108]

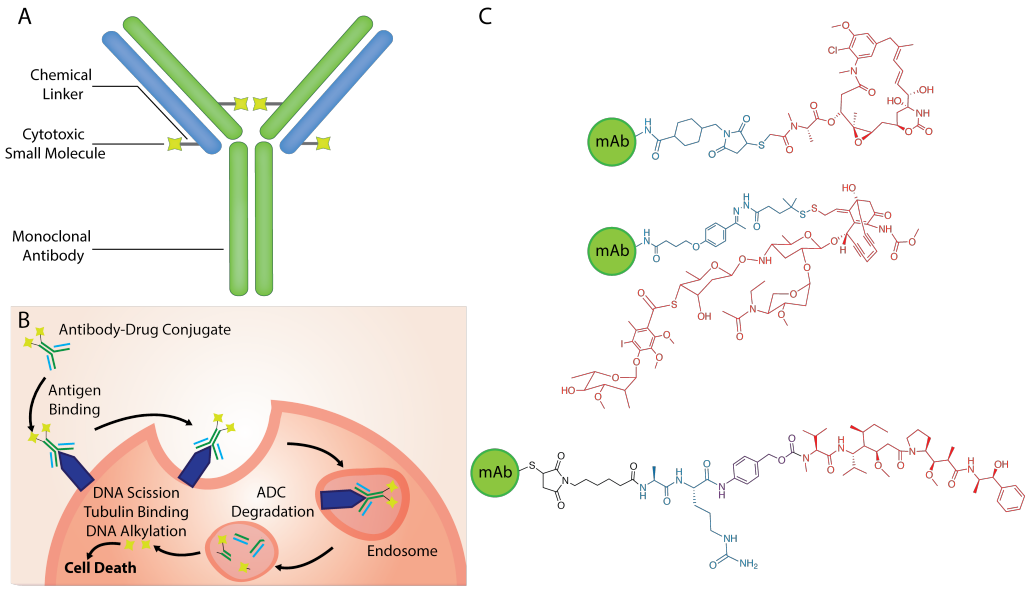

Fig. 1.4 *Overview of antibody-drug conjugates.* ***(A)*** *A schematic overview of the key components of an antibody-drug conjugate.* ***(B)*** *The process an antibody-drug conjugate undergoes from administration to death of the cancerous cell.* ***(C)*** *The chemical components of the ADCs that have received FDA approval, from top to bottom, ado-trastuzumab emtansine, gemtuzumab ozogamicin and brentuximab vedotin. Linkers are highlighted in blue, spacers in purple and toxins in red.*

The primary considerations for ADC generation are the tumor-associated antigen to which the antibody will be targeted, stable linking chemistry tethering the small molecule to the mAb and choice of toxin. Synthetic chemistry has traditionally been used to attach a cytotoxic small molecule to a monoclonal antibody (mAb) through a chemical linker and a spacer (in some cases). The linker is a stable means of attachment to native

amino acid residues of the antibody. Linkers tend to be acid-labile hydrazones, disulfide linkages, or protease cleavable peptidic linkers. Thus, internal cellular hydrolysis or proteolysis is thought to occur at the linker, releasing the small molecules from the antibody. Self-immolative spacing chemistry is often included between the linker and the small molecule, allowing for degradation of the linker without affecting the toxic drug. Finally, the active components are cytotoxic natural products, or their synthetic derivatives, such as calicheamicin, 10 or maytansine.[21,22,110,111]

1.3.3 FDA Approved ADCs

The original ADC to attain FDA approval was gemtuzumab ozogamicin, or Mylotarg in 2000. It was used for the treatment of acute myelogenous leukemia and is composed of an anti-CD33 antibody, and a hydrazine linker bound to calicheamicin, a highly toxic natural product that initiates DNA cleavage (Fig. 1.4C).[112] It was subsequently voluntarily retracted in 2010, but promising new data shows the life prolonging effect of Mylotarg used in coordination with chemotherapy compared to a treatment of solely chemotherapy.[113,114] Brentuximab vedotin, or Adcestris, is used for the treatment of relapsed Hodgkin lymphoma and systemic anaplastic large cell lymphoma. An anti-CD30 tumor necrosis factor mAb is bound to monomethyl auristatin E, a synthetic derivative of dolastatin 10 and a tubulin polymerization inhibitor, by a protease-cleavable valine-citrulline linker and a *p*-aminobenzyloxycarbonyl spacer (Fig. 1.4C).[111] It was granted accelerated approval by the FDA after a critical phase II clinical trial showed an overall response rate of 86% for patients with anaplastic large cell lymphoma, with 53% of those patients achieving a complete response.[115] Additionally, a 75% overall

response rate was attained for patients with relapsed or refractory Hodgkin lymphoma, with 34 % of patients achieving complete response and 40% a partial response.[116] Due to its success to date, it continues to be under trial for use in other CD30-positive neoplasms.[117-119]

Ado-trastuzumab emtansine (T-DM1) was granted accelerated FDA approval in 2013 for the treatment of advanced phase or metastatic human epidermal growth factor receptor 2 (HER2) positive breast cancer.[120] A thioether linker covalently bonds the microtubule inhibitor DM1, a derivative of maytansine, to an anti-HER2 mAb using lysine residues (Fig. 1.4C).[121] This case is promising for the future of natural products in cancer therapy, as maytansine was previously shelved due to systemic toxicity. Interestingly, it was shown that T-DM1 caused complete tumor regression in models where the immunotherapy trastuzumab led to regression followed by regrowth.[122] Moreover, T-DM1 is effective against trastuzumab- and lapatinib- resistant breast cancer cell lines, the standard therapies for HER2+ breast cancer.[122,123] In phase II clinical trials patients with pre-treated metastatic breast cancer saw an overall response rate of 44% with a clinical benefit rate of 73.3%.[124] Another phase II study investigated the efficacy and safety profiles of T-DM1 with trastuzumab plus docetaxel in patients with advanced or recurrent metastatic breast cancer. T-DM1 comparatively had greatly increased progression free survival rates of 14.2 months versus 9.2 with trastuzumab.[125] Thus, T-DM1 shows promise for the improvement of HER2+ cancer management and future patients' prognoses.

1.3.4 ADC Pipeline

The success of brentuximab vedotin and T-DM1 laid the groundwork for future ADCs with approximately 30 currently in clinical development, ranging from phase I-III trials.[108] This new wave of ADCs targets various "cancer-specific" antigens and includes diversified natural product toxins. Some exciting examples include: ABT-414, an anti-EGFR antibody conjugated to monomethyl auristatin F for the treatment of glioblastoma and non-small cell lung cancer; IMMU-132 and labetuzumab-SN-38, both of which introduced the use of irinotecan for the treatment of solid tumors and colorectal cancer respectively; milatuzumab doxorubicin, an anti-CD74 antibody linked to doxorubicin for the treatment of chronic lymphocytic leukemia, multiple myeloma and non-Hodgkin's lymphoma; and MDX-1203, an anti-CD70 targeted mAb loaded with duocarmycin, a DNA alkylating alkaloid, for the treatment of renal carcinoma.[126-130]

1.3.5 Antibody-Drug Conjugate Linking Technology

Although ADCs achieved clinical success, the technologies used to attach small molecule toxins to antibodies have posed significant challenges. Originally, synthetic chemistry was utilized to attach linkers and small molecules to solvent accessible native amino acid residues, including the nucleophilic amines of lysine residues (80-90 per IgG) and thiols derived from reduced interchain cysteine disulfide bonds (8 per IgG). These reactions yield heterogeneous mixtures of ADCs that vary in both drug load and conjugation site. Lysine conjugations yield mixtures of 0-6 drug-to-antibody ratio (DAR) and with approximately 20 different lysines undergoing reactions this chemistry can yield greater than one million unique ADC species.[23,90,119,131] Cysteine conjugations also yield

0-8 DAR species with over 100 different possible combinations of conjugation site and DAR.[132] These mixtures are problematic for a numerous reasons, the first being that ADCs with different drug loads deliver varied doses to cancerous cells and thus have distinct efficacy and safety profiles. The results of a particular study by Hamblett *et al.* emphasized these issues. By separating 2, 4, and 8 DAR species and testing their *in vitro* and *in vivo* effects they showed that efficacy *in vitro* directly corresponded to drug loading, with 8 DAR being the most efficacious, but interestingly *in vivo* the 4 DAR exhibited significantly better efficacy than the 8 DAR or 2 DAR species. Additionally, the toxicity profiles were very different with maximum tolerated doses of 50 mg/kg for the 8 DAR species, 100 mg/kg for the 4 DAR species and 250 mg/kg for the 2 DAR species.[133] Evidently, the therapeutic indexes of these species are quite varied. Ben-Quan Shen *et al.* also highlighted the importance of conjugation site in a study, in which cysteines were integrated into 3 unique sites to generate ADCs with the same drug loading, but that were distinctly isomeric. The *in vivo* efficacy of the isomeric ADCs were significantly different, with one species having almost no activity and another with very good efficacy, increasing survival by more than 30 days.[134] Consequently, downstream lack of standardization in drug loading and conjugation site from heterogeneous synthetic methods could potentially lead to improper dosing of patients and further compromise their health.

Another challenge has been that drug loading and conjugation site variation can engender unique *in vivo* pharmacokinetic properties.[23,24,26,134] Hamblett *et al.* demonstrated that clearance rates are directly proportional to drug loading with clearance

values of 4.4, 6.0, and 19.2 mL/day/kg for 2 DAR, 4 DAR, and 8 DAR, respectively, thus making it apparent that species with lower drug loading are better tolerated in an *in vivo* setting.[133] Ben Quan Shen *et al*. also demonstrated that the stability of antibody-drug conjugation is influenced by the site of small molecule attachment. Over a course of 30 days in mice, one isomer exhibited no loss of conjugation, while another exhibited a rapid loss of drug with only approximately 10% of antibodies remaining conjugated after 5 days.[134] Premature loss of the drug is very dangerous, since ADC natural products are extremely potent and if they are freed before reaching the cancerous cell they generate significant toxicity. Therefore, with this wide variability in properties it is necessary to have batch-to-batch standardization and homogeneous ADCs with optimized drug loading stoichiometry and conjugation site. Such consistency will ensure ADC therapeutics have ideal pharmacokinetic properties, efficacy, and safety profiles to ensure the best possible outcome for patients.

With traditional synthetic methods, extensive and diligent separation and purification is required to yield ADCs with uniform DAR. In many cases it is nearly impossible, however, to separate isomeric forms. Site-specific conjugation, in which drugs are loaded onto defined sites with highly specific stoichiometry, has been explored as a means to overcome these issues. These techniques minimize heterogeneity and therefore allow for better characterization of efficacy and pharmacokinetics and subsequently standardization of dosage.[132] Therefore, significant effort was placed on the development of unique site-selective methods to improve this class of drug.

1.3.6 Methods for Improved Conjugation Selectivity

There were numerous approaches developed to improve the precision of the chemistry involved in ADC generation (Fig. 1.5B). Here, some of the most prominent methods are discussed including the integration of unnatural amino acids, enzymatic techniques, and modification or engineering of cysteines.

1.3.6.1 Unnatural Amino Acids

An orthogonal amber suppressor tRNA/aminoacyl-tRNA synthetase can be used to incorporate unnatural amino acids into antibodies in response to an amber nonsense codon in bacterial or mammalian cells. Using this method, *p*-acetylphenylalanine is incorporated into antibodies. It is the ideal chemical group to undergo oxime ligation chemistry with an alkoxy-amine derivatized drugs to site-selectively generate ADCs. The resultant oxime bond is a stable linkage that is not susceptible to serum degradation and the technique exhibits greater than 95% formation of 2 DAR species.[27]

Alternatively, Zimmerman *et al.* developed a strategy that uses the *M. jannaschii* TyrRS, a tyrosyl-tRNA synthetase, to incorporate *p*-azidomethyl-L-phenylalanine (pAMF) into antibodies in a cell free expression system. Subsequently, copper click chemistry is used to promote an azide-alkyne cycloaddition between the unnatural amino acid and a toxin linked to dibenzocyclooctyl-polyethylene glycol (Fig. 1.5B). This technique yields species that range from an average DAR of low 1.2 to 1.9, exact proportions of the 0, 1, and 2 DAR species are not reported.[25]

Selenocysteine is seen as the 21st proteinogenic amino acid, sharing the structure of cysteine with selenium in the place of sulfur. Using a selenocysteine insertion

sequence, selenocysteine containing antibodies are generated in a mammalian cell system grown in media supplemented with selenium. Small-molecules with maleimide linkers are then site-specifically loaded onto the antibody via nucleophilic attack by selenium. When developing this technique, one selenocysteine was integrated into a Fab and the conversion efficiency from unlabeled to labeled species (1 DAR) was approximately 66%.[135]

1.3.6.2 Enzymatic Techniques

Transglutaminase

Transglutaminases are enzymes that catalyze the formation of a covalent bond between a primary amine and the side chain of glutamine. A short glutamine containing amino acid tag LLQG was developed and integrated into numerous sites in antibodies. Synthetic toxin derivatives made to include free primary amines functionalities can be loaded onto the glutamine containing tag using a transglutaminase enzyme (Fig. 1.5B). This enzymatic loading technique exhibits high levels of efficiency and site-specific loading with 98.5-99% monomeric yields. It also can be efficiently scaled up and manufactured, as the transglutaminases are readily commercially available.[26]

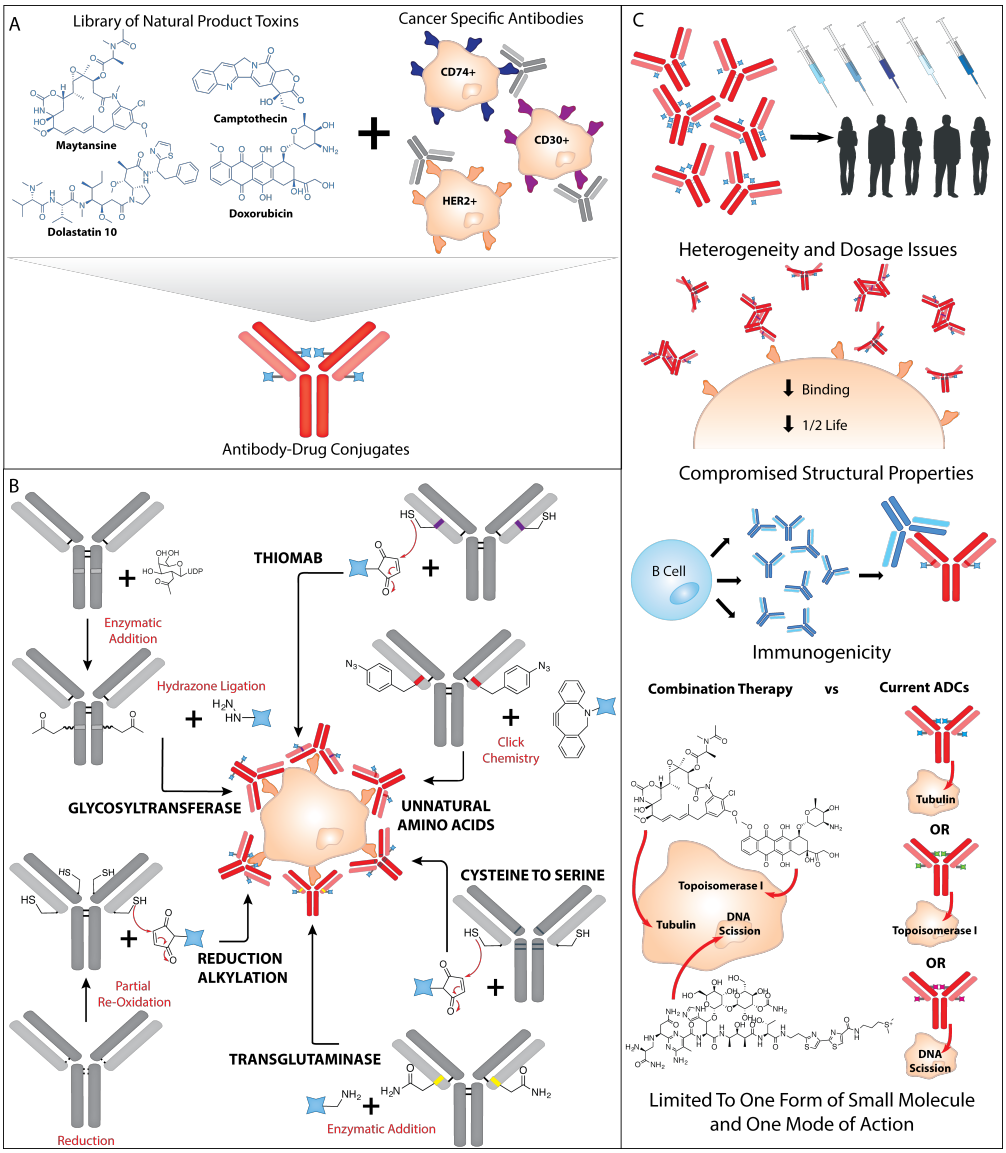

Fig. 1.5 *Overview of the current state of antibody-drug conjugates and their generation technologies.* ***(A)*** *Nature is a rich resource for toxins and many of these natural products are being linked to cancer specific antibodies to generate antibody-drug conjugates, an up-and-coming field of targeted cancer therapy. Semisynthetic derivatives of maytansine and dolastatin 10 are used in clinical ADCs tethered to anti-HER2 and anti-CD30 monoclonal antibodies.*[111,121] *Doxorubicin tethered to an anti-CD74 mAb and a semisynthetic derivative of camptothecin tethered to anti-carcinoembryonic antigen are examples of some*

of the numerous ADCs currently in clinical trial.[127,129] ***(B)*** *Heterogeneous ADC populations are inadmissible in the clinic, because heterogeneity alters their overall properties and poses dosing problems. Depicted are the controlled methods that have been developed for the generation of homogeneous ADCs, including both synthetic and enzymatic techniques. Part* ***(C)*** *highlights weaknesses that persist with certain site-selective techniques.*

Glycosyltransferase

IgGs are glycosylated at their N terminus in the CH_2 domain of their Fc fragment at the conserved Asn297. A galactosyltransferase mutant site-specifically transfers sugar residues with chemically reactive functional groups such as C2-keto-galactose from their UDP derivatives onto the terminal N-acetylglucosamine residue. Small molecules modified with hydrazine functionality are easily added to this site via a hydrazone ligation (Fig. 1.5B). This technique also generates a stable oxime linkage and causes no loss in binding activity. The efficiency and homogeneity of the technique was not reported in detail.[136]

1.3.6.3 Cysteine Modifying

Reduction-Alkylation

The reduction-alkylation strategy is used to generate brentuximab vedotin and involves manipulation of interchain disulfide bonds. During the development of this technique it was revealed that interchain disfulide bonds can be distinguished by specific chemical reduction and oxidation methods. By using appropriate molar equivalents of DTT or TCEP only partial reduction of disulfide bonds occurs in a directed fashion as certain sites are chemically favoured for reduction. Conversely, an excess of DTT can be

used to reduce all disulfide bonds, followed by a partial selective re-oxidation with DTNB to yield four available reactive thiols. Each method favours a distinct disulfide bond combination, yielding different active thiols for the formation of discrete ADC isomers. Thus, by selecting one chemical technique a prominent number of uniform antibodies are produced with the same number of free thiols in the same location ready to be alkylated by a stoichiometric amount of linker bound small molecules (Fig. 1.5B).[24]

The advancement of the reduction-alkylation technique confirmed that lower DAR species (2-4) have larger therapeutic windows and drug-loading stoichiometry impacts ADC pharmacokinetics. These chemistries also provided one of the first methods to improve the degree of homogeneity generated from cysteine conjugated ADCs.

Cysteine to Serine

In order to reduce the number of native reactive thiols from the traditional 8 down to 4 or 2, engineered antibodies were created with serine in place of certain interchain disulfide bond forming cysteines (Fig. 1.5B). Only the selected number of interchain disulfide cysteines remaining are available for reduction to free thiols for drug conjugation. Using this technique uniform ADCs were generated in a range from 89-96%, with improved conjugation precision from traditional cysteine linking methods.[137]

THIOMABS

THIOMABS are engineered antibodies containing two additional non-native reactive cysteines in each heavy chain (Fig. 1.5B). All disulfide bonds in the antibody are first reduced leading to activation of the engineered cysteines. Subsequently, through oxidation theoretically all interchain disulfide bonds reform, but the engineered cysteines

remain free and reactive. Therefore, the added drug can only conjugate to the two reactive cysteine sites, forming a homogenous 2 DAR ADC product (Fig. 1.5B).[23,138] The benefits of this technique are that it aims to retain all native internal disulfide bonds and thereby maintain the antibodies' structure and activity. It also exhibits high degrees of homogeneity for a cysteine modifying technique with near uniform loading stoichiometry. In addition, the results of THIOMAB studies have been integral in substantiating the advantages and need for site-specific conjugation techniques. The precise chemical control offered by, in this case, THIOMABs yielded homogeneous ADCs that exhibited superior safety profiles, improved efficacy and pharmacokinetic properties. For instance, the efficacy of the THIOMAB ADCs (TDC) was comparable to the randomly cysteine generated ADC (ADC), but showed the same toxicity levels in rats at a dose of 68.6 mg/kg TDC compared to a dose of 16.6 mg/kg ADC. Therefore, the TDC demonstrates that the homogeneous ADC has a wider range of safe efficacious doses, which can increase the clinical value of these drugs. Furthermore, THIOMAB generated ADCs have lower clearance rates in rats with approximately 35% TDC remaining in circulation after 12 days versus 4% ADC. Moreover, of those remaining in circulation, approximately 57% of TDCs still had at least one drug still attached compared to approximately 30% of the ADC.[23] Therefore, THIOMAB studies corroborate the concept that site-selective conjugation techniques that generate uniform ADCs yield refined therapeutics with greater potential for improved clinical outcomes.

1.3.7 Weaknesses of Site-Selective ADC Generation Techniques

Despite these efforts to site selectively engineer ADCs, improving conjugation technology remains one of the most important areas of investigation, to yield robust and reproducible techniques that eliminate ADC heterogeneity (Fig. 1.5C). Methods that replace or modify cysteine disulfide bonds, such as reduction-alkylation, cysteine to serine and THIOMAB techniques, can compromise the antibody's structural stability.[23,134] For instance, it was observed that engineered free cysteine residues can pair with those on other proteins to form protein dimers or triple light chain species.[26,132,139-141] Introduced cysteines can also form irregular intra-molecular disulfide bonds with native cysteine residues and this resultant disulfide bond shuffling can result in possible protein inactivation or compromised activity.[132,142] The elimination of disulfide bonds with reduction-alkylation and cysteine to serine strategies in particular can disrupt the antibody's ability to adopt its natural quaternary structure, which consequently negatively impact its *in vivo* activity, stability, clearance rates and its effector functions.[23,143-145]

ADC variability is another ongoing issue. For instance, conjugation mixtures continue to be generated with cysteine modifying techniques.[23,24,26] The reduction-alkylation technique generates a broad distribution of DAR species with the best conditions yielding approximately 11% 0 DAR, 19% 2 DAR, 42% 4 DAR, 23% 6 DAR and 5% 8 DAR. Moreover, within each of these DAR species there are subspecies isomers, with 2 possible 2 DAR isomers, 3 possible 4 DAR isomers, and 2 possible 6 DAR isomers, with the best conditions yielding approximately 18% and 82% of the two 2

DAR isomers, 78%, 17% and 5% for of the three 4 DAR and 97% and 3% of the two 6 DAR isomers.[24] Thus, this technique still creates significant ADC variability. The THIOMAB technique, while greatly improved, also engenders some ADC inconsistency due to the reduction and re-oxidation steps yielding unpaired native cysteines.[26,146] THIOMABS create 0.3% 0 DAR species, 3.3%1 DAR, 92.1% 2 DAR and 4.3% 3 DAR.[23] Purification and analytical techniques of different DAR and particularly isomeric species must be rigorous and can be very technologically challenging to ensure that drugs are loaded onto antibodies in equal amounts and in the same location, including HIC-HPLC followed by reverse-phased HPLC and capillary electrophoresis.[24,132] Additionally, reports suggest these techniques also face scalability issues due to the requirement of several chemical steps – reduction, oxidation, and reaction with the toxin.[27]

Another issue is that the generality of the unnatural amino acids approach has not been established and there are concerns regarding immunogenicity and scalability issues.[27,147,148] Techniques that use cell-based expression systems are challenged by low cell-line titres and the requirement for high reactant stoichiometry and all unnatural amino acid expression forms are quite complex and costly.[26,27] Moreover, the health and condition of the patient is paramount, yet it is unknown whether these unnatural amino acids will generate undesired human immune responses.[25,27] Thus, there remains a need for different approaches, which easily and consistently generate homogeneous ADCs with optimized pharmacokinetic and pharmacodynamics properties.

Another drawback of cysteine modifying, unnatural amino acid, and current enzymatic techniques is they only load one type of small molecule site-selectively onto an

antibody. Yet, it was demonstrated that combinations of synergistic molecules targeting cancer via multiple pathways have better treatment outcomes than single molecules.[149,150] Therefore, the therapeutic potential of ADCs is likely limited using current generation techniques. In order to yield more efficacious targeted therapeutics, two or more uniquely functioning natural products should be conjugated to a single antibody, generating "combination therapy" ADCs that deliver multiple hits to a cancerous cell. This is not currently possible with any degree of selectivity. Given these multiple limitations, study number two in Chapter 3 of this thesis investigates a conjugation technique that enables the site-specific stoichiometric addition of single and multiple distinct natural products onto an antibody for homogeneous polytherapy ADCs.

1.4 Hypothesis and Objectives

The overarching objective of this thesis is to better our understanding of nature's production of molecules with distinct activity toward cellular targets that may be exploited for cancer therapy and discern how these molecules might be further targeted toward the site of disease (Fig. 1.1). With this knowledge in hand, it may facilitate the future development of more sophisticated cancer therapeutics. The central hypothesis of this work is that nature's assemblies diverge to create molecules with different targets through specific modular rearrangements and biosynthetic assembly enzymes with defined group transfer activity can be additionally exploited to site-selectively transfer small molecules onto antibodies. Two bodies of work are addressed in in this thesis:

Study 1. *The Chemical and Biosynthetic Evolution of the Antimycin-Type Depsipeptides*.

I **hypothesized** that evolutionary principles have induced the recombination and divergence of nature's assembly lines through exchange of genetic information encoding distinct modular entities, leading in many cases to only modest structural differentiation, yet complete shifts in cellular target specificity.

Objective: Provide a window into nature's evolutionary principles and the slight variations and combinations of biosynthetic pathways that confer differences in activity toward targets in cancer. I aim to do this through the study of nature's assembly of a family of highly structurally related natural products that hit diverse targets in cancer, specifically the antimycin-type depsipeptides.

Study 2. *The Site-Specific Generation of Antibody-Drug Conjugates Using Phosphopantetheinyl Transferases.*

I **hypothesized** that promiscuous natural products enzymes, specifically phosphopantetheinyl transferases, can be used to direct natural product small molecules chemo- and regio-selectively onto antibodies, thereby generating ADCs that are better equipped to deliver natural products to the site of disease.

Objective: Develop a novel and improved method for the site-selective conjugation of small molecules to antibodies that will further refine the way natural products are used to treat cancer.

Chapter 2. The Chemical and Biosynthetic Evolution of the Antimycin-type Depsipeptides

2.1 Chapter Preface

To address the complexity of nature's divergence of assembly lines and the consequent distinct molecular activity, it was necessary to work with an evolutionary microcosm of nature's biosynthetic assemblies (Fig. 2.1). Therefore, we (myself and co-first author Dr. Xiang Li) elected to study a family of highly structurally related molecules that exhibit discrete anticancer activity, as we surmised they have related assembly lines conducive for investigation into evolutionary rearrangements. Specifically, we worked with the antimycin-type family of depsipeptides, which share the same loading unit, but expand in lactone ring size from 9 to 12 to 15 to 18. Interestingly, with variation in ring size there is an observed shift in activity. Antimycin, 9-membered ring, exhibits inhibitory activity toward Bcl-xL, a mitochondrial transmembrane protein up-regulated in cancer that perturbs apoptotic pathways when it undergoes protein-protein interactions.[18] JBIR-06 and neoantimycin, 12-membered and 15-membered rings, down-regulate GRP78, a chaperone protein often overexpressed in cancer cells that aids in cell survival through assistance in the unfolded protein response.[17,151,152] Respirantin, exhibits potent anti-proliferative activity toward cancer cell lines, but its current target remains unknown.[153,154] This chapter describes how we probed the chemistry available from these assembly lines and performed computational analyses and comparisons of the DNA encoding these biosynthetic assembly lines and their product enzymes. In this work we were able to reveal points of assembly line similarity and divergence within the context of

the antimycin-type family of depsipeptides, suggesting how evolution may have led to the diversification of these molecules to hit unique cellular targets that play roles in cancer.

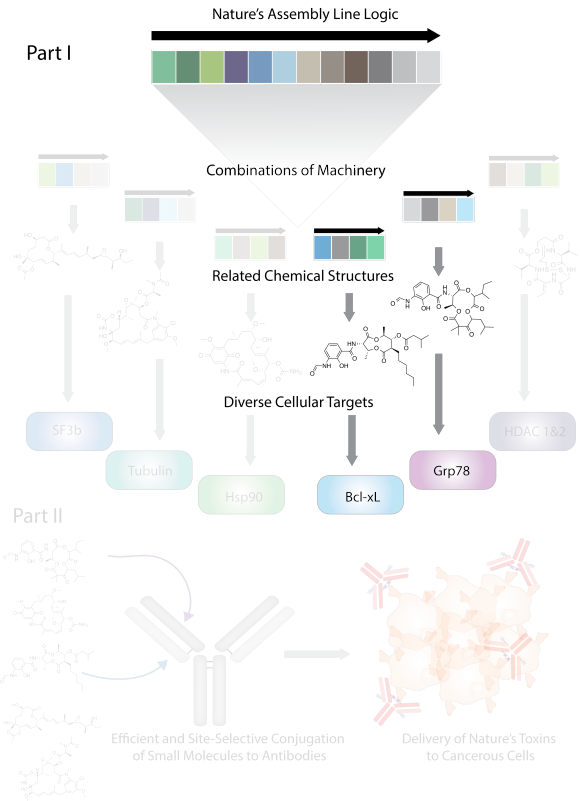

Fig. 1.1 *Chapter 2 overview. The highlighted portions indicate the topics specifically addressed in this thesis chapter. Focus is placed on the antimycin-type family of depsipeptides in particular, with investigations into combinations of biosynthetic assembly line components and how that yielded these structurally related molecules that hit the unique cellular targets Bcl-xL and GRP78.*

This work is laid out in the following chapter as a modified version of a previously published journal article for which I was the co-first author. In this work I was responsible for aiding my co-author, Dr. Xiang Li, in the genome assembly of biosynthetic clusters. I also performed the biosynthetic analyses to identify points of similarity, differentiation, and substrate flexibility across the assembly lines (with

exception of the predicted substrate-selecting amino acid sequences). I analyzed the data as a whole and wrote the manuscript (with the exception of parts of the methods section). The isolation of compounds and mass spectrometry work was completed by Dr. Xiang Li and Rostyslav Zvanych, M.Sc. candidate. Rostyslav Zvanych contributed to the figure design pertaining to the mass spectrometry work. The NMR and structural elucidation was carried out by Dr. Xiang Li. The Bcl-xL assay work was done in collaboration between Jonathon Torchia, M.Sc., under the supervision of Dr. Nathan Magarvey, and Jing Sang, under the supervision of Dr. David Andrews.

This work is now in publication in the journal *Molecular BioSystems*. The citation is as follows:

Mol. BioSyst., 2013, **9**, 2712 – Reproduced by permission of the Royal Society of Chemistry, http://pubs.rsc.org/en/content/articlepdf/2013/mb/c3mb70219g?page=search.

2.2 Abstract

Evolution of natural products, and particularly those resulting from microbial assembly line-like enzymes, such as polyketide (PK) and nonribosomal peptides (NRP), has resulted in a variety of pharmaceutically important and chemically diverse families of molecules. The antimycin-type depsipeptides are one such grouping, with a significant level of diversity and members that have noted activities against key targets governing human cellular apoptosis (e.g. Bcl-xL and GRP78). Chemical variance originates from ring size, with 9-, 12-, 15-, and 18-membered classes, and we show that such distinctions influence their molecular targeting. Further, we present here a systematic interrogation of

the chemistry and assembly line evolution of antimycin-type analogues by conducting metabolomic profiling and biosynthetic gene cluster comparative analysis of the depsipeptide assembly lines for each member of the antimycin-group. Natural molecular evolution principles of such studies should assist in artificial re-combinatorializing of PK and NRP assembly lines.

2.3 Introduction

Microbial natural products, and particularly those with biosynthetic origins arising from polyketide synthase (PKS) and nonribosomal peptide synthetase (NRPS) assembly line-like enzymes, are noted for their chemical and functional diversity. Genetic and biochemical analyses often suggest that the number of combinations and permutations plausible from PK and NRP assembly line syntheses far exceeds the number of products isolated in a laboratory setting.[1] Directed re-design of these modular assemblages, known as combinatorial biosynthesis, assists in realizing unnatural products with improved/altered functionalities and pharmacophores.[2] The suite of NRPS and PKS machinery is comprised of a vast number of enzymatic domains and modules, with distinct monomer block selectivities (>500 for NRPSs and PKSs), and tailoring actions. Our ability to leverage this large repertoire of enzymatic machinery for combinatorial biosynthesis would, however, benefit significantly from an appreciation of how systems have already been combinatorialized in nature.[3] More specifically, to appreciate how natural evolution of assembly systems occurs may provide a framework to deploy re-engineering technologies. Furthermore, in several instances laboratory engineered re-fusions of natural product assemblies have resulted in non-functional recombinant

assembly lines, undesired combined products or nearly negligible yields of the desired hybrid natural product. Unfortunately, only recent investigation into the more critical communication elements and domains (e.g. docking domains)[4] have led to an appreciation of molecular principles that enable natural interactions between modules and assembly line components. Moreover, most of the known biosynthetic gene clusters have been investigated with a focus on the functions of enzymes in their native assembly line setting rather than on attempting to reveal the natural evolutionary principles that promote successful assembly line alteration or modification.[3] One means to gain access to accepted fusion and alteration points within assembly lines, is to reveal divergence within evolutionarily related metabolites and their associated biosynthetic pathways. Retro-biosynthetic analyses, in combination with exhaustive interrogation of NRPS/PKS derived chemical diversity, may provide evidence for how nature itself evolved assembly lines.

Among these naturally selected molecular families, the antimycin-type depsipeptides are uniquely interesting with sequential macrolactone ring expansions engendering diverse anticancer activities. The most well recognized member of the group is the 9-membered antimycin and its related 9-membered congeners (e.g. UK-2A).[5,6] Functionally, this class is noted for its ability to act as a peptidomimetic and block the interaction between BH3-containing peptides and Bcl-xL.[7-9] Although, not completely understood, the interaction of antimycin with Bcl-xL is not dictated by the 2-hydroxy within the formamidosalicylic acid unit, as methylation does little to affect its targeted activity.[7,8] Methylation does, however, blunt the other noted interaction of the antimycins,

and more specifically their binding and inhibition of NADH oxidase in the mitochondrial electron transport at complex III.[7,10] Moreover, the interactions of antimycin with the BH3 groove are seemingly not a common feature of the 12-, 15-, and 18-membered ring-expanded classes of the antimycins (Fig. 2.2). The 'ring-expanded' antimycins, JBIR-06 (12-membered) and prunustatin A (15- membered), however are noted for different activity that relates to eukaryotic cell death pathways, more specifically down-regulating the expression of GRP-78, a key component of the unfolded protein response.[11,12] As such, each of these various macrocyclic natural products are leads for this second antiapoptotic pathway, up-regulated in numerous cancer cell sub-types. The antimycin-type depsipeptide family is further extended by an 18-member, respirantin, whose target is not yet known, but testing reveals a nanomolar inhibition profile of prostate cancer cell types.[13,14] The bioactivity interest in the antimycin-type series and its relationship to ring size and potentially other structural variations, presents a direct opportunity to analyze the evolution of a NRP-PK assembly line from a chemical and biological perspective. In the present study, we isolated 16 depsipeptides from *Streptomyces* sp. ADM21, *Streptomyces* sp. ML55 and *Streptoverticillium orinoci* (Fig. 2.2B) to assist in our appreciation of the spectrum of agents possible from their assembly lines.

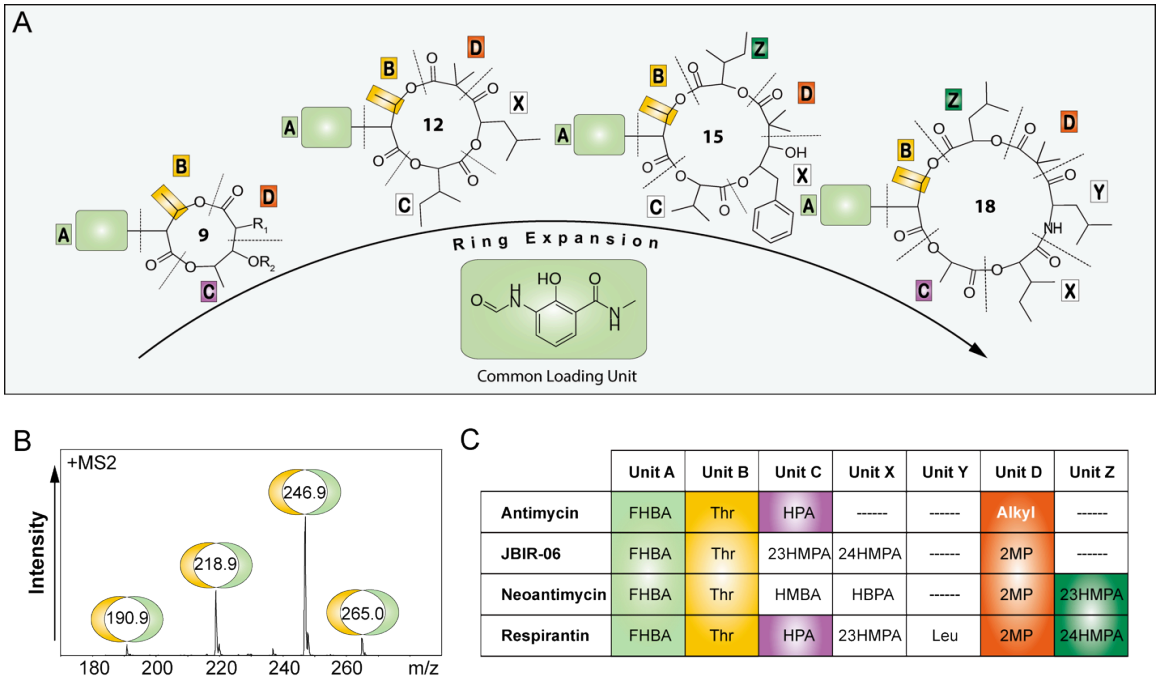

C

	Unit A	Unit B	Unit C	Unit X	Unit Y	Unit D	Unit Z
Antimycin	FHBA	Thr	HPA	------	------	Alkyl	------
JBIR-06	FHBA	Thr	23HMPA	24HMPA	------	2MP	------
Neoantimycin	FHBA	Thr	HMBA	HBPA	------	2MP	23HMPA
Respirantin	FHBA	Thr	HPA	23HMPA	Leu	2MP	24HMPA

Fig. 2.2 1*The 4 naturally occurring antimycin-type depsipeptides.* ***(A)*** *Each class is defined by divergent ring sizes to include 9-membered, 12-membered, 15-membered and 18-membered lactone macrocycle cores. Antimycin R_1: $(CH_2)_5CH_3$, R_2: $COCH_2CH(CH_3)_2$.* ***(B)*** *Screening strategy for identification of antimycin-type analogues based on diagnostic MS/MS fragmentation pattern of units A and B common across all subtypes.* ***(C)*** *Description of antimycin-type depsipeptide units A-Y FHBA: 3-formamido-2-hydroxybenzoic acid, Thr: threonine, HPA: 2-hydroxypropanoic acid, 23HMPA: 2-hydroxy-3-methylpropanoic acid, HMBA: 2-hydroxy-3-methylbutanoic acid, 24HMPA: 2-hydroxy-4-methylpropanoic acid, HBPA: α-hydroxy-benzenepropanoic acid, Leu: leucine, 2MP: 2-methylpropanal.*

To further understand the structure–activity relationships (SAR) at play within and across the classes we tested a selection from the three groups of antimycin-type depsipeptides for Bcl-xL inhibition, demonstrating that only the 9-membered antimycins disrupted the Bcl-xL–BH3 inter action and interestingly, antimycin side chain length influences activity. Moreover, we present a detailed inspection of the assembly lines for

the 4 antimycin-type ring classes to gain an appreciation of how nature drives its own combinatorial processes in order to inform possible future synthetic combinatorial studies.

2.4 Methods

2.4.1 General

^{1}H and ^{13}C NMR spectra were recorded on a Bruker AVIII 700 MHz NMR spectrometer using TMS as an internal standard. Chemical shifts (d) expressed in parts per million (ppm) and coupling constants (J) are reported in Hertz (Hz). High resolution MS spectra were collected on a Thermo LTQ OrbiTrap XL mass spectrometer (ThermoFisher Scientific, USA) with an electro-spray ionization source (ESI) and using CID with helium for fragmentation. LC-MS data was collected using a Bruker Amazon-X ion trap mass spectrometer coupled with a Dionex UltiMate 3000 HPLC system, using a Luna C18 column (250 mm x 4.6 mm, Phenomenex) for analytical separations, running acetonitrile and H_2O as the mobile phase. Column chromatography was carried out with silica gel (200–300 mesh), TLC: silica gel plates (Macherey-Nagel, SilG/UV254, 0.20 mm), spots were detected using the anisaldehyde reagent; Sephadex LH-20 was supplied by GE Health Co.

2.4.2 Extraction and Isolation

5 mL of *Streptomyces* sp. ADM21 (kindly provided by Dr Harmit Laatsch, Georg-August-Universität Göttingen, Germany), *Streptomyces* sp. ML55 (kindly provided by Dr. Shin-ya Kazuo, BIRC, Japan) and *Streptoverticiullium orinoci* (DSM 40571) seed were inoculated into 12 2.8 L Erlenmeyer flasks containing 1 L culture medium

consisting of glucose 4 g, yeast extract 4 g, malt extract 10 g and cultured at 28°C for 4 days on a rotary shaker at 160 rpm. Fermentation was concentrated and chromatographed on a Sephadex LH-20 column and eluted with MeOH. Individual fractions were purified by semi-prep HPLC with gradient MeOH–H_2O (5% to 100%) as a mobile phase to yield the pure compounds (1–16).

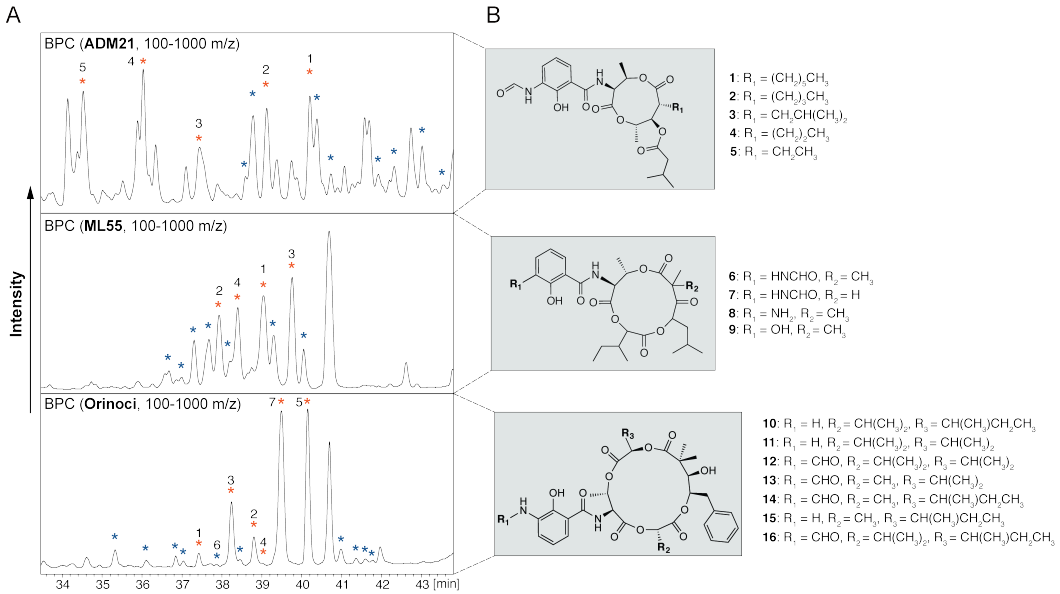

Fig. 2.3 *Chemical diversity profiling from antimycin-type depsipeptide assembly lines from strains Streptomyces sp. ADM21, Streptomyces sp. ML55 and Streptoverticillium orinoci.* ***(A)*** *Base peak chromatograms from the extracts of the 3 depsipeptide producers. Stars highlight the peaks which exhibited MS/MS fragmentation corresponding to the antimycin-type diagnostic mass fragmentation pattern, refer to Fig. 1B. Orange stars indicate the peaks, and corresponding compounds that were isolated.* ***(B)*** *The structures of the purified compounds, consistent with the orange starred chromatogram peaks.*

2.4.3 Bcl-xL Inhibition Assay

Bcl-xL inhibits membrane permeabilization by the proapopto tic proteins cBid and Bax.[9] To measure the effects of the antimycin-type depsipeptides on the activity of Bcl-

xL we measured the increase in fluorescence due to the release of the fluorophore/quencher pair 8-aminonaphthalene 1,3,6-trisulfonic acid (ANTS)/*p*-xylene-bis-pyridinium (DPX) from liposomes.[15] In this assay single addition of recombinant Bax (100 nM) or cBid (20 nM) to liposomes had little effect, but in combination the two proteins caused an increase in fluorescence due to membrane permeabilization that was inhibited by Bcl-xL (40 nM). Addition of antimycin-type depsipeptides that inhibited Bcl-xL restored the increase in fluorescence due to membrane permeabilization (Fig. 2.6A).

2.4.4 Genome Sequencing and Assembly

The Streptomyces' genomic DNA were isolated using standard phenol : chloroform extraction methods.[16] Briefly, *Streptomyces* sp. mycelia were resuspended in SET buffer (75 mM NaCl, 25 mM EDTA pH 8.0, 20 mM Tris-HCl pH 7.5) and treated with 1 mg/mL lysozyme for 60 minutes at 37°C. After incubation, proteinase K was added to a concentration of 0.5 mg/mL and SDS to a concentration of 1%, and incubated at 55°C for 2 hours. After incubation, the solution was brought to a final NaCl concentration of 1.25 M before extracting 3 times with 1:1 phenol chloroform buffered with Tris-HCl pH 8.0. After separating the organic and aqueous phase by centrifugation at 4500g, DNA was precipitated with 0.6 volume of isopropanol, and desalted with 70% ethanol. After drying, the DNA was resuspended in TE buffer. DNA samples were prepared using the Illumina protocol (TruSeq DNA Sample Preparation Guide, #15005180) and were fragmented. The DNA fragment ends were repaired and phosphorylated using Klenow T4 DNA polymerase and T4 Polynucleotide Kinase. After the ligation product was purified and PCR amplified, the library was validated and

sequenced on the Illumina Hiseq 2000 using 100 bp PE processing. Sequence reads obtained with B50 coverage were assembled into contigs using an Abyss genome sequence assembler. The gaps were filled with PCR using primers (Supplemental Table 2.1).

2.4.5 Sequence and Mauve Alignments and Phylogenetic Analysis

Nucleotide sequences were aligned using the Geneious R6 program, with default parameter settings (gap opening penalty, 10; gap extension penalty, 0.05; gap separation penalty range, 8; identity for alignment delay, 40%). The phylogenetic tree was constructed using the neighbor-joining algorithm with Geneious R6 with a gap penalty of 7 and gap extension penalty of 3. A Mauve alignment was performed using Geneious R6 progressive Mauve algorithm with a match seed weight of 20 and a minimum LCB score of 69.

2.5 Results and Discussion

2.5.1 Chemical Profiling of the Antimycin-type Chemical Diversity

A chemical analysis of the antimycin-type depsipeptides was first conducted to profile the existing diversity across the 9-, 12-, 15- and 18-membered subtypes (Fig. 2.2A). The respective depsipeptides under study include the producers of each ring class, antimycin (9-membered), JBIR-06 (12-membered), neoantimycin (15-membered), and respirantin (18-membered).[6,11,13,17] To facilitate the recognition of structural similarities and the discrimination of differences between the 4 classes, unit names have been assigned to each monomer component in the equivalent position to those across the

counterpart ring sub-types (Fig. 2.2C). The loading unit, 3-formamido-2-hydroxybenzoic acid (FHBA), unit A, and threonine (Thr), unit B, are common among all classes. Antimycin and respirantin include 2-hydroxy-propanoic acid (HPA) as unit C, whereas 2-hydroxy-3-methylpentanoic acid (23HMPA) in JBIR-06 and a 2-hydroxy-3-methylbutanoic acid (HMBA) in neoantimycin occupy this structural location. Unit X, not present in antimycin, is 2-hydroxy-4-methylpentanoic acid (24HMPA) in JBIR-06, α -hydroxy-benzenepropanoic acid (HBPA) in neoantimycin and 23HMPA in respirantin. There is a unique second amino acid component in respirantin, assigned as unit Y, which is a leucine (Leu). Unit D of JBIR-06, neoantimycin, and respirantin, is a 2-methylpropanal component (2MP), which originates from a carboxylic acid bearing a gem-dimethyl (GDM) substituent. Conversely, unit D of antimycin is composed of variants with longer straight and branched alkyl chains. Respirantin and neoantimycin are further distinguished by an additional 24HMPA and 23HMPA α-keto acid constituent respectively, designated as unit Z (Fig. 2.2C).

To gain further insight into the types of structural variety nature elicits from the antimycin-type depsipeptides respective biosynthetic pathways, an MS/MS screening strategy was developed for analogue isolation. The specific positions of structural diversity, conferred by assembly line flexibility, within each ring subtype was then easily identified. In many instances a biosynthetic assembly line will create a number of variants that are co-produced with the dominant natural product.[18] Analogues not only serve to reveal SAR, but can also be used to illuminate the promiscuous properties of a biosynthetic assembly line.[18] Advanced screening from a number of natural product

producers has shown that the variations of depsipeptides are particularly numerous. Isolation and characterization of 18 analogues of the broad-spectrum antitumour depsipeptide, cryptophycin, is a noteworthy example.[19] Often within natural product families, the greatest structural diversity arises from the incorporation of different monomer building blocks during biosynthesis, as opposed to post-assembly line modifications. As such, we devised a strategy that would be capable of identifying members based on a general diagnostic fragmentation pattern from each ring- size class. First, the known antimycin, JBIR-06 and neoantimycin diagnostic fragments were established, *m/z* at 190.9, 218.9, 246.9 and 265.0 (Fig. 2.2B). Less abundant peaks in the chromatogram, sharing the signature fragmentation pattern, were subsequently isolated (Fig. 2.3A). This approach rapidly led to the identity of 5 antimycin variants, 4 JBIR-06 analogues and 7 neoantimycin analogues, all of which have been previously characterized (Li, unpublished data.[6,11,17,20,21] Unfortunately, due to the distinct growing conditions of the respirantin producer, unrepeatable in a laboratory setting, we lacked sufficient material to purify analogues (data not shown). Structures of the 16 isolated compounds were confirmed by LC-MS/MS, 1D & 2D nuclear magnetic resonance (NMR) and by correlation of the spectral data to literature values (Supplemental Fig. 2.1 and 2.6-2.55).[11,17]

It is apparent from the sites of structural deviation across the subtypes and rich diversity of monomer building blocks within each subtype, that nature's antimycin-type assembly lines exhibit broad enzymatic flexibility (Fig. 2.3B). All five antimycin analogues (1–5), and one of the JBIR-06 analogues (7) differed in unit D. The antimycins

contained varying alkyl chain tail lengths from two carbons, up to six in length and also an isobutyl group, whereas one of the gem-dimethyl alkyl groups in JBIR-06 was replaced by hydrogen. Analogues of JBIR-06 and neoantimycin were both found to vary in unit A, in which the formamido group (6 and 7) was replaced by an amine (5) or hydroxyl group (9) in JBIR-06 and a hydrogen (10, 11, and 15) or formyl group (12, 13, 14 and 15) in neoantimycin. Rich chemical diversity is found amongst the neoantimycins in particular, with deviations occurring additionally at units C and Z. The differing α-keto acid building blocks include those with an isopropyl moiety (10, 11, 12, and 16), or a methyl group (13, 14 and 15) for unit C and 2-methylbutyl (10, 14, 15 and 16), or an isopropyl moiety (11, 12, and 13) for unit Z. The isolation of 16 analogues reflects the promiscuity of unit A loading module, the unit D PKS module, and the α-keto acid loading units C and Z within the antimycin-type assembly lines, suggesting where future modifications could be made to these molecules through natural incorporations.

2.5.2 Antimycin-type Assembly Lines

For comparative purposes and to uncover assembly line diversification within the antimycin-type depsipeptides, we conducted genomic sequencing of the antimycin (*Streptomyces* sp. ADM21), JBIR-06 (*Streptomyces* sp. ML55), neoantimycin (*Streptoverticillium orinoci*), and respirantin (Alaskan *Kitasatospora* sp.) producers. 100 bp paired end libraries were constructed and DNA used for the HiSeq2000 sequencing protocol. Each genomic sequencing scan yielded approximately 325, 310, 380 and 450 Mbp of DNA sequence of which assemblies lead to 210, 176, 128 and 392 large contigs. Recently antimycin biosynthetic clusters have been revealed from several strains

including, *Streptomyces* sp. S4, *S. ambofaciens* ATCC 23877, *S. albus* J1074, *Streptomyces* sp. NRRL 2288, and *S. blastmyceticus* NBRC 12747.[22,23] We therefore used the *Streptomyces* sp. S4 antimycin gene cluster as a seed to search for the homologous antimycin cluster within *Streptomyces* sp. ADM21. The search results, specifically using AntH and AntI, those that encode for unit A, produced only one possible candidate for the antimycin gene cluster, with a sequence similarity of 93.5%. Additionally, a Basic Local Alignment Search (BLAST) was performed on the 3 larger ring-sized subtype producers against *Streptomyces* sp. S4 to locate their depsipeptide clusters. Leads were identified with similarities of 72.3%, 71.0%, and 69.1% for the JBIR-06 (*S.* sp. ML55), neoantimycin (*S. orinoci*), and respirantin (Alaskan *Kitasatospora* sp.) clusters respectively. Extension from each of the homologs produced antimycin-like assembly lines. However, with increasing product ring size came a higher number of modules, with *S.* sp. ML55 (12-membered JBIR-06 producer) containing 5 modules, *S. orinoci* (15-membered neoantimycin producer) 6 modules, and Alaskan *Kitasatospora* sp. (18-membered respirantin producer) 7 modules (Fig. 2.4). Sequence interrogation of these biosynthetic loci is in keeping with the anticipated co-linearity and coding for each of the respective antimycin-type depsipeptides. Identification of the candidate depsipeptide clusters provided a logical starting point to assess how the antimycin-type assembly lines diverge.

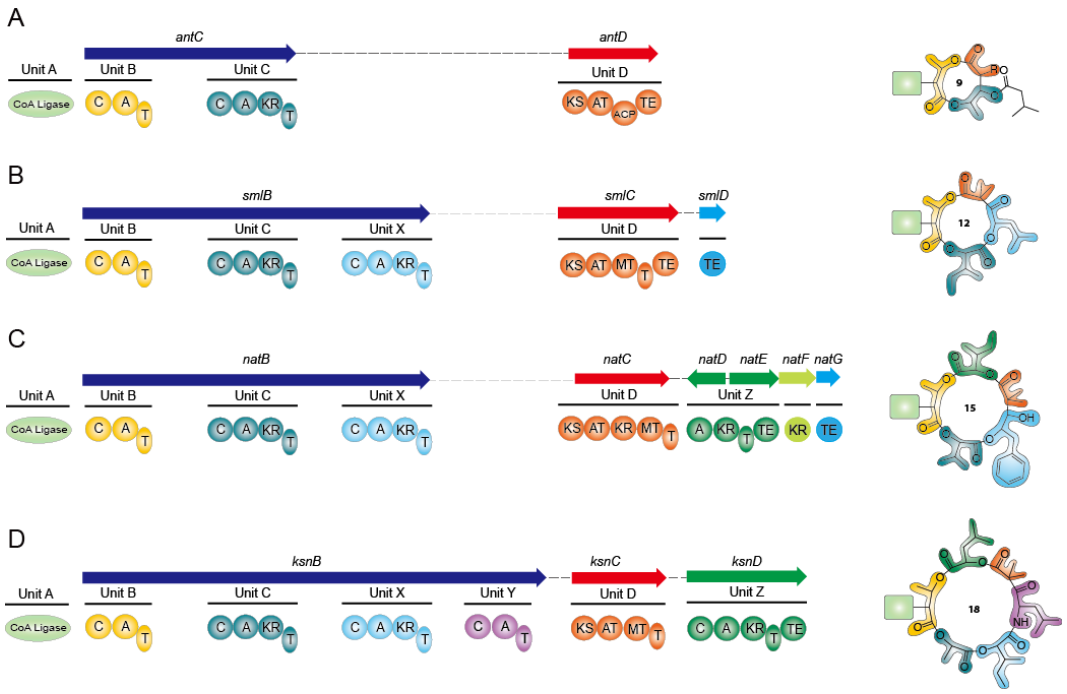

Fig. 2.4 *The NRPS–PKS biosynthetic clusters that produce the 4 classes of antimycin-type depsipeptides,* ***(A)*** *antimycin,* ***(B)*** *JBIR-06,* ***(C)*** *neoantimycin, and* ***(D)*** *respirantin.*

Threonine-loading unit B appears to be highly conserved across the 4 assembly lines, thus it was the point of departure for further investigation. A multiple pairwise alignment of the 4 unit Bs revealed high percent sequence identities for the expanded ring sub-type producers to the *S.* sp. ADM21 antimycin cluster, with JBIR-06 (*Streptomyces* sp. ML55) at 79.2%, neoantimycin (*S. orinoci*) at 78.7%, and respirantin (Alaskan *Kitasatospora* sp.) at 76.7%, demonstrating the similarities in composition and arrangement of base pairs in the unit B encoding portion of all 4 clusters. A narrower focus on the unit B adenylation domains, responsible for substrate selection and ultimate product chemistry, corroborated said results. Genetic similarity was further exhibited through phylogenetic analysis and adenylation domain sequence alignment of all

adenylation domains present within the 4 depsipeptide assembly lines (Supplemental Fig. 2.3B and 2.5A). The unit B adenylation domains were found to have the highest percent sequence identity across all of the assembly line adenylation domains, ranging from 73.8–80.9%, and had the closest level of ancestry as indicated by their grouping in the phylogenetic tree. A protein level analysis of the unit B adenylation domains revealed that the substrate-selectivity governing amino acid sequence is highly conserved across the antimycin, JBIR-06, neoantimycin, and respirantin assembly lines, as indicated by the top line of amino acids in Supplemetal Fig. 3A. These genetic and protein data, in hand with the chemical structural relationships of the depsipeptides, indicate as expected that *Streptomyces* sp. ADM21, *Streptomyces* sp. ML55, *S. orinoci*, and *Kitasatospora* sp., and consequently their products, antimycin, JBIR-06, neoantimycin and respirantin, evolved tangentially from a common route.

2.5.3 Bioinformatic Investigation of Assembly Line Relationships

Recognizing that the initiating units of the antimycin-type assembly lines are most likely derived from the same source, led us to query how the genetic, and consequent enzymatic, insertions and extensions to assembly lines came about. It appears that there are three possible means by which highly structurally related families of natural products could arise from a common enzymatic root. The first means being through duplications of previous assembly line modules, the second by incorporation of novel DNA from the same bacterial source upon which point mutations could occur, and the third through the incorporation of novel DNA from distinct bacterial sources that leads to the greatest assembly line divergence. In the case of the three unit Xs, they do not appear to be

duplications of unit Cs. The loaded α-keto acids are distinct and a multiple pairwise alignment of all 4 unit C and the 3 unit X sequences yielded relatively low sequence similarities between the C and X units, ranging from 57.3–64.7%. Moreover, it does not seem likely that the JBIR-06, neoantimycin and respirantin producers have incorporated this new unit from the same source, as the alignment produced sequence identities spanning from 58.9–65.7% for the 3 unit Xs. Further probing of the adenylation domain similarities showed that unit X of the respirantin producer is almost certainly an addition from a disparate source, with low sequence identity to that of the JBIR- 06 and neoantimycin producers and diverging as its own branch in a phylogenetic analysis (54A). The unit X origins for JBIR-06 and neoantimycin remain unclear, however, with an adenylation domain sequence identity of 68.5% and a close phylogenetic grouping (Fig. 2.5A and Supplemental Fig. 2.3A).

An alignment of the additional C-A-T module, unit Y, nucleotide sequence from the respirantin assembly line was performed with those of the 4 unit Bs, the conserved threonine-loading C-A-T found in all assembly lines, to provide insight on whether the distinctive unit is derived from a module duplication. The percent sequence identities are notably lower for the relationship between those encoding unit Y and the unit Bs (59.5–61.9%) than across the unit Bs (75.0–78.4%) from the different depsipeptide producers, suggesting that the unit Y sequence was integrated from an unrelated source. Further investigation was performed through a focus on the adenylation domains. A multiple alignment of the 4 unit B adenylation domains with the Y adenylation domain demonstrated that the unit Y adenylation domain is only 66.4–66.7% similar to those of

the 4 unit Bs, whereas the unit Bs are 77.7–83.5% similar. Furthermore, the amino acid sequence governing substrate incorporation in unit Y diverges from the conserved sequence of the unit Bs, as indicated by the bottom line of amino acids in Supplemental Fig. 2.3A, therefore substantiating that unit Y is not derived from an antimycin-type assembly line DNA replication.

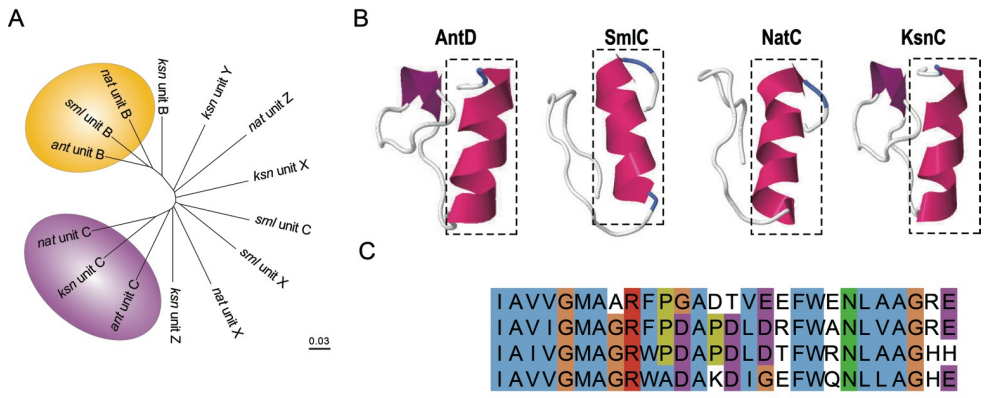

Fig. 2.5 *Genetic alignment analyses of components from the 4 antimycin-type depsipeptide clusters* ***(A)*** *Phylogenetic analysis of the adenylation domains of the depsipeptides' biosynthetic clusters.* ***(B)*** *Simulated possible recognition/binding domain between the NRPS and PKS enzymes.* ***(C)*** *A 28 amino acid conserved domain representing a possible recognition/binding sequence between the NRPS and PKS enzymes.*

We proceeded to investigate the relationship of unit Z to the other antimycin-type C-A-KR-T modules. The neoantimycin unit Z shares a sequence identity ranging from 51.0–56.2% with units C and X and the respirantin unit Z has a sequence identity of 55.7–59.5% to these same units upon performing a multiple alignment of all C, X, and Z units. The low homologies between the unit Z nucleotide sequences and those of previous

C-A-KR-T modules, units C or X, suggest that they have not likely arisen through DNA duplication. The unit Z incorporations also appear to have come from different sources, as the sequence alignment produced a similarity of 53.7% between that from the neoantimycin and respirantin assembly lines.

A Mauve analysis was next performed to gain a more complete view of the genetic evolution relationships between the 4 full-length antimycin-type depsipeptide biosynthetic clusters (Supplemental Fig. 2.4). Mauve is a more sophisticated multiple genome alignment program, capable of processing large-scale evolutionary events, including insertions and rearrangements.[24] It groups nucleotide sequences sharing ancestral roots by colour and the level of similarity is indicated by the intensity on the plot. The pink alignment component is suggestive that unit B is the same across the antimycin, JBIR-06, neoantimycin and respirantin assembly lines, further corroborating our previous computational homology investigations. It is interesting to note that module insertions do not appear to occur after T domains, but more likely around C domains as indicated by the alignment colour transitions from pink to green/red and yellow to red/green across the 4 assembly lines. Our examination yielded another definitive common sequence across the 4 antimycin-type clusters located at the beginning of the PKS modules (Fig. 2.5C), which we propose to be a conserved docking domain. A protein interaction that docks NRPS to PKS units must occur, but has been uncharacterized to date. Looking at the antimycin-type NRPS termini there are no clear sequence patterns that could partner a PKS docking domain, for recent structural studies have provided important new insights relating to the architecture and mechanism of type I

PKS associations. By X-ray crystallographic analysis of the PikAIII/PikAIV docking domain interface, Buchholz *et al.* suggested α-helical regions are involved in protein–protein interaction between two PKS module.[4] An 80–100 amino acid sequence is known to be the docking component on the C' terminus of the acyl carrier protein (ACP), with which a 30–40 N-terminal sequence of the ketosynthase (KS) interacts.[25] The identified conserved sequence in the antimycin-type assembly lines was 28 amino acids found near the N terminus of the KS domain. We, therefore, proceeded to generate 3D models of 4 PKS enzymes within each depsipeptide cluster based on reported PKS crystal structures (Fig. 2.5B). Each contains a conserved α-helical region at the very beginning of the sequence, which could potentially serve as an NRPS–PKS interaction surface. Although the question remains of how an NRPS specifically interacts with its PKS cognate, the data indicates another potential shared evolutionary trait of the 4 antimycin-type depsipeptides.

Next, we sought to further characterize the unit D PKS domains to unveil the divergences in substrate selectivity as the antimycin assembly line alone incorporates alkyl-chain containing monomers. We anticipated that the antimycin assembly line acyltransferase (AT) would be sufficiently different from ATs in the other systems, however a nucleotide alignment revealed a 66.4%, 67.5%, and 67.2% sequence similarity between the antimycin AT encoding DNA and that of JBIR-06, neoantimycin, and respirantin respectively. Moreover, a near identical conserved 13 amino acid sequence was predicted for the substrate-selecting domain of the AT in all 4 assembly lines (Supplemental Fig. 2.5), perhaps suggesting that site-specific mutations at other locations

within the conserved acyltransferases are responsible for conferring different substrate selectivity. The keto-synthases are also relatively similar, with shared nucleotide identity of 71.9% (JBIR-06), 69.5% (neoantimycin), and 73.5% (respirantin) to the antimycin producer. Noted divergence occurs, however, after the AT, with insertions of ketoreductase (KR) and methyltransferase (MT) domains. It appears therefore that the conserved KS-AT di-domain is sufficiently hyper-variable to imbue antimycin with unique chemistry in comparison to the other ring subtypes. With knowledge of such KS-AT promiscuity, it is reasonable to propose rational future combinatorial manipulations that specifically leverage this unit D di-domain.

2.5.4 Bioactivity Assessment of the Antimycin-type Depsipeptides

The differences within and across the antimycin-type ring classes begs the question, is the noted protein–protein blocking interaction of antimycin in keeping with the common unit A of all the subtype structures, or with one of the ancillary components? To probe this, we tested JBIR-06 and neoantimycin against the known inhibitor of BH3–Bcl-xL binding, antimycin 3A (Fig. 2.6B). The results of these experiments imply that the action of antimycin A3 in blocking BH3 binding is not exclusive to unit A. Furthermore, they are consistent with alterations to unit A in the methoxy antimycin series, which is a current clinical lead that exhibits no change in activity from antimycin A3.[7]

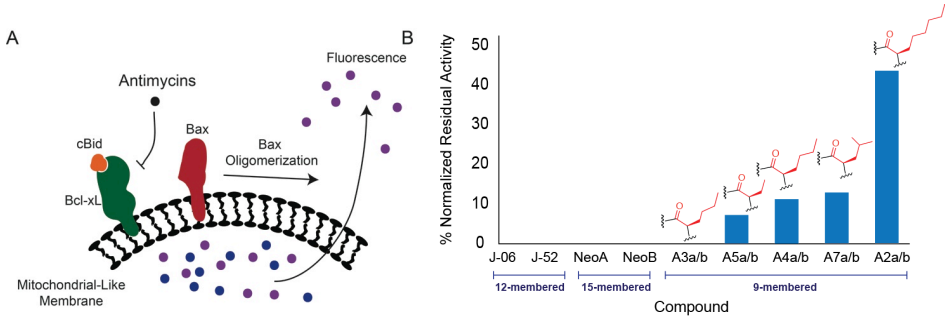

Fig. 2.6 *Bioactivity assessment of antimycin-type depsipeptides* ***(A)*** *Schematic overview of fluorescent polarization Bcl-xL inhibition assay.* ***(B)*** *Inhibition of Bcl-xL by isolated compounds, J-06 (JB1R-06),*[11] *J-52 (JBIR-52),*[20] *NeoA (neoantimycin A),*[17] *NeoB (neoantimycin B)*[26] *and A2, A3, A4,*[6] *A5*[27] *and A7*[28] *represent antimycin 2, 3, 4, 5 and 7.*

Our ability to profile the antimycin type depsipeptides led us to further query actions of the antimycin series exclusively. We isolated a variety of antimycin analogues with varying chain lengths in the fatty acid chain component, unit D, and found that the chain length is a driving factor for Bcl-xL inhibition (Fig. 2.6B). Antimycin A3a/b, 4 carbon alkyl chain, was not as active as the longer tailed variant antimycin A2a/b, a 6 carbon alkyl chain, which demonstrated the most potent activity and thus the importance of the alkyl component to Bcl-xL inhibition. Such systematic chemical profiling and bioactivity assessment, not only shows the diversification enabled by the assembly lines, but also the molecular and functional uniqueness of independent members of the antimycin-type depispeptides.

2.6 Conclusions

In this work, we were able to interrogate the various structures of the antimycin-type depsipeptides from variant biosynthetic sources and reveal the assembly line

machinery for each of the 9-, 12-, 15-, 18-membered ring subtypes. Through computational probing and comparison of their assembly lines, we generated a picture for how these biosynthetic machineries are related to one another. Furthermore, we have perhaps uncovered modules of promiscuity, one of which is the acyltransferase, unit D, as in the antimycin series it leads to the incorporation of substrates with varying fatty acid tails, where in other types loading is constrained to methylmalonate and malonate monomers. Investigations of chemical and biosynthetic evolution of natural assembly lines, such as this, may importantly create opportunities to appreciate how nature evolves assembly lines, which in turn may be useful and significant for future combinatorial biosynthetic efforts.

2.7 References

1. S. Donadio, P. Monciardini and M. Sosio, *Nat. Prod. Rep.*, 2007, **24**, 1073–1109.
2. F. T. Wong and C. Khosla, *Curr. Opin. Chem. Biol.*, 2012, **1**, 117–123.
3. M. A. Fischbach and C. T. Walsh, *Chem. Rev.*, 2006, **106**, 3468.
4. T. J. Buchholz, T. W. Geders, F. E. Bartley III, K. A. Reynolds, J. L. Smith and D.H. Sherman, *ACS Chem. Biol.*, 2009, **4**, 41–52.
5. K. Tani, Y. Usuki, K. Motoba, K. Fujita and M. Taniguchi, *J. Antibiot.*, 2002, **55**, 315–321.
6. W. Liu and F. M. Strong, *J. Am. Chem. Soc.*, 1959, **81**, 4387–4390.
7. S. P. Tzung, K. M. Kim, G. Basañez, C. D. Giedt, J. Simon, J. Zimmerberg, K. Y. Zhang and D. M. Hockenbery, *Nat. Cell Biol.*, 2001, **3**, 183–191.
8. K. M. Kim, C. D. Giedt, G. Basañez, J. W. O'Neill, J. J. Hill, Y. H. Han, S. P.

Tzung, J. Zimmerberg, D. M. Hockenbery and K. Y. J. Zhang, *Biochemistry*, 2001, **40**, 4911–4922.

9. S. Cory and J. M. Adams, *Nat. Rev. Cancer*, 2002, **2**, 647–656.

10. N. Tokutake, H. Miyoshi, T. Satoh, T. Hatano and H. Iwamura, *Biochim. Biophys. Acta*, 1994, **1185**, 271–278.

11. J. Y. Ueda, A. Nagai, M. Izumikawa, S. Chijiwa, M. Takagi and K. Shin-ya, *J. Antibiot.*, 2008, **61**, 241–244.

12. Y. Umeda, S. Chijiwa, K. Furihata, K. Furihata, S. Sakuda, H. Nagasawa, H. Watanabe and K. Shin-ya, *J. Antibiot.*, 2005, **58**, 206–209.

13. I. Urushibata, A. Isogai, S. Matsumoto and A. Suzuki, *J. Antibiot.*, 1993, **46**, 701–703.

14. G. R. Pettit, T. H. Smith, S. Feng, J. C. Knight, R. Tan, R. K. Pettit and P. A. Hinrichs, *J. Nat. Prod.*, 2007, **70**, 1073–1083.

15. J. A. Yethon, R. F. Epand, B. Leber, R. M. Epand and D. W. Andrews, *J. Biol. Chem.*, 2003, **278**, 48935–48941.

16. K. Smalla, N. Cresswell, L. C. Mendonca-Hagler, A. Wolters and J. D. van Elsas, *J. Appl. Bacteriol.*, 1993, **74**, 70–75.

17. G. Cassinelli, A. Grein, P. Orezzi, P. Pennella and A. Sanfilippo, *Arch. Mikrobiol.*, 1967, **55**, 358–368.

18. M. Nett, H. Ikeda and B. S. Moore, *Nat. Prod. Rep.*, 2009, **26**, 1362–1384.

19. T. Golakoti, J. Ogino, C. E. Heltzel, T. L. Husebo, C. M. Jensen, L. K. Larsen, G. M. L. Patterson, R. E. Moore and S. L. Mooberry, *J. Am. Chem. Soc.*, 1995, **117**,

12030–12049.

20. I. Kozone, J. Ueda, M. Takagi and K. Shin-ya, *J. Antibiot.*, 2009, **62**, 593–595.

21. Y. Takeda, T. Masuda, T. Matsumoto, Y. Takechi, T. Shingu and H. G. Floss, *J. Nat. Prod.*, 1998, **61**, 978–981.

22. M. Sandy, Z. Rui, J. Gallagher and W. Zhang, *ACS Chem. Biol.*, 2012, **7**, 1956–1961.

23. R. F. Seipke, J. Barke, C. Brearley, L. Hill, D. W. Yu, R. J. M. Goss and M. I. Hutchings, *PLoS One*, 2011, **6**, e22028.

24. A. E. Darling, T. J. Treangen, X. Messeguer and N. T. Perna, *Methods Mol. Biol.*, 2007, **396**, 135–152.

25. R. W. Broadhurst, D. Nietlispach, M. P. Wheatcroft, P. F. Leadlay and K. J. Weissman, *Chem. Biol.*, 2003, **10**, 723–731.

26. K. Takahashi, E. Tsuda and K. Kurosawa, *J. Antibiot.*, 2001, **54**, 867–873.

27. G. Schilling, D. Berti and D. J. Kluepfel, *J. Antibiot.*, 1970, **23**, 81–90.

28. C. J. Barrow, J. J. Oleynek, V. Marinelli, H. H. Sun, P. Kaplita, D. M. Sedlock, A. M. Gillum, C. C. Chadwick and R. Cooper, *J. Antibiot.*, 1997, **50**, 729–733.

2.8 Supplemental Tables

Primer Names	Forward	Reverse
ADM21-GAP-1	5'-GCGCGGTCGGTCAGATCGT-3'	5'-GAATTCCCCTACAGCGCG-3'
ADM21-GAP-2	5'-TCTCCATGGCCGACTTCTT-3'	5'-CCGTCCAGCTGGTTGAGG-3'
ADM21-GAP-3	5'-GCAGCTCAACGCGCACTTC-3'	5'-GCTCCCCGGCCGCGAGCA-3'
ML55-GAP-1	5'-CAACGCCCATGTGATCCT-3'	5'-AGGACATCGGGGAGTTCTG-3'
ML55-GAP-2	5'-CCTCGGACAGCACGAGAC-3'	5'-TGCTTCTTGAGGATCTTCCC-3'
ORINO-GAP-1	5'-GCTATGGCTACACCCTGGTC-3'	5'-GCCTATCTGTACCGGGTCAC-3'
ORINO - GAP-2	5'-GTGGGGCCCGCTGCTGT-3'	5'-TGACCCGCTCCTCGCGC-3'
ORINO - GAP-3	5'-CGGTGTGCCCGCGCCCGGGG-3'	5'-TCATCACATGGTGCGCGCCC-3'
ORINO - GAP-4	5'-CTCGGCGACGGTTCGCTGG-3'	5'-TCCTCATGCGCCGCCACC-3'

Supplemental Table 2.11*Primers used in this study.*

2.9 Supplemental Figures

2.9.1 General

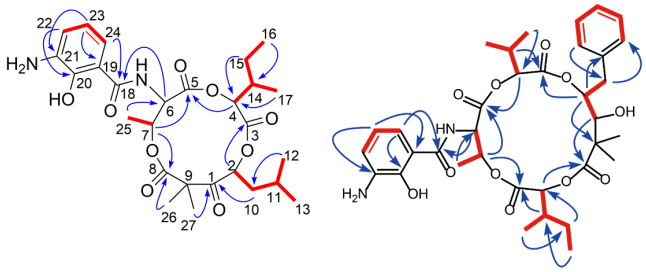

Supplemental Fig. 2.1 *Representative ^{1}H-^{1}H COSY and ^{1}H-^{13}C HMBC correlations of isolated compounds.*

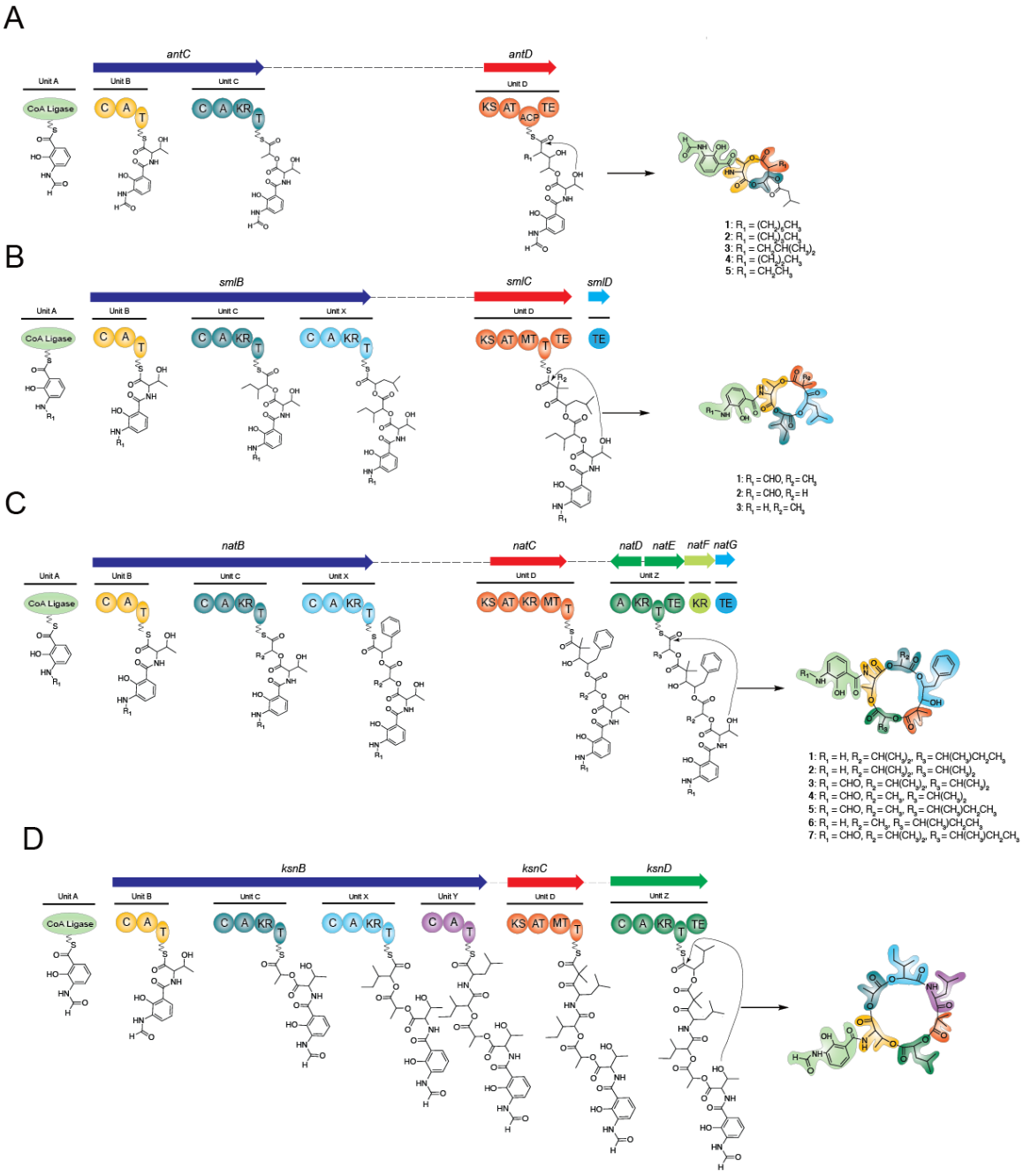

Supplemental Fig. 2.2 *Representation of the PKS-NRPS biosynthetic pathway for the 9-, 12-, 15-, and 18-membered antimycin-type depsipeptide subclasses, highlighting the flexibility of the biosynthetic units, X, Y, and Z.*

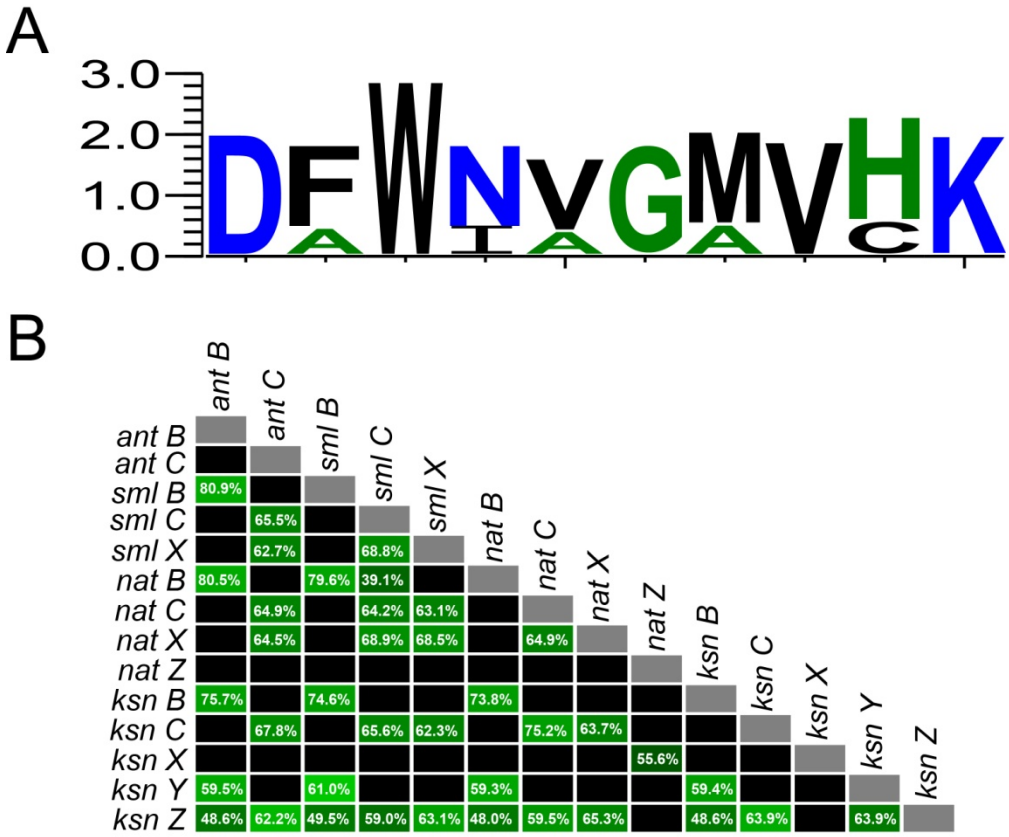

Supplemental Fig. 2.3 *Adenylation domain analyses* ***(A)*** *Predicted adenylation domains loading amino acid codes.* ***(B)*** *Heatmap of the Geneious nucleotide alignment of the adenylation domains of the antimycin (ant), JBIR-06 (sml), neoantimycin (nat) and respirantin (ksn) NRPS clusters, demonstrating the genetic similarity in colour and percentage.*

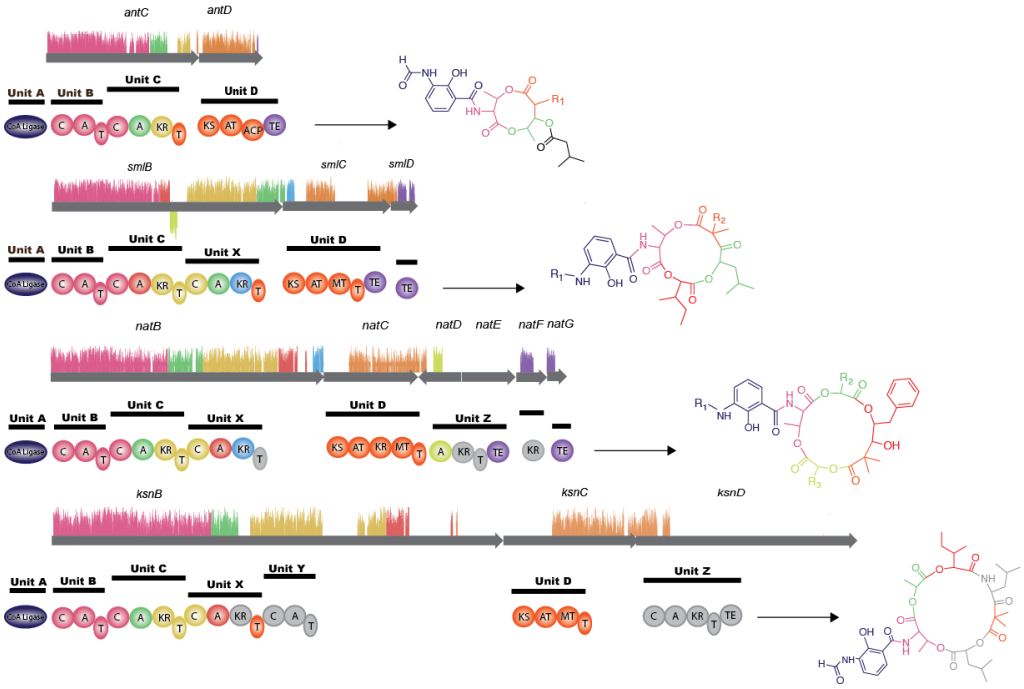

Supplemental Fig. 2.4 *Mauve analysis of the nucleotide sequences encoding the antimycin-type PKS-NRPS enzymology from Streptomyces sp. ADM21 (ant), Streptomyces sp. ML55 (sml), Streptoverticillium orinoci (nat) and Alaskan Kitasataspora sp. (ksn). Nucleotide sequences were pairwise aligned using the program Geneious. Colour indicates genetic similarity, and the height and frequency of the coloured lines depicts the degree of similarity.*

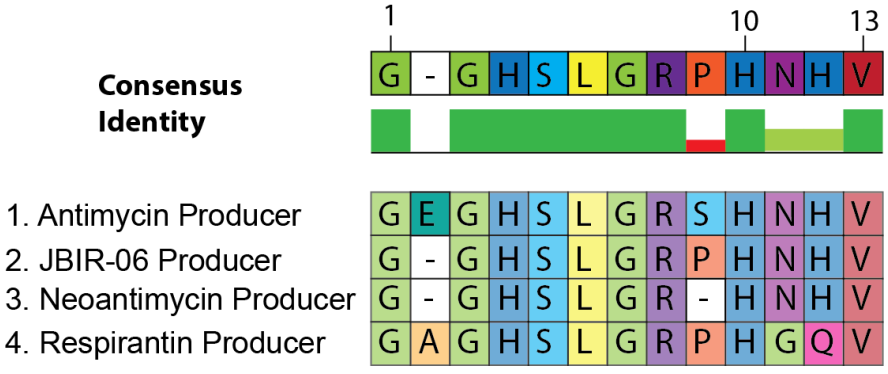

Supplemental Fig. 2.5 *Predicted conserved amino acid sequence of acyltransferases.*

2.9.2 NMR and Mass Spectra for Structural Elucidation

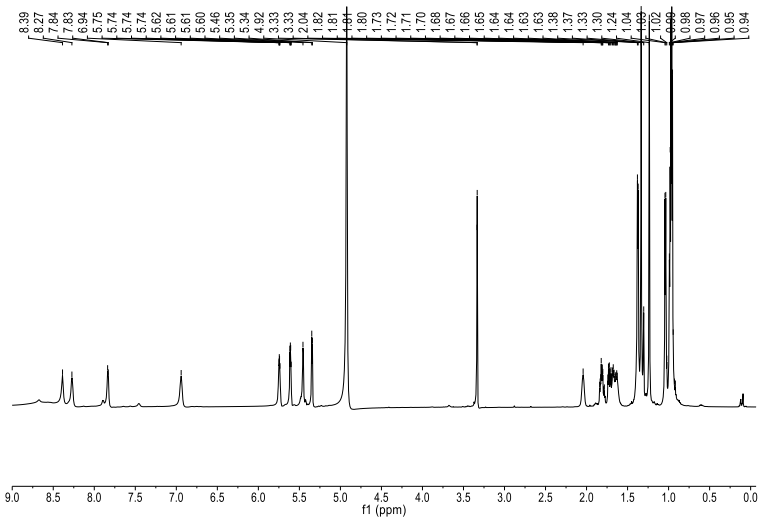

Supplemental Fig. 2.6 *^{1}H NMR spectrum of JBIR-06.*

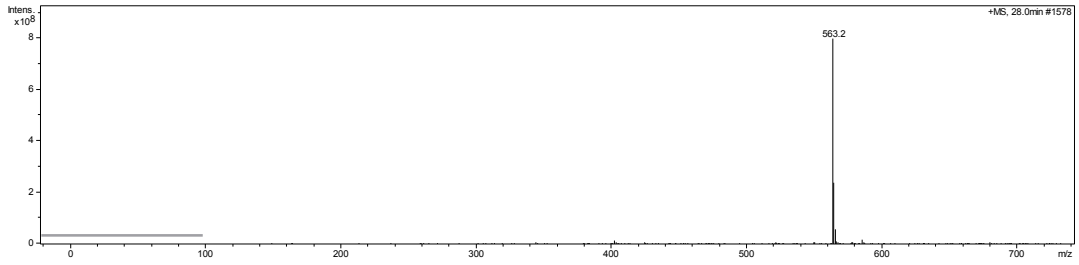

Supplemental Fig. 2.7 *MS spectrum of JBIR-06.*

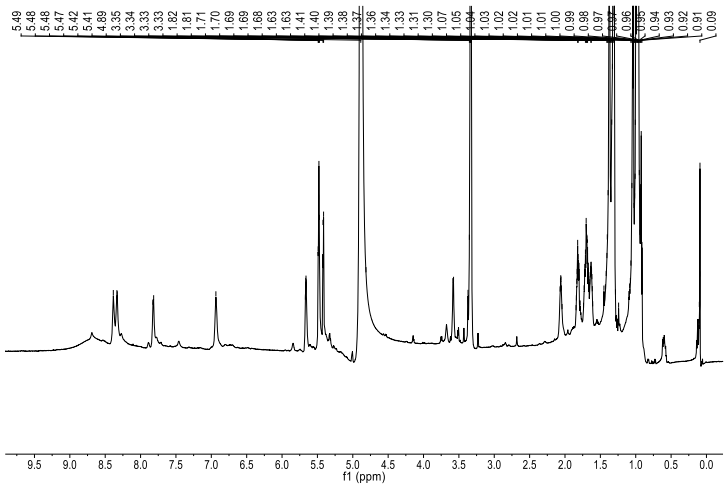

Supplemental Fig. 2.8 *^{1}H NMR spectrum of JBIR-52.*

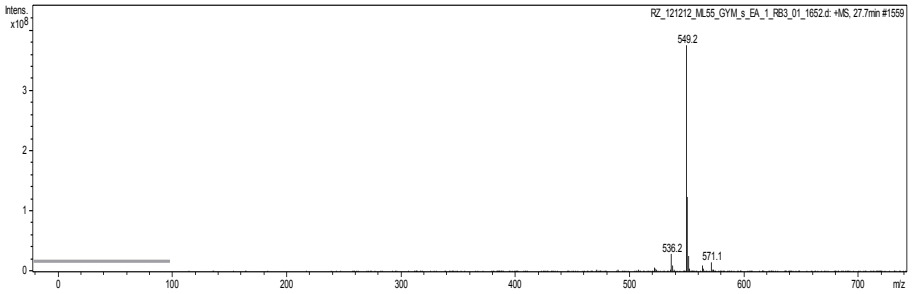

Supplemental Fig. 2.9 *MS spectrum of JBIR-52.*

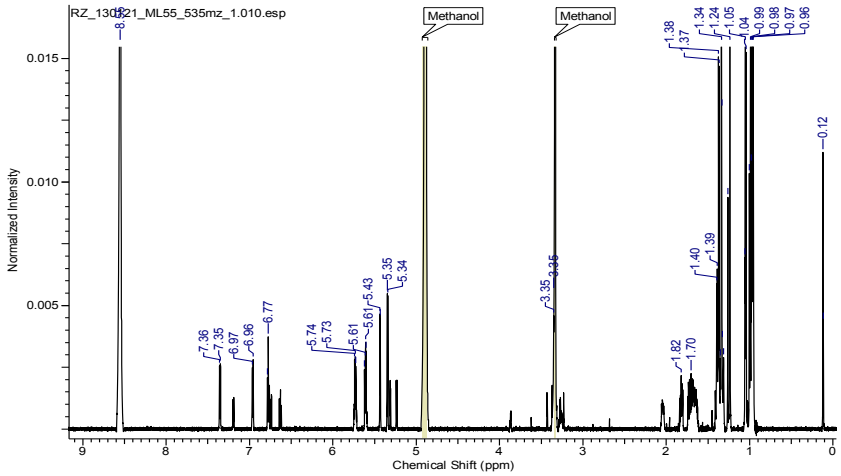

Supplemental Fig. 2.10 *^{1}H NMR spectrum of compound JBIR-06-1.*

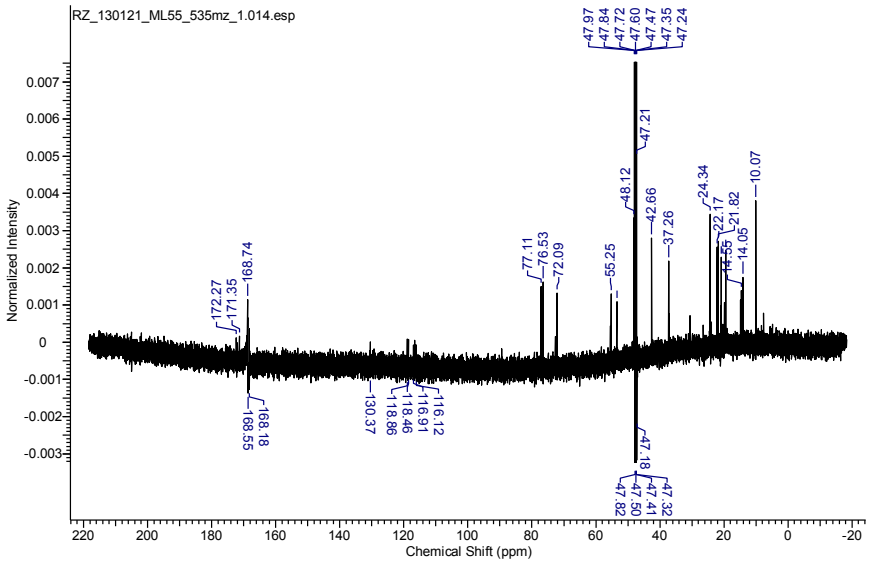

Supplemental Fig. 2.11 *^{13}C NMR spectrum of compound JBIR-06-1.*

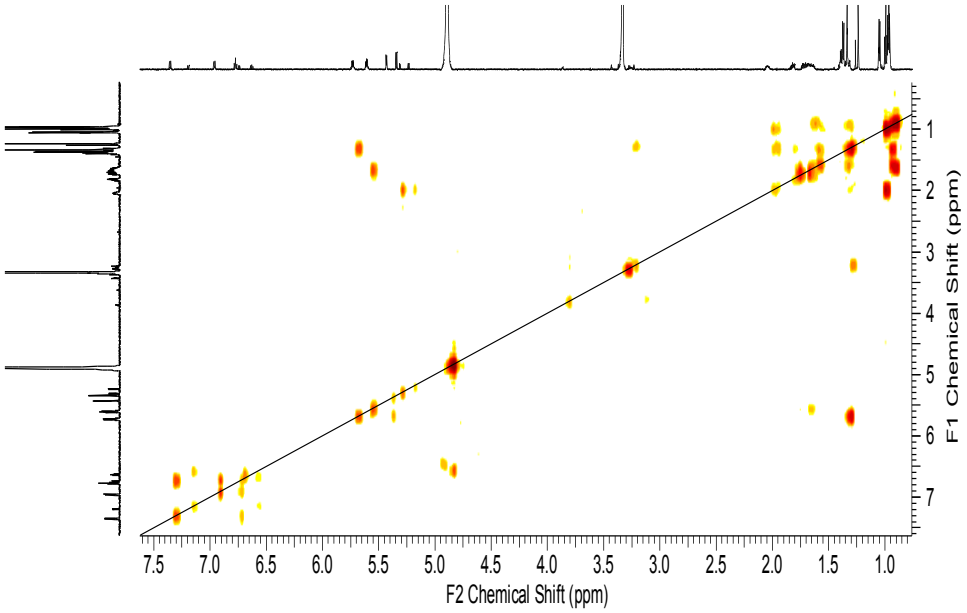

Supplemental Fig. 2.12 *^{1}H-^{1}H COSY spectrum of compound JBIR-06-1.*

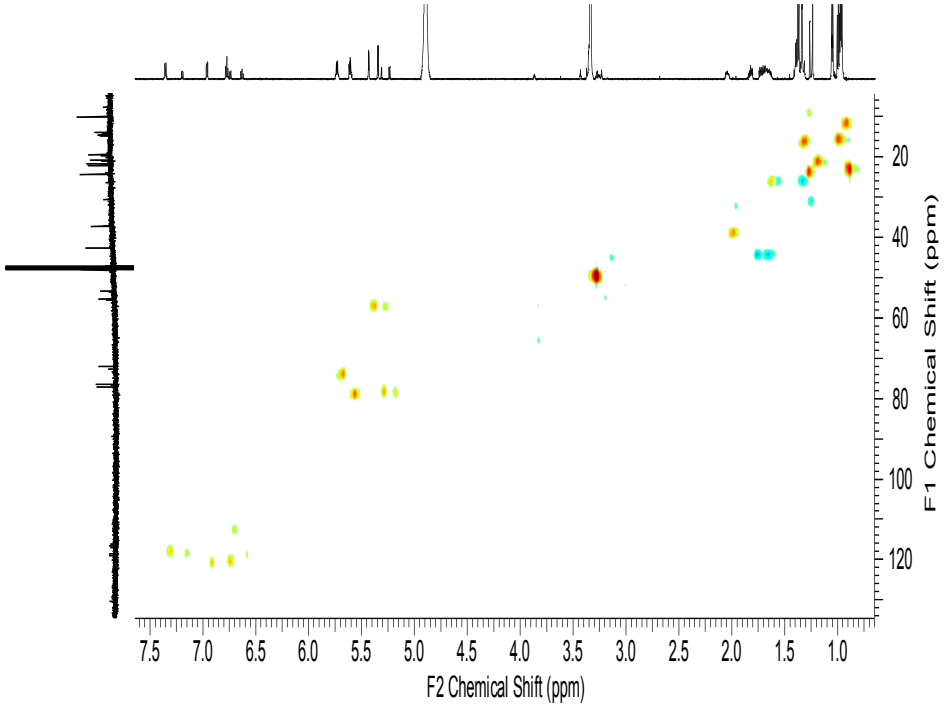

Supplemental Fig. 2.13 *HMQC spectrum of compound JBIR-06-1.*

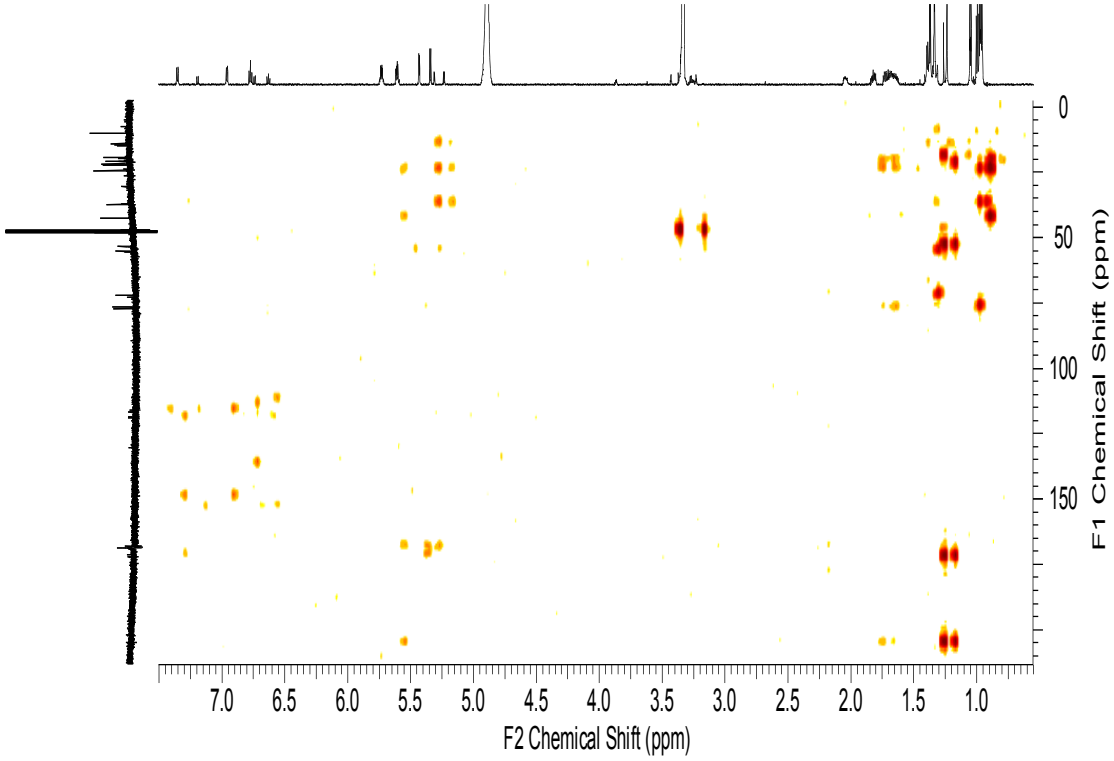

Supplemental Fig. 2.14 *HMBC spectrum of compound JBIR-06-1.*

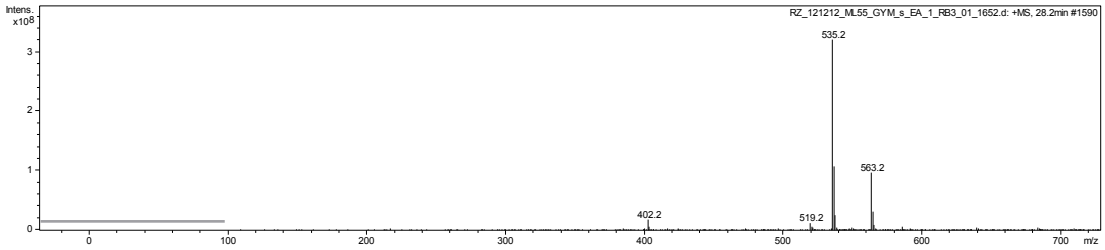

Supplemental Fig. 2.15*MS spectrum of JBIR-06-01.*

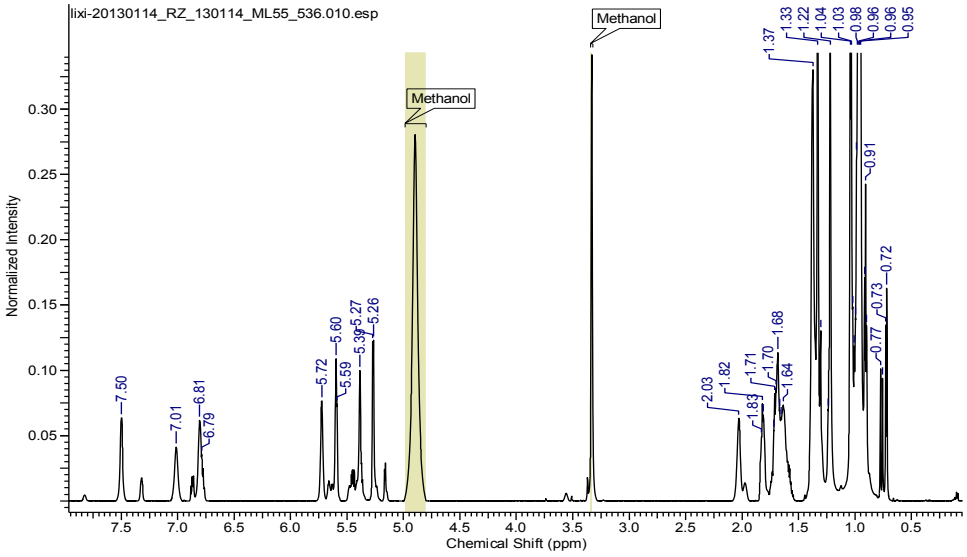

Supplemental Fig. 2.16 *^{1}H NMR spectrum of compound JBIR-06-2.*

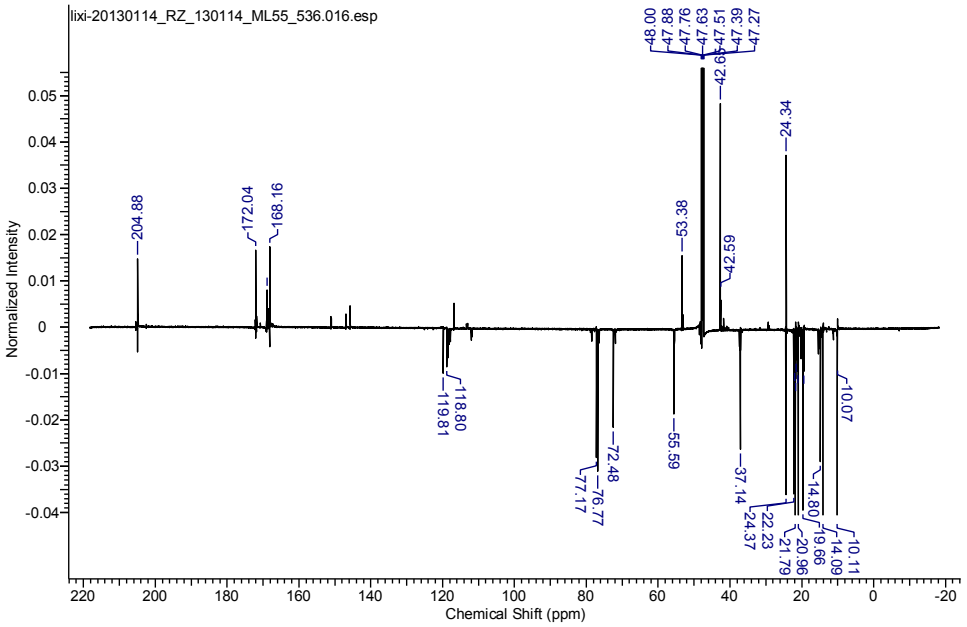

Supplemental Fig. 2.17 *^{13}C NMR spectrum of compound JBIR-06-2.*

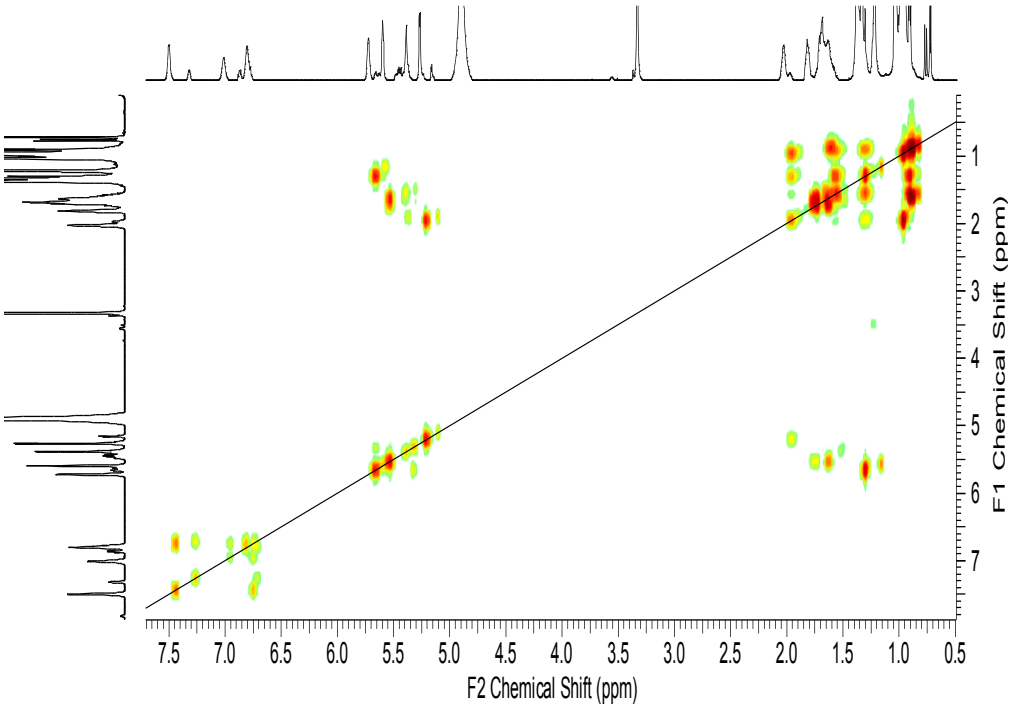

Supplemental Fig. 2.18 *^{1}H-^{1}H COSY spectrum of compound JBIR-06-2.*

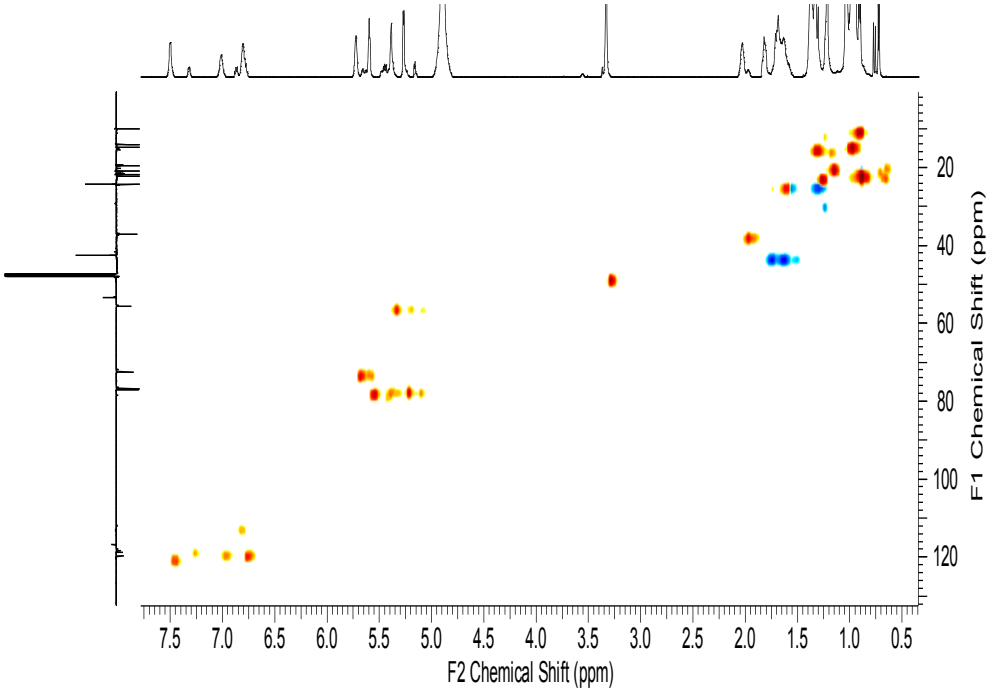

Supplemental Fig. 2.19 *HMQC spectrum of compound JBIR-06-2.*

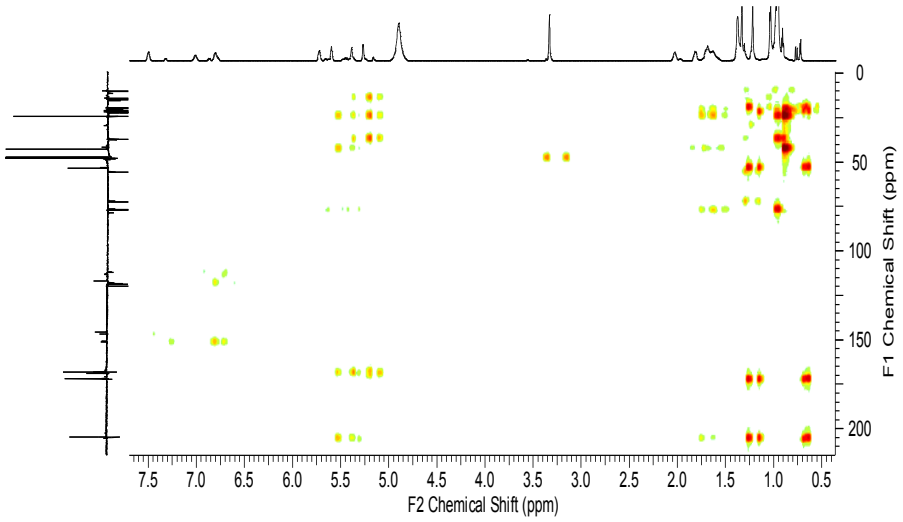

Supplemental Fig. 2.20 *HMBC spectrum of compound JBIR-06-2.*

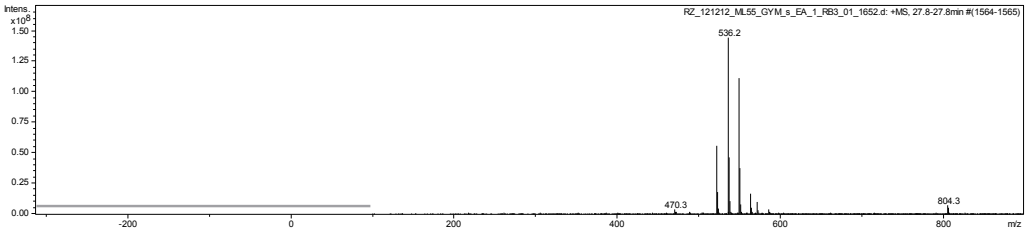

Supplemental Fig. 2.21 *MS spectrum of JBIR-06.*

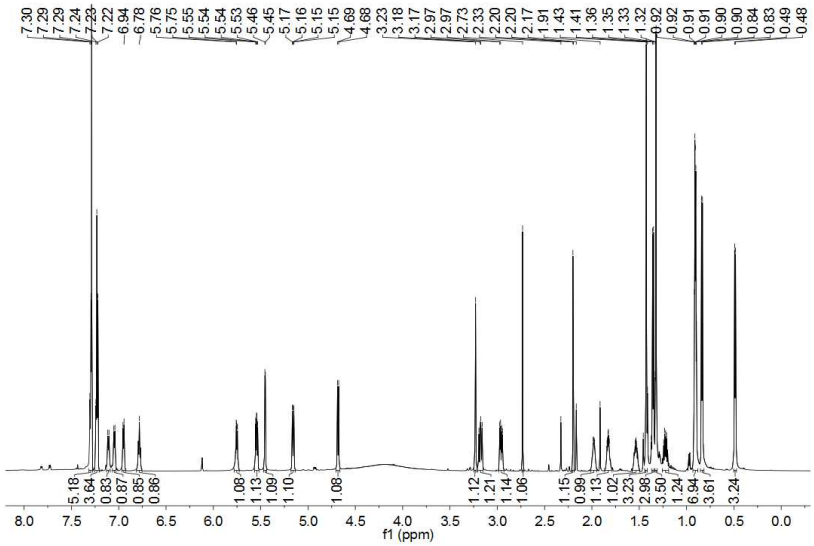

Supplemental Fig. 2.22 *^{1}H NMR spectrum of Neo-1.*

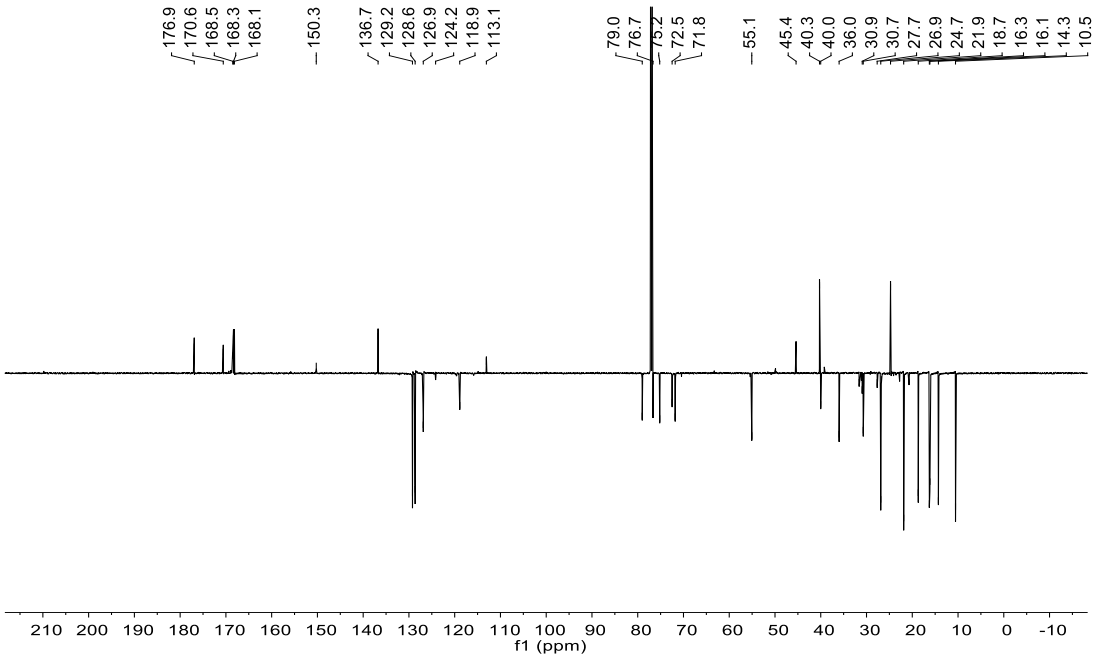

Supplemental Fig. 2.23 *^{13}C NMR spectrum of Neo-1.*

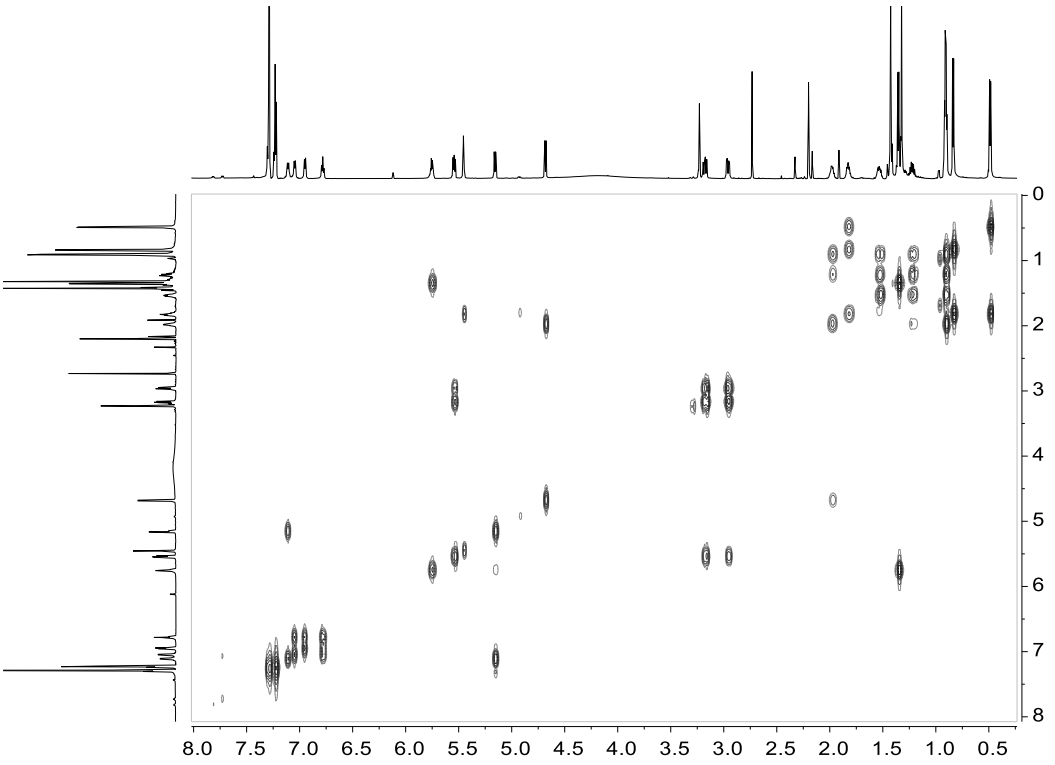

Supplemental Fig. 2.24 *^{1}H-^{1}H COSY spectrum of Neo-1.*

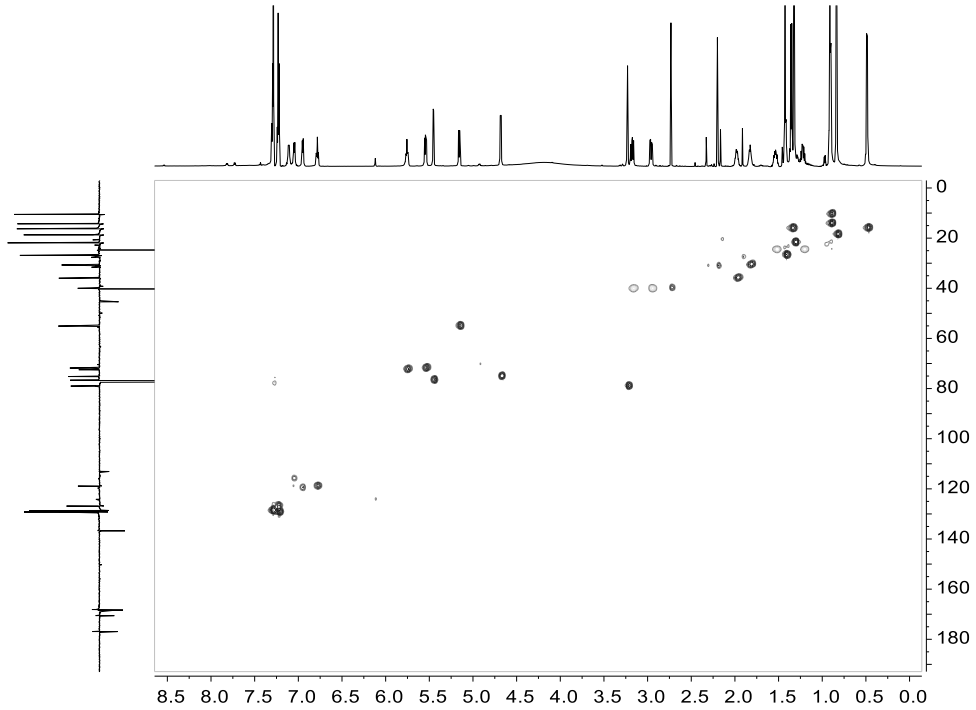

Supplemental Fig. 2.25 *^{1}H-^{13}C HMQC spectrum of Neo-1.*

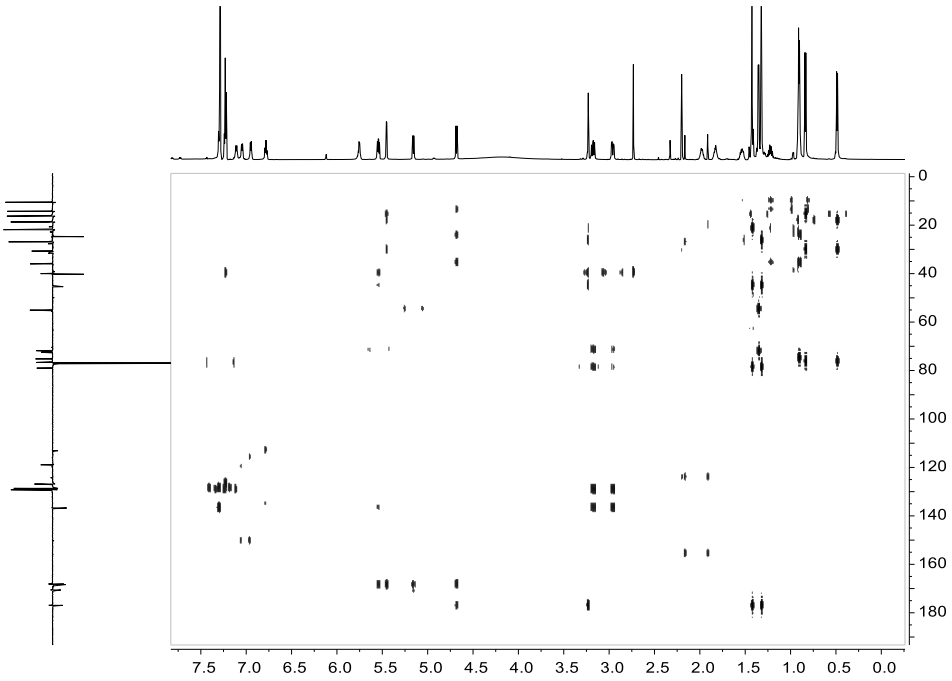

Supplemental Fig. 2.26 *^{1}H-^{13}C HMBC spectrum of Neo-1.*

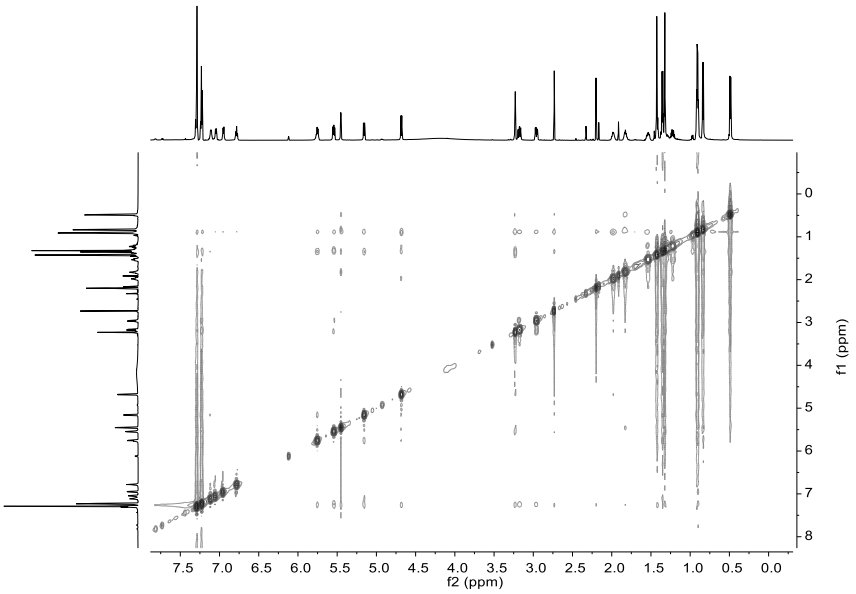

Supplemental Fig. 2.27 *^{1}H-^{1}H NOESY spectrum of Neo-1.*

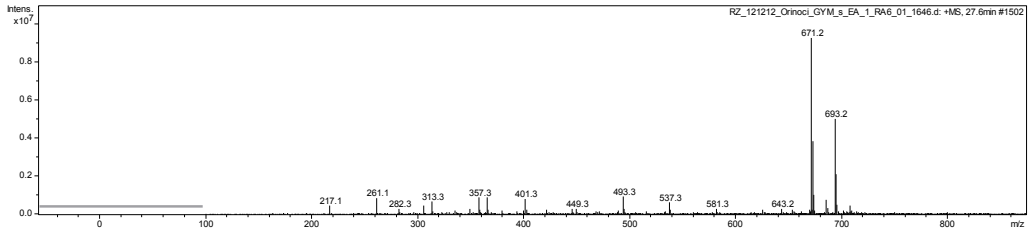

Supplemental Fig. 2.28 *MS spectrum of Neo-1.*

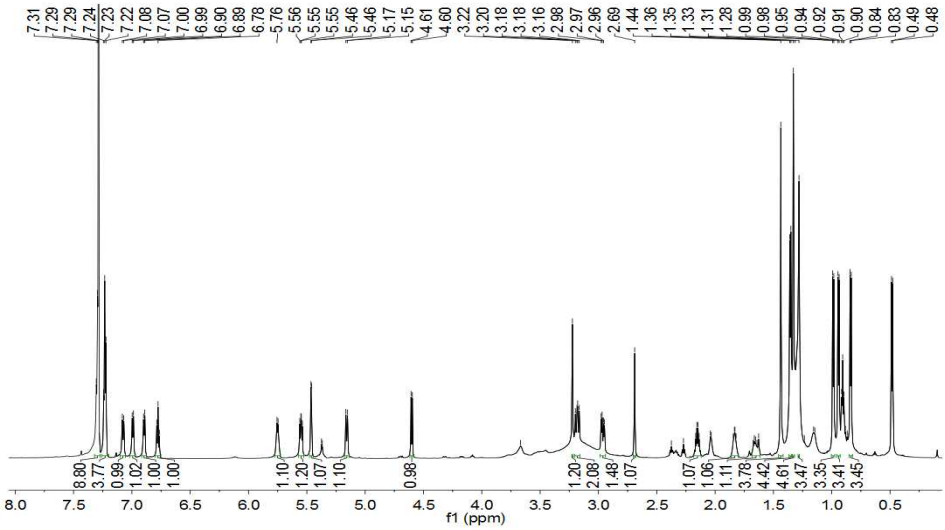

Supplemental Fig. 2.29 *^{1}H NMR spectrum of Neo-2.*

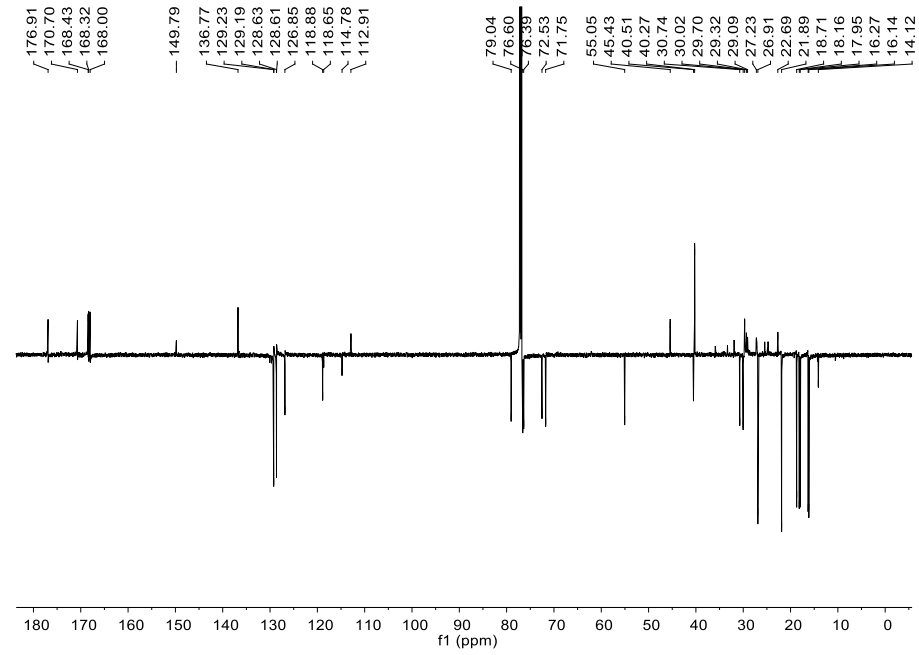

Supplemental Fig. 2.30 *^{13}C NMR spectrum of Neo-2.*

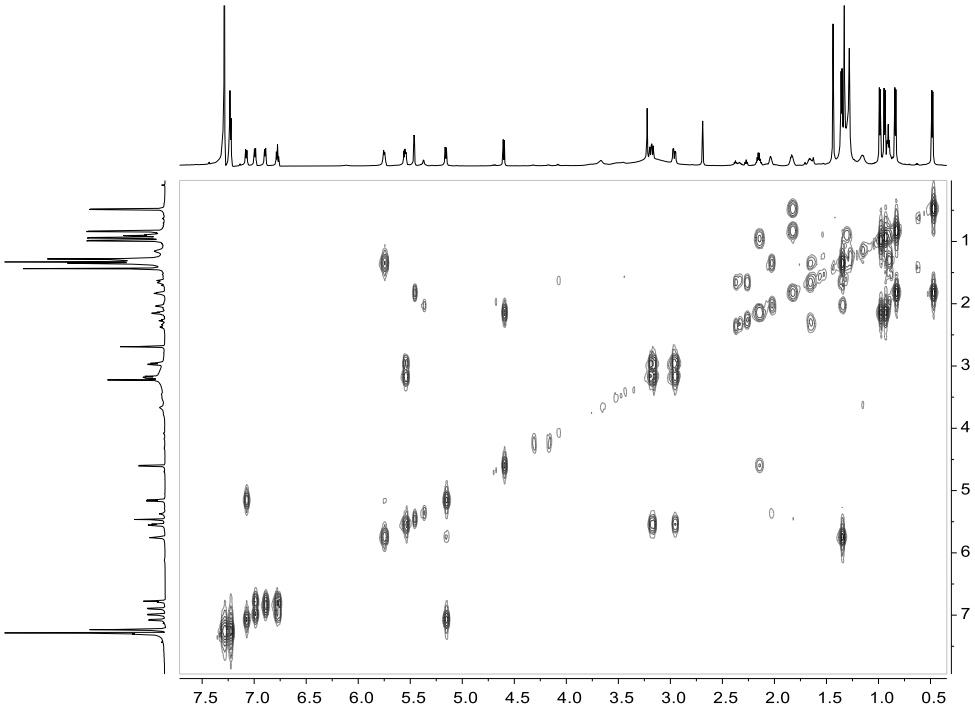

Supplemental Fig. 2.31 *^{1}H-^{1}H COSY spectrum of Neo-2.*

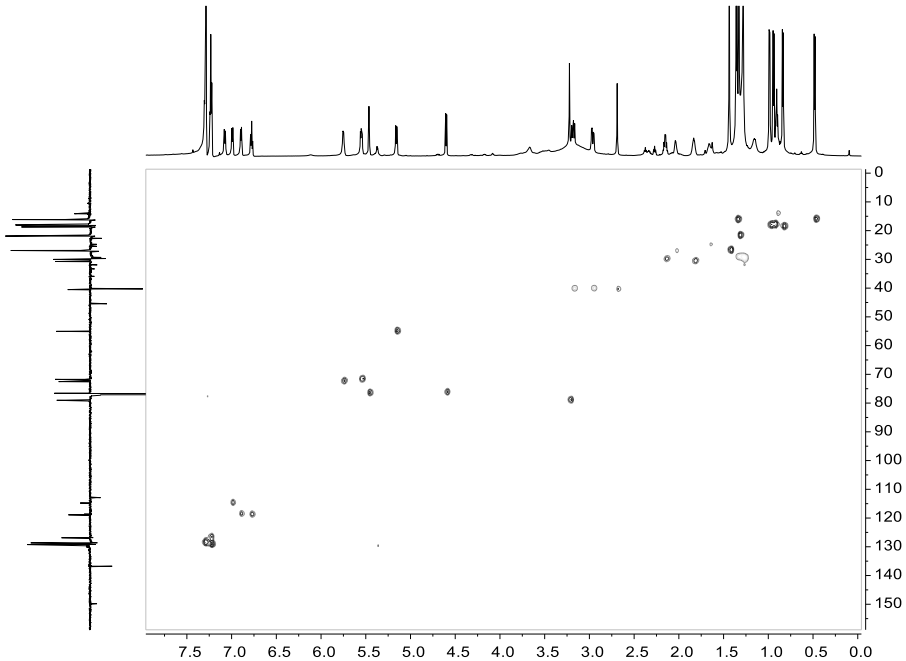

Supplemental Fig. 2.32 *^{1}H-^{13}C HMQC spectrum of Neo-2.*

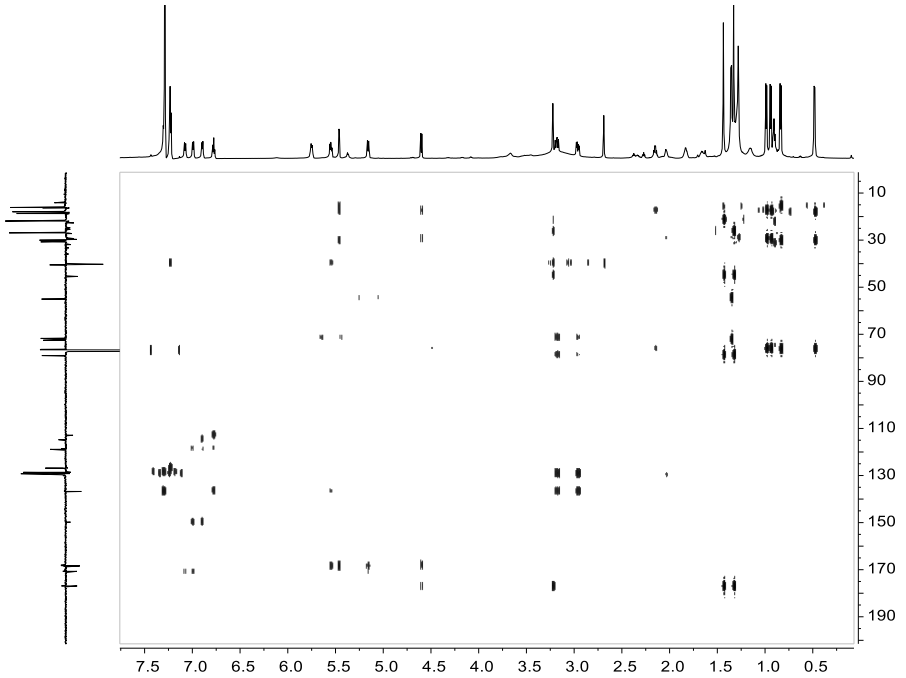

Supplemental Fig. 2..33 *^{1}H-^{13}C HMBC spectrum of Neo-2.*

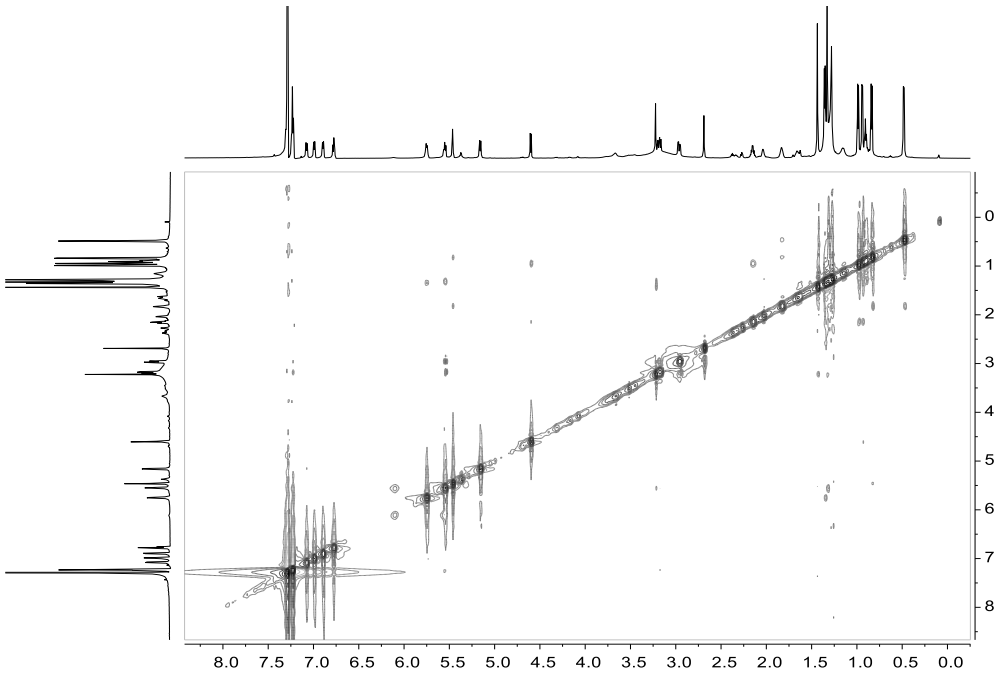

Supplemental Fig. 2.34 *^{1}H-^{1}H NOESY spectrum of Neo-2.*

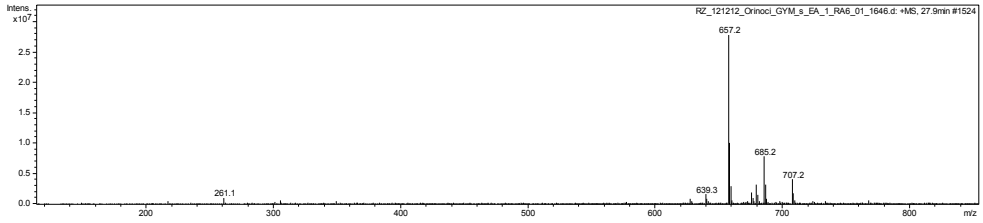

Supplemental Fig. 2.35 *MS spectrum of Neo-2.*

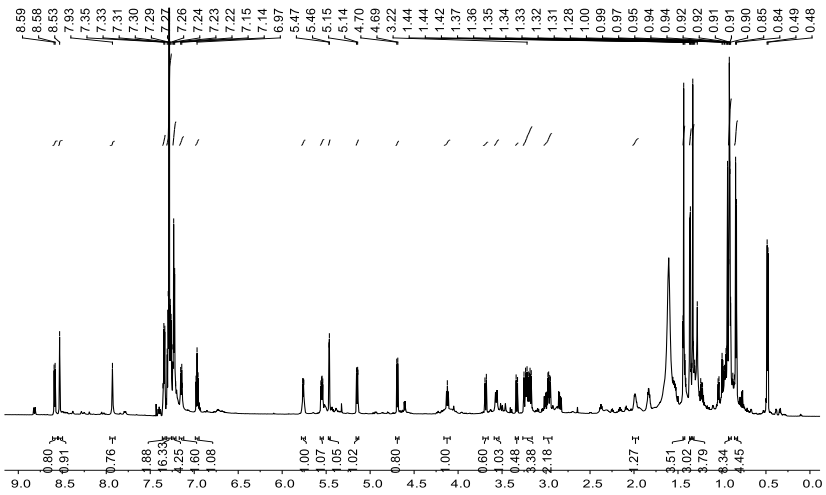

Supplemental Fig. 2.36 *^{1}H NMR spectrum of Neo-3.*

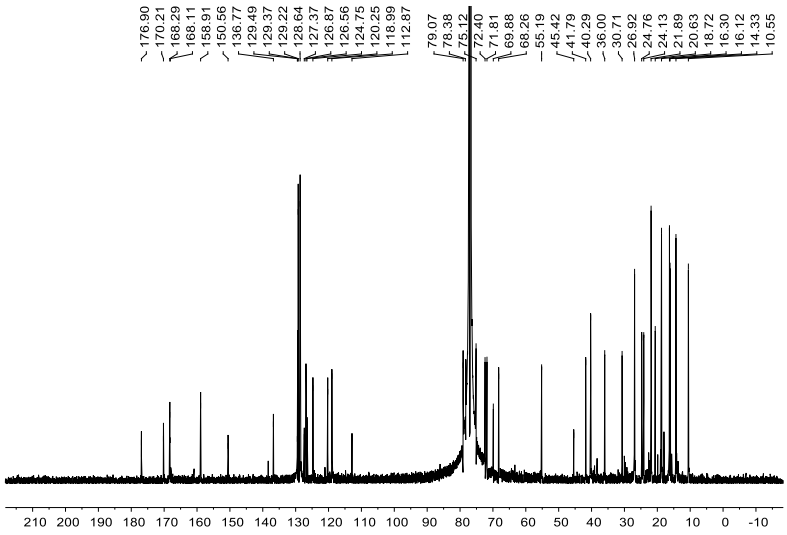

Supplemental Fig. 2.37 *^{13}C NMR spectrum of Neo-3.*

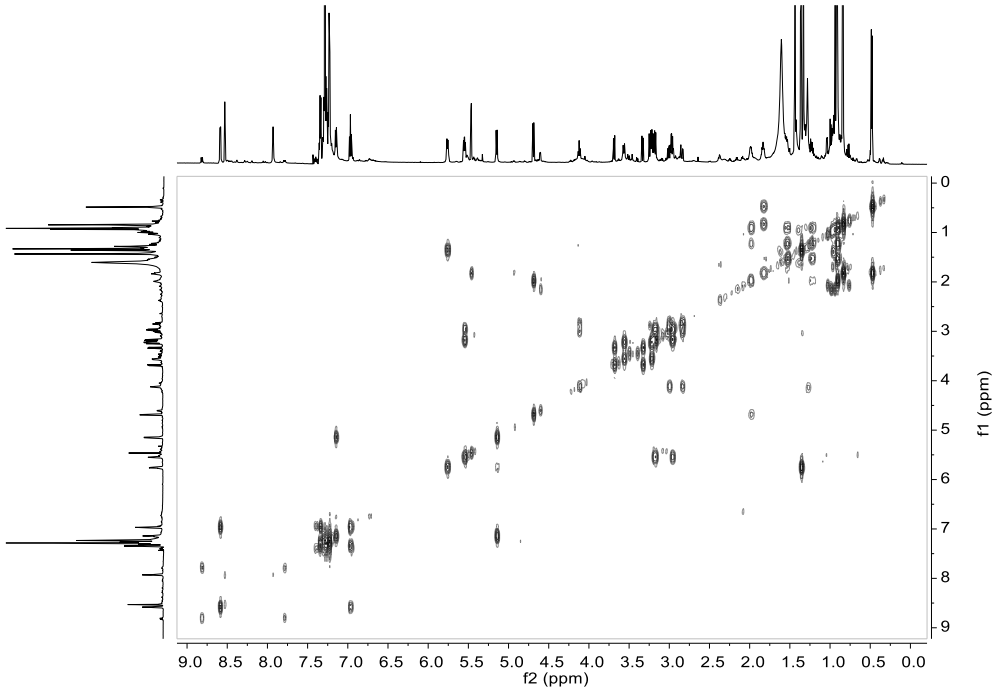

Supplemental Fig. 2.38 *^{1}H-^{1}H COSY spectrum of Neo-3.*

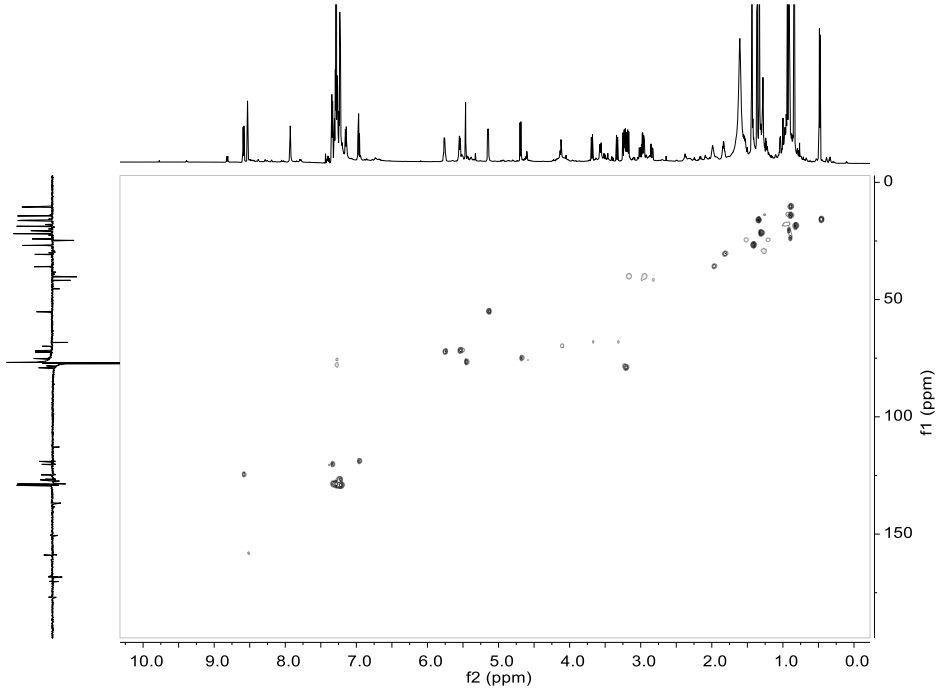

Supplemental Fig. 2.39 *^{1}H-^{13}C HMQC spectrum of Neo-3.*

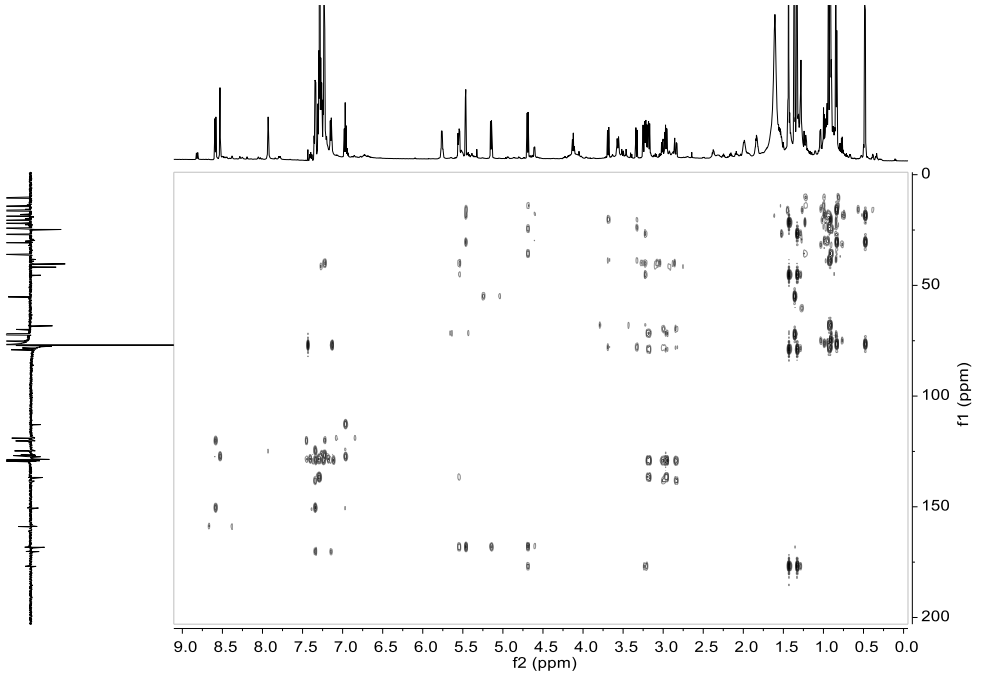

Supplemental Fig. 2.40 *^{1}H-^{13}C HMBC spectrum of Neo-3.*

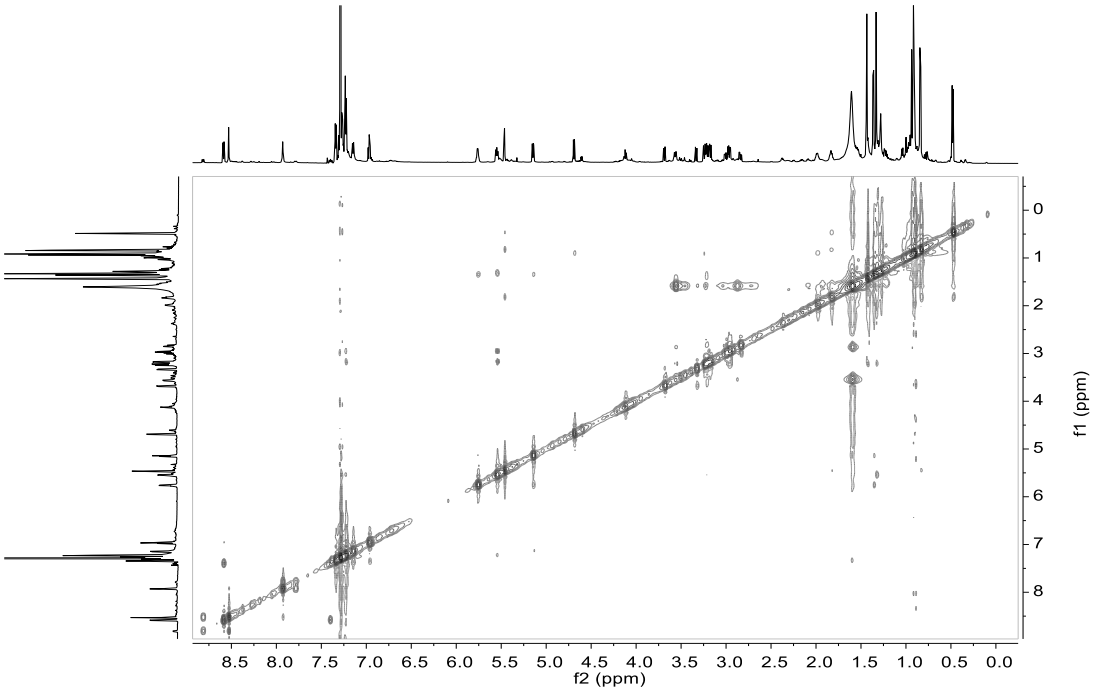

Supplemental Fig. 2.41 *^{1}H-^{1}H NOESY spectrum of Neo-3.*

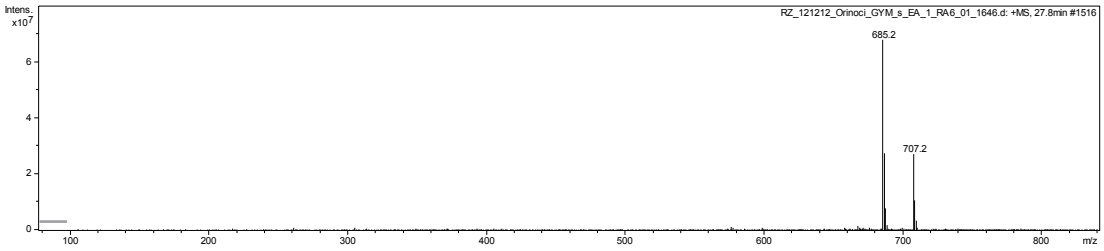

Supplemental Fig. 2.42 *MS spectrum of Neo-3.*

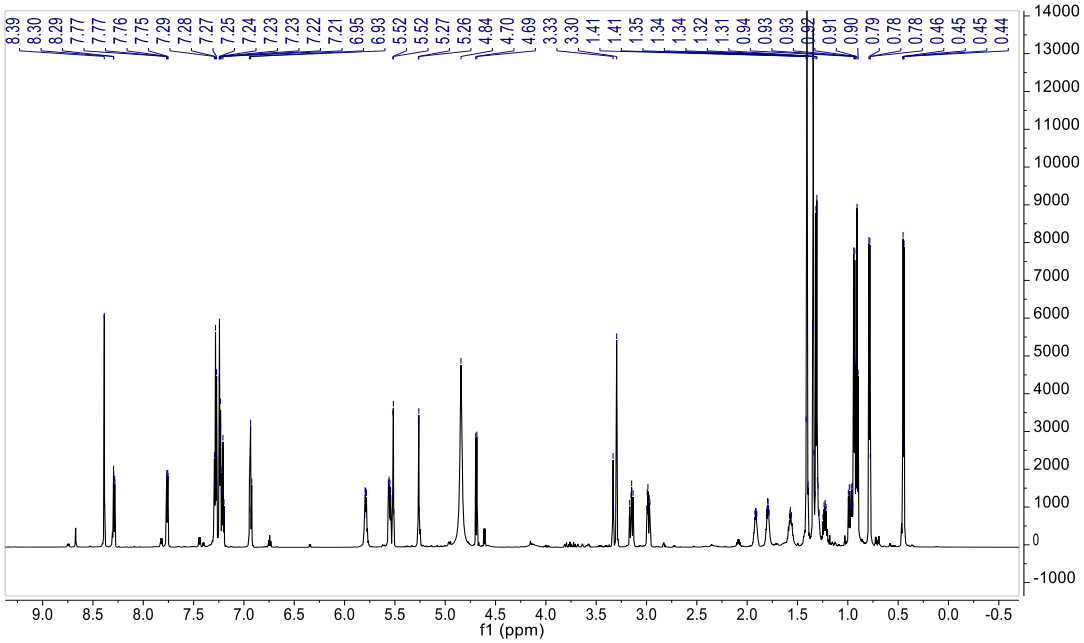

Supplemental Fig. 2.43 *^{1}H NMR spectrum of Neo-4.*

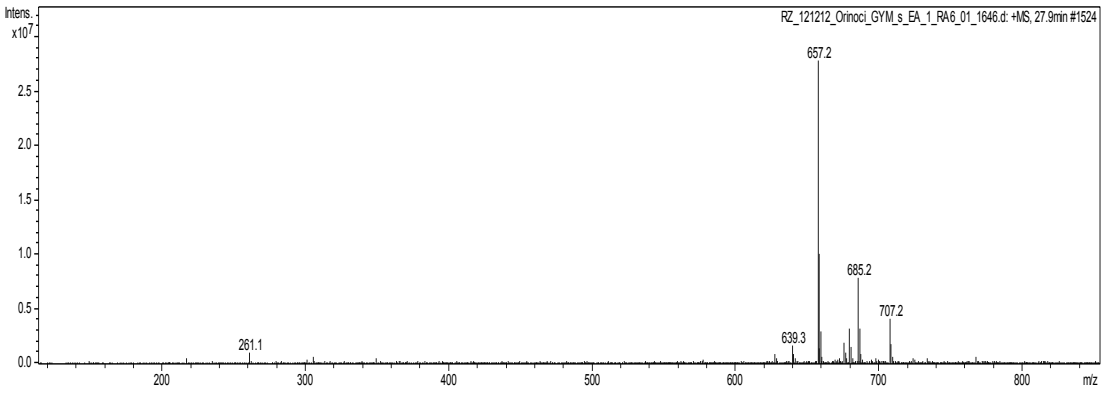

Supplemental Fig. 2.44 *MS spectrum of Neo-4.*

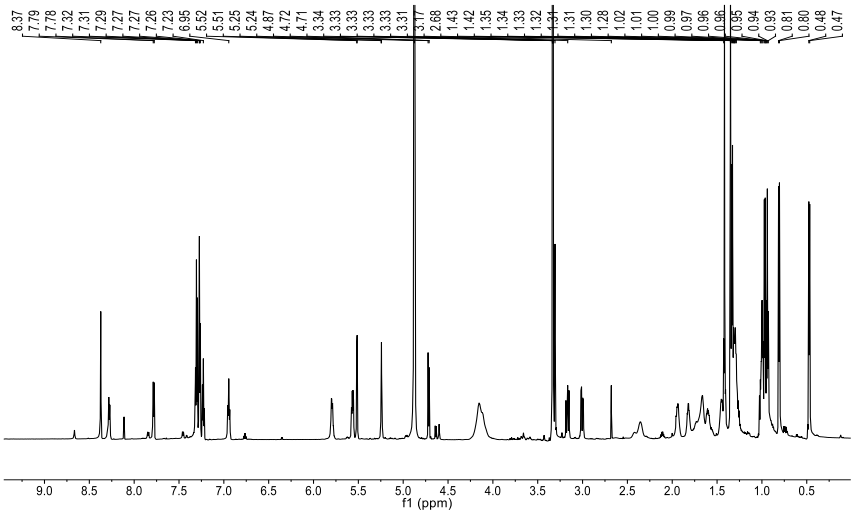

Supplemental Fig. 2.45 *^{1}H NMR spectrum of Neo-5.*

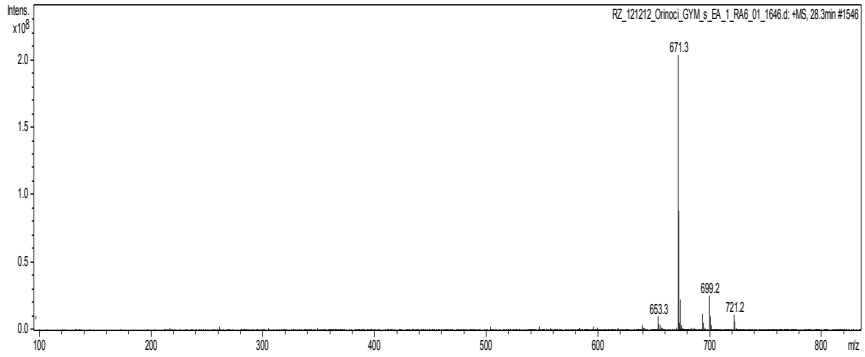

Supplemental Fig. 2.46 *MS spectrum of Neo-05.*

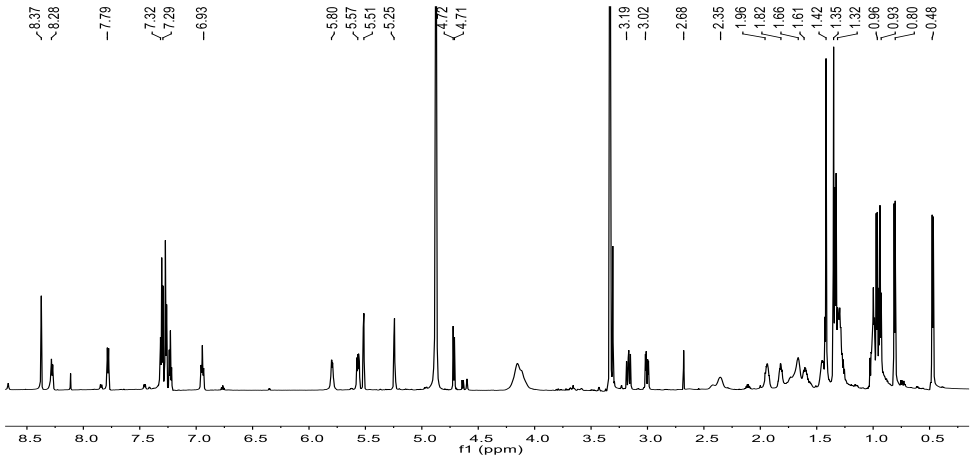

Supplemental Fig. 2.47 *^{1}H NMR spectrum of Neo-6.*

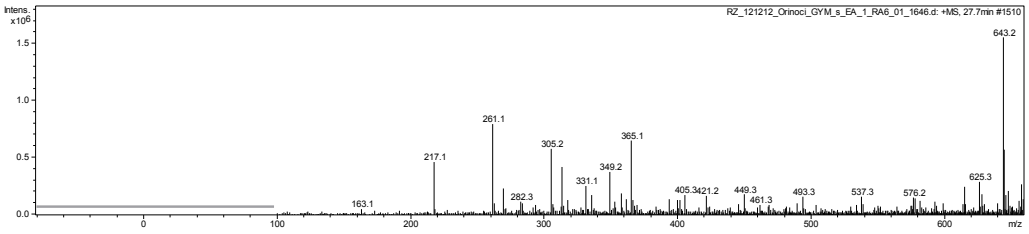

Supplemental Fig. 2.48 *MS spectrum of Neo-6.*

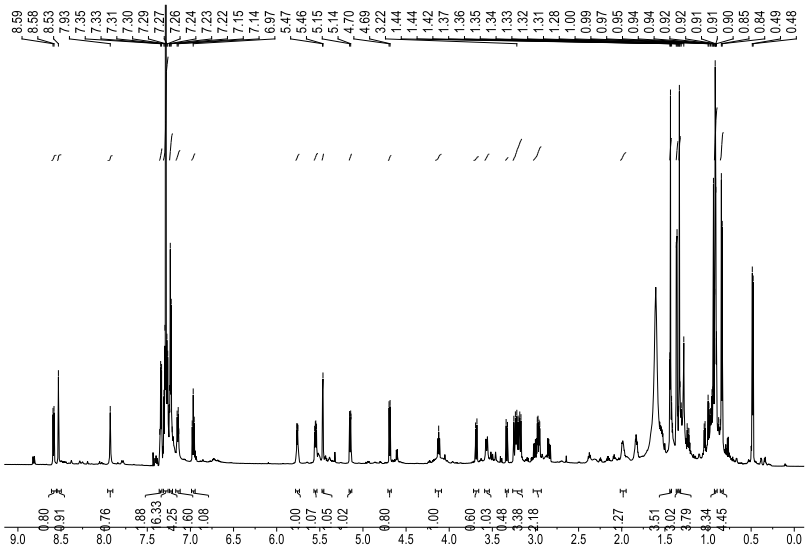

Supplemental Fig. 2.49 *^{1}H NMR spectrum of Neo-7.*

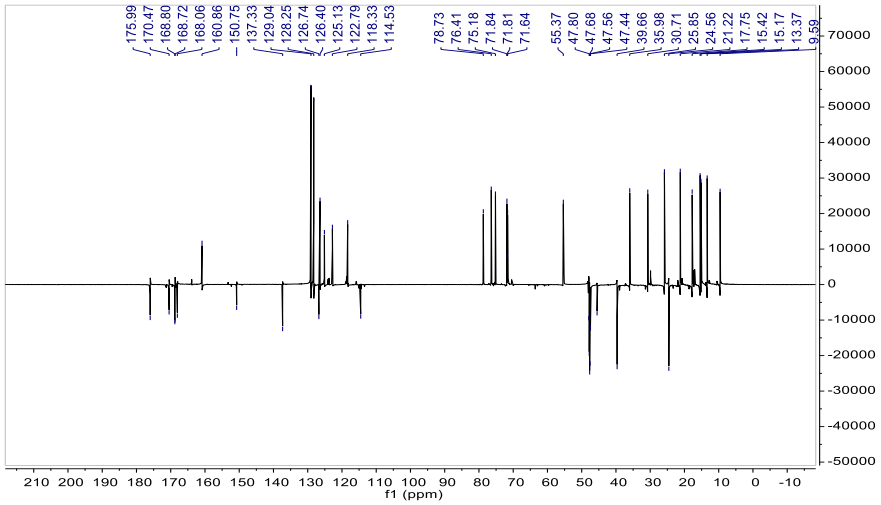

Supplemental Fig. 2.50 *^{13}C NMR spectrum of Neo-7.*

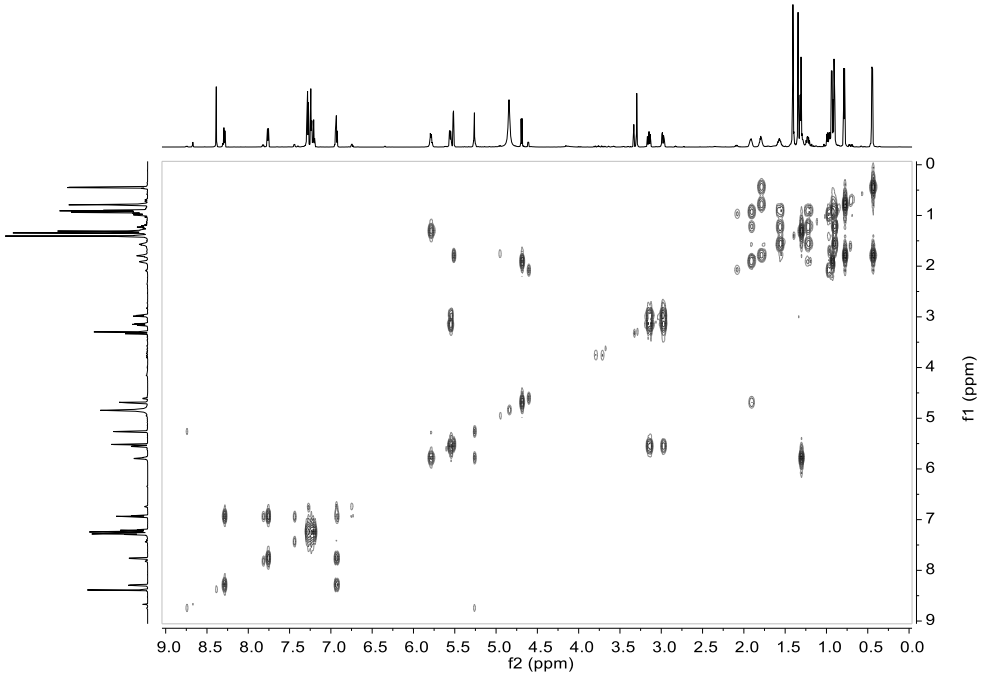

Supplemental Fig. 2.51 *^{1}H-^{1}H COSY spectrum of Neo-7.*

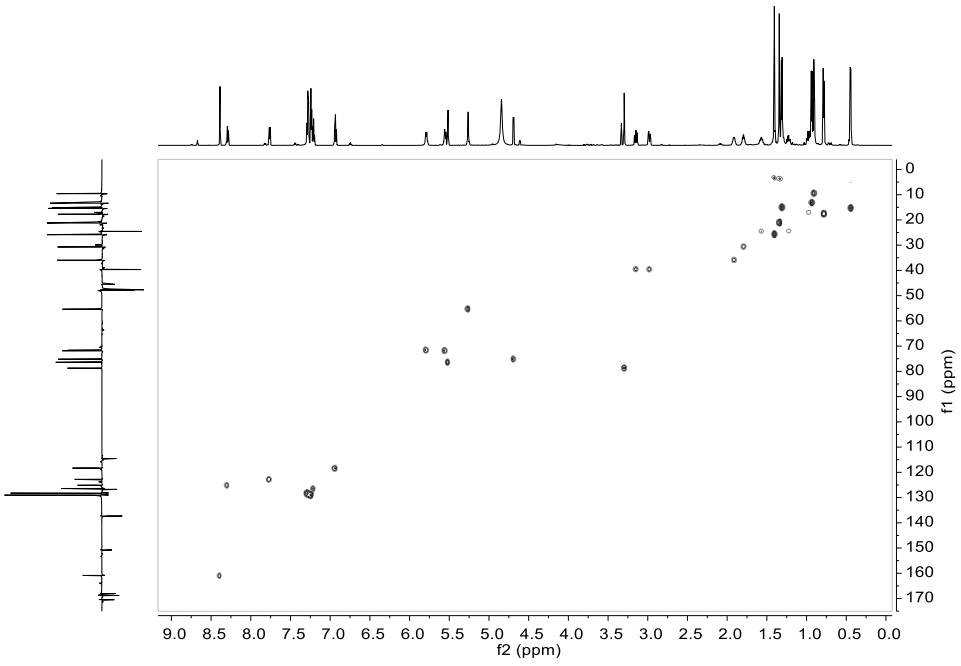

Supplemental Fig. 2.52 *^{1}H-^{13}C HMQC spectrum of Neo-7.*

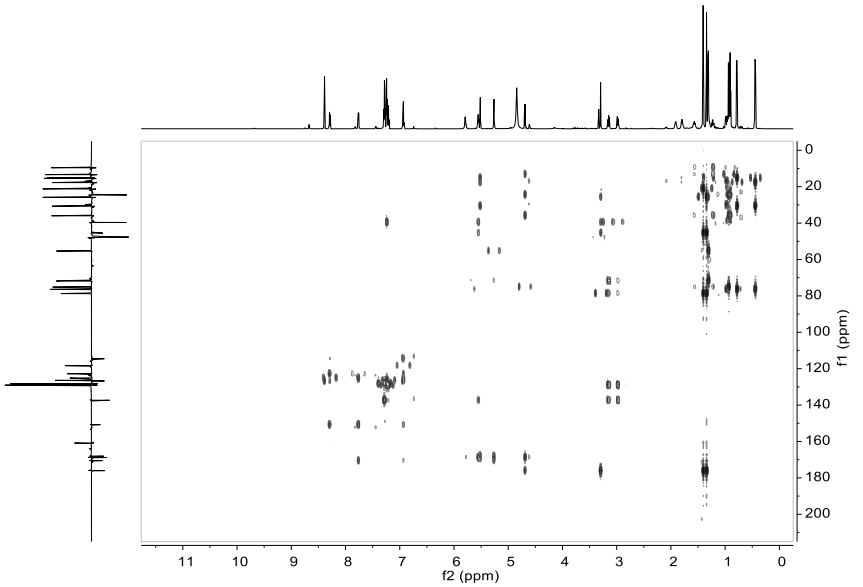

Supplemental Fig. 2.53 *^{1}H-^{13}C HMBC spectrum of Neo-7.*

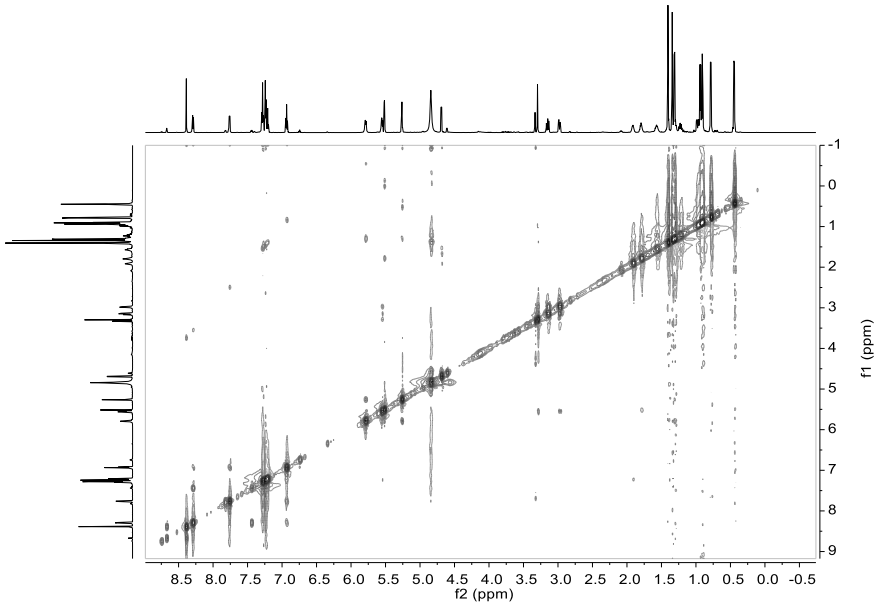

Supplemental Fig. 2.54 *^{1}H-^{1}H NOESY spectrum of Neo-7.*

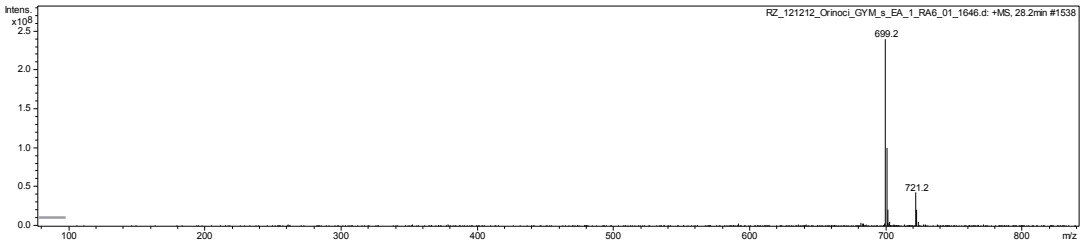

Supplemental Fig. 2.55 *MS spectrum of Neo-7.*

Chapter 3. The Site-Selective Generation of Antibody-Drug Conjugates Using Phosphopantetheinyl Transferases

3.1 Chapter Preface

With a better comprehension of how natural assembly line evolution occurs, synthetic efforts to manipulate assembly lines to yield targets with diversified and multiple activities toward cellular targets up-regulated in cancer may be more successful. However, even though natural products affect divergent eukaryotic cellular targets, they did not evolve within the context of humans and therefore a means to deliver them specifically to cancer cells and avoid healthy cells is required (Fig. 3.1). This chapter outlines the work done to develop an improved methodology for the attachment of small molecules to antibodies, which act as a cancer cell-honing tool. Here I establish in a preliminary manner a novel biosynthetic enzymatic technique, using phosphopantetheinyl transferases, for the site-specific and efficient loading of small molecules onto antibodies. Moreover, I begin to explore the natural ability of these enzymes to selectively load multiple unique molecules onto an antibody for the future generation of antibody-drug conjugates that deliver several natural products directly to cancer cells and attack these

cells via diverse cellular targets.

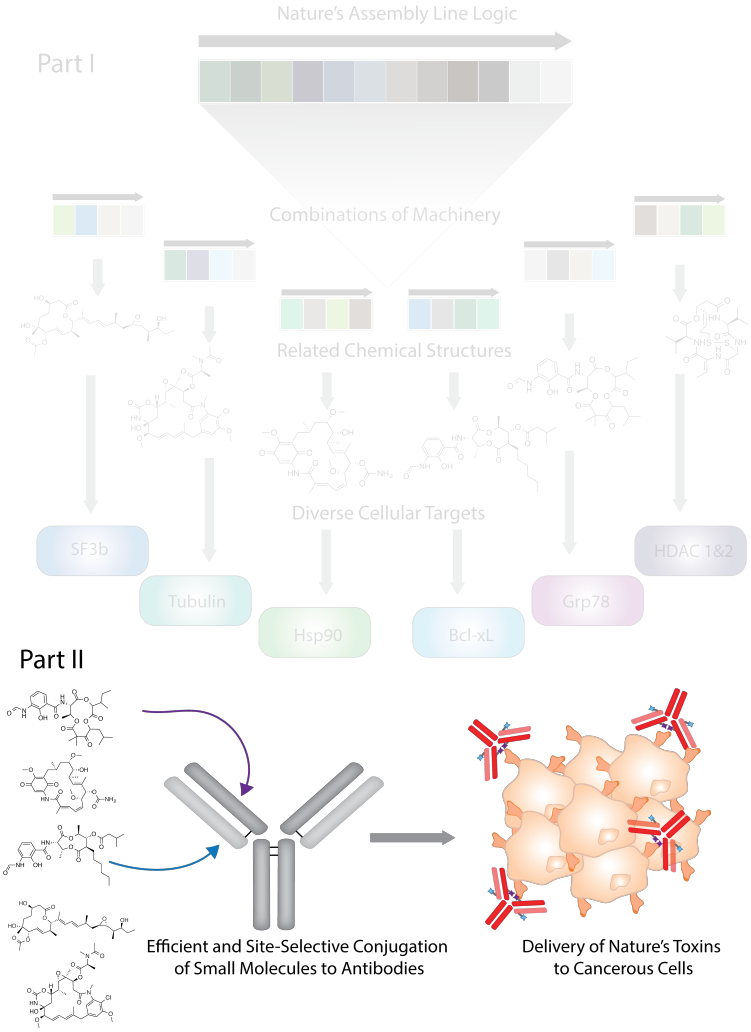

Fig. 3.1 *Chapter 3 overview. The highlighted portion indicates the topics that are specifically addressed in this thesis chapter. Antibody-drug conjugates (ADC) provide a means to deliver natural products directly to cancer cells that have overexpressed cell membrane markers, enhancing their potential as chemotherapeutics. However, there remains a need for robust and reproducible techniques that site-selectively add single and multiple molecules to antibodies for the generation of antibody-drug conjugates. This thesis chapter addresses this need through the development of a technique using natural product enzymology that can generate site-specific antibody-drug conjugates and can offer a degree of*

stoichiometric- and site-selectivity when loading uniquely functioning small molecules onto an antibody for polytherapy ADCs.

I was responsible for this work in its entirety except for the following specified portions. The synthesis of the podophyllotoxin-PMPI was done with the assistance of Robert Gale. The sequence and expression vector for the Parent J Fab and Fab purification protocol was provided by the Sidhu laboratory at the University of Toronto. The binding study was performed at the University of Toronto by Dr. Shane Miersch. All other work was performed under the supervision and guidance of Dr. Nathan Magarvey.

This chapter is formatted for journal publication and therefore the references directly follow this body of work.

3.2 Introduction

There is a vast catalogue of synthetic and natural product toxins structurally primed to kill cancerous cells, but many traditional chemotherapies often fail in clinical trials or clinical care.[1,2] This is due largely to the severe off-target activities of these drugs providing very narrow therapeutic windows. However, small molecule natural products (or their semisynthetic derivatives) and antibodies *together* exhibit high levels of chemotherapeutic complementarity. In several instances they have been jointly administered or linked specifically to create antibody-drug conjugates (ADC). Linking complex natural product toxins, with diverse cancer cell killing properties (tubulin, actin and DNA damaging), to antibodies with selectivity to epitopes characteristically overexpressed on cancerous cells provides a promising approach for delivering toxic

agents specifically to a diseased site (Fig. 3.2A).[3,4] Key examples include FDA approved brentuximab vedotin (Adcetris) with monomethyl auristatin E (a derivative of the natural product dolastatin 10) tethered to an anti-CD30 antibody for the treatment of Hodgkin's lymphoma, and ado-trastuzumab emtansine (Kadcyla) with mertansine (a derivative of the natural product maytansine) tethered to an anti-HER2+ antibody for the treatment of metastatic breast cancer.[5-6]

Despite the initial clinical success of this therapeutic class, significant challenges arose with ADC synthesis technology, particularly in the realm of their controlled formation. Original efforts to generate ADCs exploited the nucleophilic side chains of native amino acid residues, including lysine and interchain disulfide bridge forming cysteines. Synthetic techniques, such as these, yield hugely diverse drug populations with varied drug-to-antibody ratios, typically ranging from 1-8 drugs loaded per antibody, and also numerous isomeric species. Drug variation, referring to the number of small molecules loaded and the location of these small molecules, is highly problematic as it impacts ADCs' efficacy, safety, pharmacokinetic and pharmacodynamic profiles. Without methods of standardization, it is extremely challenging to determine the appropriate dosage for patients and can ultimately compromise their treatment outcome and health. As a result, designing novel site-selective methods for the generation of homogeneous antibody-drug conjugates is an area of significant interest (Fig. 3.2B).[8-12]

State-of-the-art techniques include controlled synthesis using interchain disulfide bonds (reduction-alkylation strategy), the incorporation of new cysteines (THIOMAB) or unnatural amino acids for site-selective loading, and the utilization or integration of

amino acid sequences specific for enzymatic transfer (Fig. 3.2B).[8,13-17] Although these methods generate superior ADCs, weaknesses persist. For example, techniques relying upon cysteine thiol chemistry (reduction-alkylation, cysteine to serine and THIOMAB) tend to generate heterogeneous species. Furthermore, these methods can result in compromised structural integrity of the antibody and consequently altered pharmacokinetic and pharmacodynamic properties.[8,13,18-22] Unnatural amino acids offer highly specific loading methods, but may lead to immunogenicity and the scalability of these processes pose a critical difficulty (Fig 3.2C).[14,15,17,23] Enzymatic transfer methods, such as transglutaminases, have shown particular promise as easily up-scalable methods that yield homogenous ADCs.[14,16] However, these enzymatic classes, in addition to other site-selective techniques, are limited in their capacity to specifically load numerous structurally diverse small molecules that function via unique mechanisms onto a single antibody construct.

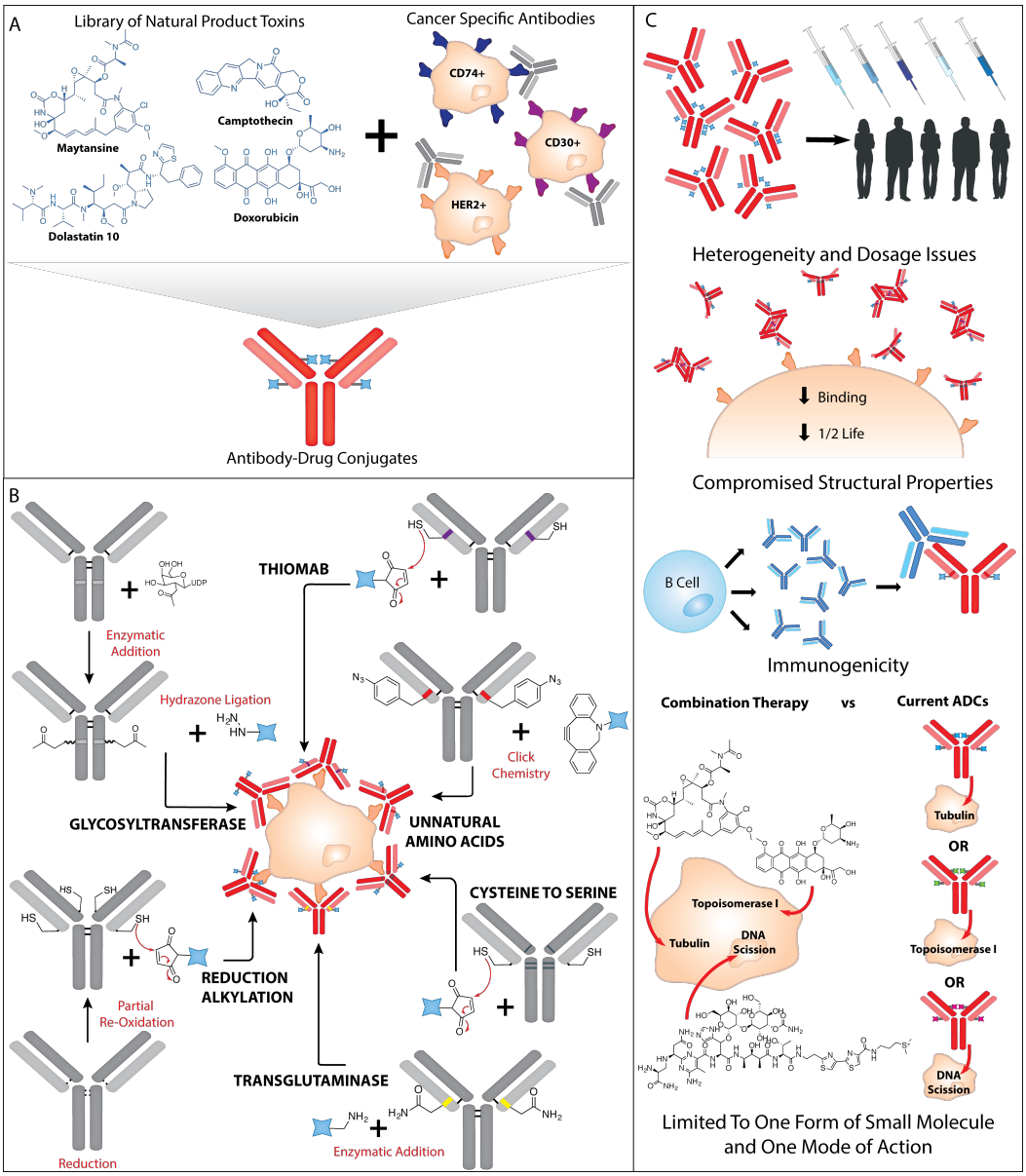

Fig. 3.2 *Overview of the current state of antibody-drug conjugates and their generation technologies.* ***(A)*** *Nature is a rich resource for toxins and many of these natural products are being linked to cancer specific antibodies to generate antibody-drug conjugates, an up-and-coming field of targeted cancer therapy. Semisynthetic derivatives of maytansine and dolastatin 10 are used in clinical ADCs tethered to anti-HER2*

and anti-CD30 monoclonal antibodies. Doxorubicin tethered to an anti-CD74 mAb and a semisynthetic derivative of camptothecin tethered to anti-carcinoembryonic antigen are examples of some of the numerous ADCs currently in clinical trial. ***(B)*** *Heterogeneous ADC populations are inadmissible in the clinic, because heterogeneity alters their overall properties and poses dosing problems. Depicted are the controlled methods that have been developed for the generation of homogeneous ADCs, including both synthetic and enzymatic techniques. Part* ***(C)*** *highlights weaknesses that persist with certain site-selective techniques.*

Utilizing multiple synergistic molecules to hit diverse targets within cancerous cells delivers a more effective and toxic dose and decreases chances of resistance (Fig 3.2C). Therefore, combination chemotherapy is most often used to treat cancer in the clinic.[24-26] Consequently, it is highly desirable to have an ADC generation method that provides the ability to site-specifically load multiple small molecules with distinct modes of action onto an antibody. This approach would yield ADCs that can target cancer in a multi-pronged approach.

To address these needs we looked toward other biosynthetic enzymes responsible for the assembly of natural products, specifically bond forming group transfer enzymes such as acyltransferases, phosphopantetheinyl transferases and transpeptidases that have been studied for their promiscuity.[27-31] Phosphopantetheinyl transferases are specifically attractive as a robust, efficient and chemo- and regioselective approach for generating ADCs because they exhibit extensive substrate loading flexibility and recognize a unique amino acid sequence from that of an antibody.[28,32-35] In nature, the role of these enzymes is to activate biosynthetic assembly lines by loading the flexible phosphopantetheine from

coenzyme A (CoA) onto a specific serine residue present in peptidyl/acyl carrier proteins (80-100 amino acid residues).[28] However, the work of Jun Yin *et al.* demonstrated that phosphopantetheinyl transferases recognition site can be condensed down from 80-100 amino acids to an optimized short 12 amino acid sequence, ideal for protein tagging.[32,36] Moreover, there are a variety of phosphopantetheinyl transferases available from this class and they demonstrated that different phosphopantetheinyl transferases show preference for unique 12 amino acid sequences, providing the capacity to perform orthogonal tandem loading onto a single protein construct.[36]

Here, we designed Fab constructs, integrating phosphopantetheinyl transferase tags into the J Fab sequence, a derivative of the clinically validated HER2+ specific antibody trastuzumab used for breast cancer therapy. We demonstrated that phosphopantetheinyl transferases selectively load fluorophore-CoA molecules onto the phosphopantetheinyl transferase sites in the engineered J Fabs, providing a novel technique for the generation of homogeneous ADCs. We then verified that the amino acid tag and phosphopantetheine-small molecule modifications did not completely compromise the Fabs binding ability. Subsequently, we proceeded to synthesize a toxin-CoA conjugate for future phosphopantetheinyl transferase loading to generate a true ADC. Finally, we determined that Fabs loaded with two unique small molecules may be produced with an unprecedented degree of selectivity using two distinct phosphopantetheinyl transferases. The results of this study therefore suggest that phosphopantetheinyl transferases may offer the ability to generate homogeneous ADCs

and potentially those that target cancer cells through various pathways and can therefore generate better clinical outcomes.

3.3 Materials and Methods

3.3.1 General

LC-MS/MS data was collected using a Bruker Amazon-X ion trap mass spectrometer (ESI source, positive mode) coupled with a Dionex UltiMate 3000 HPLC system for analytical separations. Samples were run on a Luna 5 μm C18(2) 100Å Phenomenex 150x4.6mm column for 3 minutes at 5% ACN (0.1% TFA) at 1.5 ml/minute, followed by a linear ramp to 100% ACN at 30 minutes. SDS-PAGE analyses were run on 12%, 12 well, Genscript ExpressPlus PAGE gels with a Bio-Rad Precision Plus Protein™ Dual Color Standard ladder, unless otherwise specified. Fluorescent scans were performed on a GE Healthcare Typhoon TRIO+ Variable Mode Imager.

3.3.2 Construct Design, Strains, and Vectors

The anti-HER2 Fab, J Fab, construct was kindly provided by the laboratory of Dr. Sachdev Sidhu in an in-house expression vector and contains a FLAG tag at the C' terminus of the light chain and a His_6 tag at the C' terminus of the heavy chain.[37] Phosphopantetheinyl transferase tag nucleotide sequences S6 and A1 were developed from amino acid sequences published by Zhou *et al*. and integrated into the J Fab nucleotide sequence (Supplemental Table 3.1).[36] The J PPTM (phosphopantetheinyl transferase marker) Fab construct contains the S6 sequence flanked on either side with DNA encoding a linker of 10 glycines at the C' terminus of the J Fab light chain before the FLAG tag sequence (between Ser217 and Asp 218 in translated protein sequence).

The J S6A1 Fab construct contains the S6 sequence at the transition from the variable to constant domain of the light chain (between Lys107 and Arg 108 in translated protein sequence) and the A1 sequence at the transition from the variable to constant domain of the heavy chain (between Ser117 and Ala 118 in translated protein sequence). The nucleotide sequence for AcpS was modeled to match that from *E. coli* K-12, GenBank accession number P24224, with a His_6 tag added to the C' terminus. J PPTM Fab, J S6A1, and AcpS sequences were optimized and ordered as synthetic constructs from DNA2.0 in pJExpress401 vectors, which have T5 promoters and are IPTG inducible. The sfp construct was developed in-house and cloned into a pET28 vector. All plasmids were cloned into BL21 DE3 *E. coli* cells for expression.

3.3.3 Fab Expression and Purification

Large scale cultures were prepared in Luria-Bertani (LB Lenox EMD Millipore) broth and inoculated with a 1:100 fold dilution from a liquid overnight culture (O/N) and grown for 3 hours at 37°C and 250 rpm. Cultures were placed on ice for 20 minutes, after which they were induced with IPTG to a final concentration of 500 μM and left to shake O/N at 15°C. All cultures were centrifuged for 15 minutes at 8000 rpm and pellets were resuspended in 50 ml of lysis buffer (1ml Triton 100x, 100 μL of 200 mM PMSF, 100 μL of 2M $MgCl_2$, 1 μL Benzonase, and 100 mg lysozyme per 100 mL of lysis buffer) per litre of bacteria. Lysis was carried out rotating samples at 4°C for one hour. Samples were centrifuged for 1 hour at 4750 rpm, 4°C and the lysates were decanted from the pellets.

Parent J Fab

The Parent J Fab was purified on a FPLC AKTA Purifier system using the His_6 tag. A final concentration of 10 mM imidazole was added to lysate and injected onto a HisTrap FF Crude 1 mL column (GE Healthcare) at 1 ml/min. Column was washed with 5 column volumes (CV) of Buffer A (10 mM imidazole, TRIS-HCl 20mM, pH 8) followed by a linear gradient from 0% Buffer B (500 mM imidazole, Tris-HCl 20mM, pH 8) to 100% Buffer B at 20 CV. Fractions were analyzed on SDS-PAGE gel and clean fractions were collected. Buffer was extensively exchanged using Macrosep Advance 30 kDa centrifugal filters intro a Tris Buffer (20mM Tris-HCl, 200 mM NaCl, pH8).

J PPTM

Lysate was incubated with anti-FLAG resin (GenScript) for 30 minutes at room temperature. Using a gravity column, the resin was thoroughly washed with Tris Buffer (20mM Tris-HCl, 200 mM NaCl, pH8). Protein was eluted using 4M NaCl, 50 mM Tris-HCl, pH 7. Buffer was extensively exchanged using Microsep Advance 30 kDa centrifugal filters intro a Tris Buffer (20mM Tris-HCl, 200 mM NaCl, pH8).

J S6A1

Lysate was incubated with Protein A-Agarose beads (Biovision) for 1 hour at 4°C. Using a gravity column, the resin was thoroughly washed with Tris Buffer (20mM Tris-HCl, 200 mM NaCl, pH8). Protein was eluted with 3.5M $MgCl_2$ ($MgCl_2$□6H2O Bioshop) Tris-HCl 20 mM, pH 7. Buffer was extensively exchanged using Microsep Advance 30 kDa centrifugal filters into a Tris Buffer (20mM Tris-HCl, 200 mM NaCl, pH 8).

3.3.4 Enzyme Expression and Purification

Large scale cultures were prepared in Luria-Bertani broth and inoculated with a 1:100 fold dilution from a liquid overnight cultures and grown to OD_{600}=0.6-0.9 at 37°C at 250 rpm. Cultures were then placed on ice for 20 minutes, after which they were induced with 500 μM IPTG and left to shake O/N at 15°C at 200 rpm. All cultures were centrifuged for 30 minutes at 5000 rpm and the pellets were then resuspended in 50 mL of Buffer X (20 mM Tris-Hcl, 200 mM NaCl, 20 mM imidazole, pH 8). Lysis was carried out using a Constant Systems Cell Disrupter TS Series 0.75 kW (Model TS2/40/BA/AA), through which samples were passed 2x at 20,000 psi. The lysate was centrifuged at 15,000 rpm at 4°C for 45 minutes and purified using Ni-NTA agarose using a gravity column and eluted with 3 10 mL aliquots of Buffer X with increasing concentrations of imidazole (50 mM, 100 mM and 200 mM). Fractions were analysed by SDS-PAGE and clean fractions were collected. Buffer was extensively exchanged using Macrosep Advance 10 kDa centrifugal filters into a Tris Buffer (20mM Tris-HCl, 200 mM NaCl, pH 8).

3.3.5 Fluorophore-Coenzyme A Synthesis

BODIPY-CoA

Reaction and purification were performed using a previously established protocol.[38] Coenzyme A trilithium salt was dissolved in phosphate buffered saline solution (PBS) with 50 mM $MgCl_2$ and BODIPY FL N-(2-aminoethyl) maleimide was dissolved in DMSO. Reagents were combined in a 2 ml reaction in PBS to final concentrations of 0.51 mM coenzyme A trilithium salt, 1.5 mM BODIPY FL N-(2-

aminoethyl) maleimide and 10% DMSO. Reaction was placed in the dark and agitated for 85 minutes on a VWR Incubating Rocker. Reaction was purified by ethyl acetate extraction.

Texas red-CoA

Sulforhodamine 101 C_2-maleimide or Texas red C_2-maleimide (Setareh Biotech), 7.3 mg, was dissolved in 600 µL of DMSO and 24.6 mg of Coenzyme A trilithium salt dehydrate (Affymetrix) was dissolved in 1400 µL of 100 mM sodium phosphate buffer pH 7. Mixtures were combined to final concentrations of 5 mM Texas red C_2-maleimide and 15 mM Coenzyme A trilithium salt dihydrate and stirred for one hour in the dark.

The product was purified using a Teledyne Isco Combiflash system. Reaction mixture was injected onto a RediSep R_f High Performance Gold 50 g HP C18 column at a flow rate of 40 mL/min. Method was run for 5 minutes at 10% solvent B, acetonitrile, and 90% solvent A, water, which was followed by a linear gradient up to 50% B over 30 minutes. Fractions were monitored using λ_1 214 nm and λ_2 254 nm and uncontaminated fractions were collected.

3.3.6 Loading Assays

J PPTM Fab and Parent J Fab

Reactions were performed in a Tris-HCl buffer (Tris-HCl 20mM, NaCl 200 mM, pH8) with Fabs at a concentration of 1.5 µM, $MgCl_2$ at 1 mM, Texas red-CoA at 50 µM in a final reaction volume of 80 µL. Reactions were performed with 0.5 µM sfp and J PPTM Fab and Parent J Fab respectively. Controls were performed with 0.5 µM AcpS, or with no enzyme.

Reactions were carried out for 1 hour at 37°C after which they were washed extensively with Tris-HCl buffer in Pall Microsep Advance Centrifugal Devices, 3K MWCO. Samples were run on a 12% SDS-PAGE gel, Genscript and visualized on a Typhoon scanner, 610 nm emission filter, 526 nm laser, 100 pixel, 3+mm focal plane. Gel was stained using silver stain.

J S6A1 Fab

Single Enzyme

Three 70 *u*L reactions were performed in a Tris-HCl buffer (Tris-HCl 20mM, NaCl 200 mM, pH8) with 55 µL of J S6A1 Fab (below quantifiable concentration levels), 1 mM $MgCl_2$, 50 µM Texas red-CoA and either 1.3 µM sfp, 0.68 µM AcpS, or no enzyme. The reactions were incubated at 37°C for 1 hour and washed extensively with Tris-HCl buffer in Pall Microsep Advance Centrifugal Devices, 3K MWCO. Samples were run on a SDS-PAGE gel and visualized on a Typhoon scanner with 610 nm emission filter and 526 nm laser. Gel was subsequently silver stained.

Tandem Loading

Three 70 µL reactions were performed in a Tris-HCl buffer (Tris-HCl 20mM, NaCl 200 mM, pH 8) with 55 µL of J S6A1 Fab (below quantifiable concentration levels), 1 mM $MgCl_2$, 50 µM Texas red-CoA and 0.7 µM AcpS. The reactions were incubated at 37°C for 45 minutes and washed extensively with Tris-HCl buffer in Pall Microsep Advance Centrifugal Devices, 3K MWCO. Washed reactions were prepared for a subsequent step. All three reactions were brought to a final concentration of 1 mM $MgCl_2$ and 147 µM BODIPY-CoA. Sfp was added to reaction 1 to a final concentration

of 1.3 μM, no enzyme was added to reaction 2 and AcpS was added to reaction 3 to a final concentration of 0.7 μM. All reactions were brought to a final volume of 70 μL with Tris-HCl buffer (Tris-HCl 20mM, NaCl 200 mM, pH 8). Reactions were once again incubated at 37°C for 45 minutes and washed extensively with Tris-HCl buffer (Tris-HCl 20mM, NaCl 200 mM, pH 8) in Pall Microsep Advance Centrifugal Devices, 3K MWCO. Samples were run on a 6-18%, 10 well ExpressPlus PAGE gel (Genscript) and visualized on a Typhoon scanner first with 610 nm emission filter and 526 nm laser followed by a second scan with a 520 nm emission filter and 488 nm laser.

ELISA 3.3.7

Parent J Fab, J PPTM Fab, and the tagged form of J PPTM Fab (J PPTM Fab+TR-CoA) were tested. J PPTM Fab was tagged with Texas red-CoA, as described in loading assay procedure, except the reaction was carried out at room temperature and subsequently re-purified using anti-FLAG resin to remove unbound fluorophore and sfp. ELISA protocol was adapted from *Making and Using Antibodies- A Practical Handbook*, *Chapter 8 Making Antibodies in Bacteria*, *Direct Binding Phage ELISA 8.3.3.3.1*.[39] 30 μL of 2 μg/mL HER2 (from R&D Systems) in PBS was plated onto 384 well plates as the extracellular domain (ECD). Variations from the protocol include the use of specified purified Fabs in place of phage supernatants. A Bradford assay with a murine mAb standard was used to determine protein concentrations and normalize the three Fabs. Six protein serial dilutions were used, starting at a maximum concentration of 5 μg/mL and

decreasing by five-fold concentration steps down to .00032 µg/mL. Additionally, in place of horseradish peroxidase/anti-M13 antibody conjugate an anti-FLAG antibody (the M2 antibody from Sigma with the HRP fusion) was used.

3.3.8 Podophyllotoxin-PMPI-Coenzyme A Synthesis

Step 1: Podophyllotoxin (Enzo Life Sciences) was reacted with *p*-maleimidophenyl isocyanate, PMPI (Thermo Scientific Pierce) under argon in anhydrous DMSO, 1:10 molar excess of podophyllotoxin: PMPI. Reaction was stirred overnight at room temperature in the dark. Product formation was confirmed using TLC (normal phase, 2:98 methanol:chloroform) and LC-MS/MS.[40] *Step 2:* Coenzyme A trilithium salt dihydrate (Affymetrix) was dissolved in 100 mM sodium phosphate, pH 7 and a 2x molar excess was added to the first reaction of the original PMPI, DMSO 33.3% and sodium phosphate buffer 66.6%. Reaction was stirred in the dark at room temperature for 2.5 hours. Product was confirmed using LC-MS/MS.

3.3.9 Podophyllotoxin-Tosylate Synthesis

The reaction was performed under previously established conditions with molar ratios of alcohol: *p*-toluenesulfonyl chloride: pyridine at 1:1.5:2.[41] Podophyllotoxin was dissolved in chloroform to a final concentration of 10 mM and placed in an ice bath. After the vessel and components had chilled pyridine was added to a final concentration of 20 mM, and stirred. The *p*-toluenesulfonyl chloride was then added to a final concentration of 15mM. The reaction proceeded for 8 hrs. Product formation was confirmed using LC-MS/MS (results described in next section, Chapter 4, as work is still in progress).

3.4 Results and Discussion

3.4.1 Design and Verification of a Phosphopantetheinyl Transferase Site-Specific Anti-HER2 Fab

The phosphopantetheinyl transferase sfp, originally isolated from *Bacillus subtilis*, is highly characterized. It is particularly noted for its capacity to recognize and load assorted chemistries bound to coenzyme A (through a stable thioether linkage) onto specific serines in full length thiolation domains/peptidyl carrier proteins or condensed tags, such as S6 (GDSLWLLRLLN) (Fig. 3.3A).[28,34-36] The reaction yields a covalent bond between the molecule-phosphopantetheine arm fusion and the serine residue through a strong phosphodiester bond. This enzyme therefore affords the ability to utilize a variety of toxins for antibody conjugation that are both structurally diverse and chemically complex. Moreover, this enzyme is readily available through heterologous expression, as explicated in well-established protocols, or is commercially available from sources such as New England Biolabs, making this enzymatic approach easily affordable, accessible and scalable.[42] To test whether phosphopantetheinyl transferases can site-specifically generate antibody-drug conjugates we integrated the S6 tag into the C' terminus of the anti-HER2 Fab, known as the J Fab, to yield J PPTM Fab (Fig 3.3B, Supplemental Table 3.1). A 10 glycine linker was placed on either side of the S6 tag to ensure that both the Fab and tag could adopt their native conformations. The J PPTM Fab was computationally designed and ordered as a synthetic construct from DNA2.0.

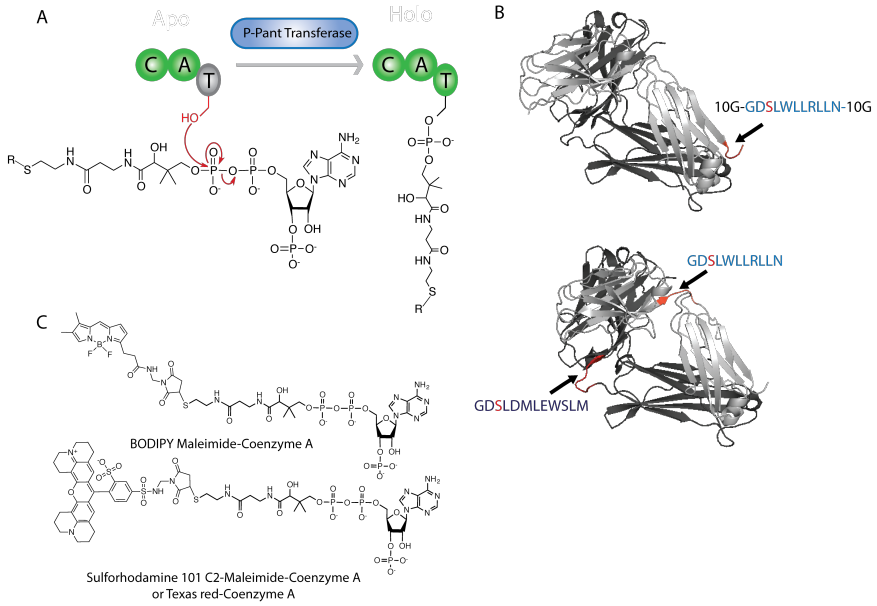

Fig. 3.3 *Approach to phosphopantetheinyl transferase catalyzed site-specific generation of antibody-drug conjugates.* ***(A)*** *Phosphopantetheinyl transferase catalyzed transfer of phosphopantetheine arm from CoA to site-specific serine in a thiolation domain T. in its native context, a natural product assembly line (C. condensation domain, A. adenylation domain). This chemical addition transitions the T. domain from its apo to active holo form as indicated be the change from grey to green. Phosphopantetheinyl transferases are promiscuous with the ability to recognize diverse chemistries linked to the free thiol of CoA, illustrated by the R group.* ***(B)*** *Parent J Fab positions that were derivatized with phosphopantetheinyl transferase tags to generate novel Fab constructs are highlighted in red. J PPTM Fab (top) contains the S6 marker (light blue with site-selective serine in red) specific for sfp flanked on either side with a 10 glycine linker at the C' terminus of the light chain (light grey). J S6A1 Fab (bottom) contains the S6 marker (light blue with site-selective serine in red) specific for sfp at the transition from the variable to the constant of the light chain (light grey) and the A1 marker (navy blue with site-selective serine in red) specific for AcpS at the transition from the variable to the constant of the heavy chain (dark grey).* ***(C)*** *Examples of fluorophore-CoA molecules synthesized and conjugated to antibodies to verify the technique.*

We strategically chose to work with a HER2 (ERBB2) specific Fab, a certified breast cancer target found to be up-regulated in 20-30% of all breast cancer cases and particularly those with resistance to traditional chemotherapies and the worst prognoses.[43] Furthermore, it is an approved and effective therapeutic target with clinical examples specific for this receptor such as trastuzumab, the anti-HER2 monoclonal antibody, and the ADC ado-trastuzumab emtansine.[44,45] In place of the classical anti-HER2 Fab Trastuzumab, we opted to use the J Fab, developed at the University of Toronto by the Sidhu laboratory. This novel anti-HER2 construct is particularly advantageous for ADC development as it binds to a distinct epitope on HER2, offering the possibility of trastuzumab combination therapy. Furthermore, the full length IgG (of J Fab) exhibits superior cellular internalization properties to Trastuzumab.[37] A higher fraction of J IgG ADCs and thus toxic payload would be internalized and delivered to their targets, presumably resulting in lower doses exhibiting better efficacy.

Heterologous overexpression and purification of sfp, Parent J Fab and J PPTM Fab yielded expected proteins at ~26 kDa, ~50 kDa and ~52 kDa respectively and the appropriate reduced forms of the Fabs, as analyzed by SDS-PAGE (Supplemental Fig. 3.1). A surrogate fluorophore-CoA, Texas red-CoA, was synthesized and utilized in place of a toxin-CoA for visualization purposes (Fig. 3.3C). Conjugation reactions were conducted with J PPTM Fab and Parent J Fab in combination with Texas red-CoA and the phosphopantetheinyl transferase sfp (Fig. 3.4A). Additional controls were carried out without sfp and with an alternative phosphopantetheinyl transferase, AcpS, that should not have specificity for the S6 tag. Fluorescence was observed at J PPTM Fab protein

bands, full length and reduced, in the presence of sfp, but no fluorescence was detected in the controls without sfp, suggesting that the observed fluorescence is due to covalent bond formation between Texas red-CoA and J PPTM Fab and not unspecific staining. Therefore, sfp successfully catalyzed the conjugation of the small molecule onto the J PPTM Fab, but the question of site-selectivity remained. Parent J Fab reactions with and without sfp showed no fluorescence, therefore no transfer of Texas red-CoA occurred by the phosphopantetheinyl transferase onto the unmodified J Fab sequence. It is, therefore, reasonable to conclude that sfp does not recognize the native sequence of the Parent J Fab and must be loading the phosphopantetheine arm-Texas red from Texas red-CoA onto the unique and specific serine of the S6 tag present in only the J PPTM Fab. Furthermore, no loading is observed in the presence of another phosphopantetheinyl transferase AcpS, emphasizing the exclusive affinity sfp has for the J PPTM Fab S6 tag. Therefore, having established that sfp site-selectively can load small molecules onto S6 tagged Fab constructs, this method can be applied using toxin-CoA molecules to generate homogeneous ADCs in the future.

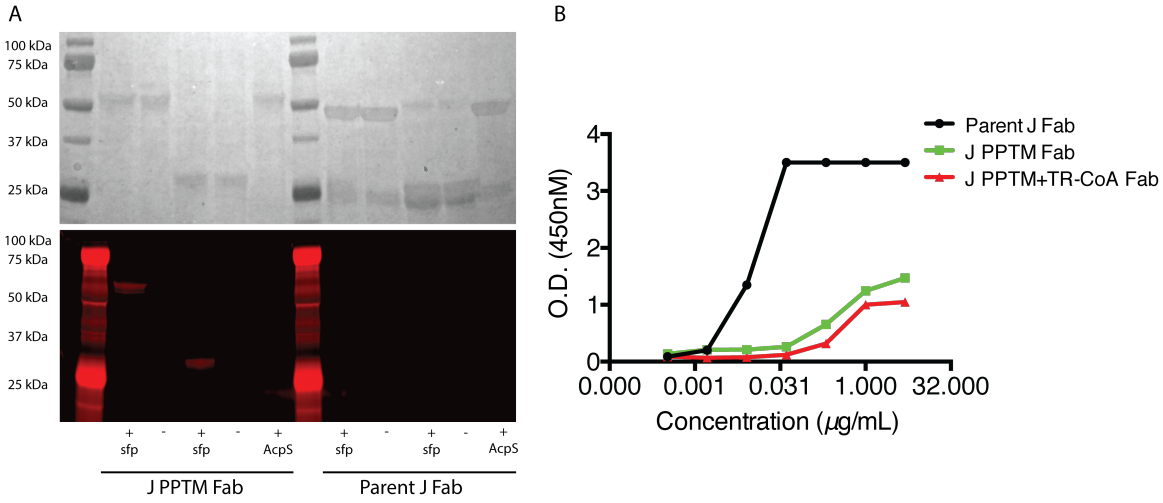

Fig. 3.4 *Validation of J PPTM Fab.* ***(A)*** *SDS-PAGE gel and fluorescent scan establishing phosphopantetheinyl transferase generated site specific J PPTM Fab-fluorophore conjugate. Lane 1: Ladder, Lane 2: J PPTM Fab + TR-CoA + sfp, Lane 3: J PPTM Fab + TR-CoA, Lane 4: J PPTM Fab reduced + TR-CoA + sfp, Lane 5: J PPTM Fab reduced + TR-CoA, Lane 6: J PPTM Fab + TR-CoA + AcpS, Lane 7: Ladder, Lane 8: Parent J Fab + TR-CoA + sfp, Lane 9: Parent J Fab + TR-CoA, Lane 10: Parent J Fab reduced + TR-CoA + sfp, Lane 11: Parent J Fab reduced + TR-CoA, Lane 12: Parent J Fab + TR-CoA + AcpS. It is evident that TR-CoA is only successfully loaded in the presence of sfp onto J Fab PPTM (Lane 2 and 4) indicating that this conjugation is occurring site-specifically onto the S6 tag present in J Fab PPTM and not the parent J Fab.* ***(B)*** *Immobilized ECD HER2 was incubated with various concentrations of Parent J Fab, J PPTM Fab, a J PPTM Fab loaded with Texas red-CoA by sfp (J PPTM+TR-CoA Fab), or BSA as a control. Plates were assayed for bound HER2-Fab complexes using HRP conjugated anti-FLAG antibody. J PPTM Fab retains ability to bind to HER2, however at a substantially decreased level from Parent J Fab. The addition of the phosphopantetheine arm and small molecule does not seem to further compromise binding ability.*

3.4.2 *In vitro* Binding

We next sought to assess the effect of the S6 tag and glycine linker and the additional small molecule-phosphopantetheine arm on HER2 binding of the J fab *in vitro*

(Fig. 3.3B). An ELISA revealed that there is a notable change in binding from the Parent J Fab to the J Fab PPTM, with an approximately 100-fold increase in concentration required for the J Fab PPTM to attain the same binding level as the Parent J Fab. There was not, however, a substantial difference in binding between the J Fab PPTM versus the sfp loaded J Fab PPTM with Texas red-phosphopantetheine arm (J Fab PPTM+TR-CoA) with an approximate 5-fold concentration deviation required to attain the same level of binding. This therefore suggests that the addition of a phosphopantetheine arm-small molecule to a Fab does not greatly alter its binding properties. This is significant as the phosphopantetheine linking chemistry and thiol tethered small molecule are necessary for the use of phosphopantetheinyl transferases to generate site-selective ADCs. Conversely, the 10G-S6-10G tag appears to engender the main binding deviation from the Parent J Fab. This is likely due to the size of the amino acid modification and its location. The additional 20 amino acid linker flanking the critical 12 amino acid S6 tag adds bulk to the construct and may compromise the Fabs ability to adopt its native conformation. Similarly, the location of the tag in the Fab may negatively affect structural properties that are integral to binding HER2. Therefore, it may be beneficial for future technology development to modify the site of S6 tag integration and experiment with varying lengths of glycine linkers and without in order to optimize HER2 binding. Alternatively, the addition of the 10G-S6-10G adjacent to the FLAG tag may have compromised the conformation or accessibility of the FLAG sequence. In this case, the decrease in signal may be attributed to a disruption of the binding between the J PPTM Fab and the anti-FLAG HRP and not the HER2 J PPTM Fab binding. It can be determined if this is the

case by repeating the experiment using an anti-His_6 HRP for signal generation as there is a His_6 tag on the unmodified heavy chain of both the Parent J Fab and the J PPTM Fab. Currently, however, it is important to recognize that the J PPTM Fab still successfully recognizes and binds to HER2 and thus maintains its potential as a site-selective ADC construct.

3.4.3 Synthesis of Toxin-CoA Conjugate

In order to generate a phosphopantetheinyl transferase conjugated ADC it was necessary to synthesize a toxin-CoA molecule. We drew upon nature's catalogue of potent anticancer agents and selected to use podophyllotoxin, a lignin produced from *Podophyllum* plant species. The cytotoxicity of podophyllotoxin is derived from its activity as an antimitotic microtubule inhibitor.[46-48] It is particularly noteworthy that numerous chemical modifications have been made to podophyllotoxin at the C4 position of the C ring, shifting the activity of the compound away from microtubule disruption to DNA Topoisomerase II inhibition (Fig 3.4).[49-51] An important clinical example is etoposide, derivatized with a 4,6-O-ethyldiene-β-D-glucopyranoside group at the C4 location, which exhibits potent activity toward DNA Topoisomerase II and is used for the treatment of testicular cancer and small cell lung cancer.[51] Evidently, podophyllotoxin derivatives at the C4 site are well characterized and maintain important anticancer activity, therefore the C4 alcohol provided a natural site for coenzyme A attachment.

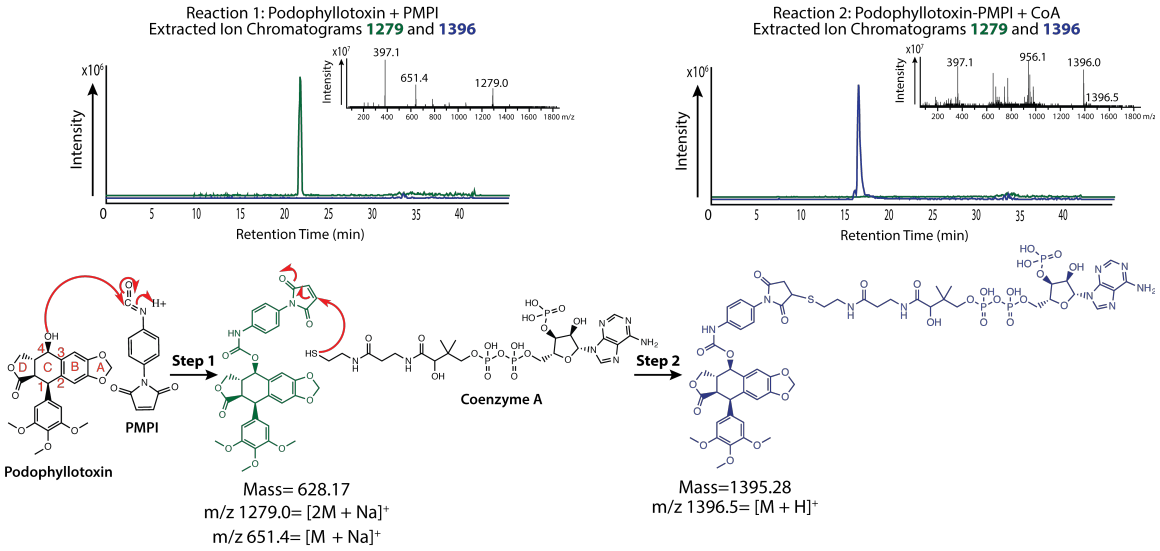

Fig. 3.5 *The two-step synthetic route used to generate podophyllotoxin-PMPI-CoA with the extracted ion chromatograms of appropriate product masses. The labeled rings (A-D) and carbons (1-4) are highlighted in red on podophyllotoxin to show the C4 site that has previously been derivatized. The extracted ion chromatogram m/z=1279 (green) of reaction 1 corresponds to the [2M + Na]* $^{+}$ *species of podophyllotoxin-PMPI (green), the peak at retention time 21.5 minutes verifies product formation. The extracted ion chromatogram m/z=1396 (blue) of reaction 2 corresponds to the [M + H]* $^{+}$ *species of podophyllotoxin-PMPI-CoA (blue), the peak at retention time 16.4 minutes verifies product formation. Furthermore, the extracted m/z=1279 (green) peak has disappeared in the reaction 2 chromatogram indicating that the podophyllotoxin-PMPI was consumed in the formation of podophyllotoxin-PMPI-CoA and it is confirmed to be a new trace as the extracted ion chromatogram m/z=1279 (blue) of reaction 1 shows no peak.*

To link the podophyllotoxin hydroxyl with the free thiol of coenzyme A we elected to use a heterobifunctional linker, *p*-maleimidophenyl isocyanate (PMPI), that includes an isocyanate group specific for hydroxyl nucleophilic attack and a maleimide group specific for attack by thiols.[40] The reaction was performed in two steps, first combining podophyllotoxin with the PMPI linker under inert atmosphere and second

reacting coenzyme A with the podophyllotoxin-PMPI formed in step 1. Step one product formation was confirmed using LC-MS/MS. A new peak at a retention time of 21.5 minutes was identified in the reaction UV base peak chromatogram compared to the podophyllotoxin and linker standards, indicating that product formed (Supplemental Fig. 3.2). The mass spectra and fragmentation of that peak corresponds to the expected podophoyllotoxin-PMPI product (628.17 Da), with a parent mass of 651.4 *m/z* corresponding to $[M + Na]^+$ and a dimer at 1279.0 m/z corresponding to $[2M + Na]^+$ (Fig 3.5). The fragmentation patterns of these species further confirmed the correct product with the 1279.0 *m/z* dimer fragmenting to 651.1 *m/z* $[M + Na]^+$ and 419.0 *m/z* corresponding to a loss of the PMPI linker + Na^+. The parent mass 651.4 *m/z* shared the same 419 *m/z* fragment (Supplemental Fig. 3.3). Having confirmed the formation of podophyllotoxin-PMPI, coenzyme A was added in the second reaction step to attack the PMPI maleimide. Product formation was confirmed using LC-MS/MS. The UV chromatogram showed that the PMPI-podophyllotoxin peak at retention time 21.5 minutes disappeared, indicating that it was consumed in the reaction (Supplemental Fig. 3.4). The mass of the expected product was 1395.28 Da, therefore an extracted ion chromatogram of *m/z* =1396.0 +/- 0.5 was used to reveal the new peak at retention time of 16.4 minutes. The parent mass of this peak was *m/z*= 1396.5 corresponding to $[M + H]^+$ of the successfully formed product podophyllotoxin-PMPI-CoA (Fig 3.5, Supplemental Fig. 3.5). Equipped with this CoA derivatized toxin it is now possible to generate ADCs using J Fab PPTM and phosphopantetheinyl transferases for bioactivity tests upon HER2+ cell lines.

3.4.4 Design and Verification of a Site-Specific Dually Loaded Anti-HER2 Fab

In addition to the use of phosphopantetheinyl transferases for the generation of homogeneous ADCs, we wanted to explore the possibility of using numerous enzymes of this class to site-specifically load multiple unique small molecules selectively onto Fabs, thereby generating ADCs that could hit various targets in cancerous cells. To do this, we designed a novel J Fab construct, J S6A1 Fab that contained the sfp S6 sequence in the flexible loop of the light chain at the transition from the variable to constant domain (Fig. 3.3B). It additionally contained a sequence known as A1, GDSLDMLEWSLM, which has specificity for the phosphopantetheinyl transferase AcpS, originally isolated from *E. coli* K-12 (Supplemental Table 3.1). The A1 tag was located in the flexible loop of the heavy chain from the variable to constant domain. The S6 and A1 tags were specifically developed for the tandem orthogonal loading of unique species onto proteins, with sfp and AcpS showing high selectivity toward their respective serine containing tags.[36] Thus, we sought to test if these enzymes could be used in tandem in the context of ADCs to generate a J S6A1 Fab loaded stoichiometrically and site-selectively with two distinct small molecule-CoA species.

The J S6A1 Fab and AcpS sequences were ordered as synthetic constructs from DNA2.0 and the proteins were subsequently heterologously overexpressed, purified and verified using SDS-PAGE analysis (Supplemental Figures 3.1 and 3.6). We first established that both enzymes exhibited activity toward the J S6A1 Fab construct by loading Texas red-CoA (Supplemental Fig. 3.7). However, we noted that AcpS loading was more efficient onto the Fab with a significantly greater fluorescent signal observed

than in the sfp conjugation. This is likely due to the native conformation of J S6A1 Fab limiting the solvent accessibility to the S6 tag compared to the A1 tag. In future, this could potentially be overcome by pre-reducing the chains, performing the enzymatic conjugation, and then re-oxidizing the constructs. After establishing that the two phosphopantetheinyl transferases successfully conjugate small molecule-CoAs to the J S6A1 Fab, we looked to determine if this could be done in a tandem fashion (Fig. 3.6). A reaction first was carried out with AcpS and Texas red-CoA to occupy all A1 sites. Subsequently, all excess fluorophore was washed away and a second reaction was performed with BODIPY-CoA and sfp (1), no additional enzyme (2), or AcpS (3) (Fig. 3.2C). The green normalized to red fluorescence intensity of reaction (1) was the highest – 10x greater than reaction (2) and 1.5x greater than reaction (3). This suggests that there is a degree of enzymatic selectivity occurring, with sfp offering the best activity toward the unreacted serines of the S6 tag in comparison to the remaining AcpS in reaction (2) or the additional AcpS in reaction (3) which should not recognize this site. Therefore, using AcpS and sfp in tandem provides an improved capacity, from the available synthetic techniques, for stoichiometric site-selective loading of two unique small molecule-CoA species onto Fabs.

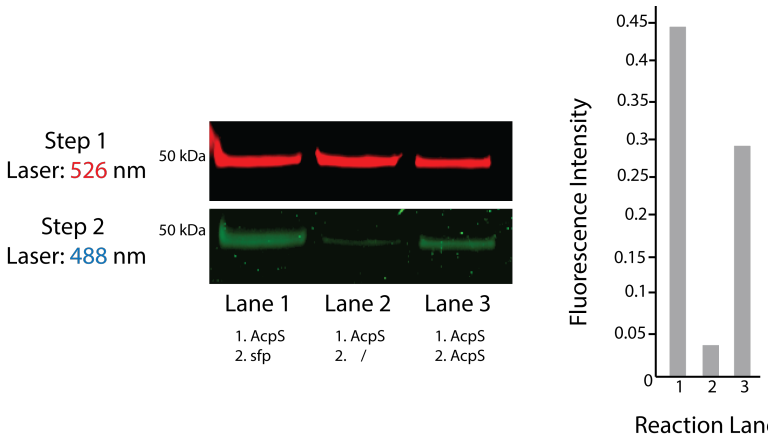

Fig. 3.6 *AcpS and sfp tandem loading reactions with J S6A1 Fab analyzed with a fluorescence scan of SDS-PAGE gel and bar graph depicting green normalized to red fluorescent intensities. Reactions were first performed with AcpS and Texas red-CoA to occupy A1 sites. Excess texas red-CoA excess was then removed. To establish ability of enzymes to work site-specifically, BODIPY-CoA and either sfp (reaction 1, lane 1), no additional enzyme (reaction 2, lane 2), or AcpS (reaction 3, lane 3) were added in a second reaction step. Fluorescent spectrums of Texas red and BODIPY do not overlap, therefore the reaction gel was first scanned with a 526 nm laser and 610 emission filter to observe the uniform conjugation of Texas red in step 1 of all three reactions. The gel was next scanned with a 488 nm laser and 520 nm emission filter to observe differences in loading of BODIPY. It is apparent that reaction 1, namely sfp, exhibits the highest selectivity and activity toward the remaining unreacted enzymatic site S6. Fluorescent intensities were quantified and green was normalized to red to be plotted into the bar graph. It is evident that tandem fluorophore loading using AcpS followed by sfp occurs with a degree of specificity since BODIPY conjugation occurred at noticeably higher levels using sfp than in the reactions with remaining or additional AcpS (intensity of reaction 1 is 10 times greater than reaction 2 and 1.5 times greater than reaction 3).*

Although the combination of AcpS followed by sfp provided the highest efficiency of fluorophore conjugation (presumably due to their tag selectivity), the

observable green fluorescence in reactions (2) and (3) was unexpected. This could be attributed to several reasons, the first being that the enzymes are not highly specific to their tags and therefore the remaining AcpS in reaction (2) and the added AcpS in reaction (3) loaded BODIPY-CoA onto the S6 tag. This option seems improbable as previous controls were performed using J Fab PPTM which contains the same S6 tag and no fluorophore loading was observed using AcpS (Fig. 3.4A). An alternative is that BODIPY-CoA is "sticky" and therefore some of the fluorescence can be attributed to protein staining rather than phosphopantetheinyl transferase catalyzed bond formation. The most compelling hypothesis, however, is that not all A1 sites were occupied in the first reaction step, leaving free A1 serines to be loaded with BODIPY-CoA by AcpS in the second reaction step. If this is the issue, then it may be overcome experimental optimization. To this end, it may be useful to lengthen the reaction time and vary enzyme and small molecule-CoA concentrations to identify the ideal ratios for maximal conjugation. Switching the enzymatic order of reactions might also be useful, it may be easier to occupy all of the S6 sites with sfp first and subsequently derivatize the A1 site with AcpS. With these optimizations it is likely that the selectivity of this tandem enzymatic method can be dramatically increased, providing a very promising method to conjugate antibodies with unique small molecule species for polytherapy ADCs.

3.5 Conclusion

In this work, we lay the groundwork for a novel site-specific ADC generation technique, establishing that phosphopantetheinyl transferases site-selectively transfer small molecule-CoA compounds onto serine containing tags of modified anti-HER2 Fab

constructs. Additionally, we determined that the phosphopantetheinyl transferase tagged Fabs retain their ability to recognize and bind to HER2. We therefore synthesized a toxin-CoA compound for future phosphopantetheinyl transferase catalyzed ADC generation. Additionally, we determined in a preliminary manner that the phosphopantetheinyl transferases, sfp and AcpS can be used in an orthogonal tandem fashion to provide a degree of site-selectivity (over available synthetic techniques) when looking to load multiple unique small molecule species onto antibodies for polytherapy ADC generation. With this foundation in place, it is possible to validate the clinical potential of phosphopantetheinyl transferases for the site-specific conjugation of single and multiple toxin ADCs. Therefore, this study has provided the basis for a novel enzymatic technique to improve small molecule to antibody conjugation and consequently our ability to produce better cancer therapies.

3.6 References

1. Newman, D.J., Cragg, G.M. & Snader, K.M. The influence of natural products upon drug discovery. *Nat. Prod. Rep.* **17**, 215-234 (2000).
2. da Rocha, A.B., Lopes, R.M. & Schwartsmann, G. Natural products in anticancer therapy. *Curr. Opin. Pharmacol.* **1**, 364-369 (2001).
3. Ducry, L. & Stump, B. Antibody-drug conjugates: linking cytotoxic payloads to monoclonal antibodies. *Bioconjugate Chem.* **21**, 5-13 (2010).
4. Chari, R.V., Miller, M.L. & Widdison, W.C. Antibody-drug conjugates: an emerging concept in cancer therapy. *Angew. Chem. Int. Ed.* **53**, 3796-3827 (2014).

5. Senter, P.D. & Sievers, E.L. The discovery and development of brentuximab vedotin for use in relapsed Hodgkin lymphoma and systemic anaplastic large cell lymphoma. *Nat. Biotechnol.* **30**, 631-637 (2012).

6. Traynor, K. Ado-trastuzumab emtansine approved for advanced breast cancer. *Am, J. Health-Syst. Pharm.* **70**, 562 (2013).

7. Hurvitz, S. *et al.* Trastuzumab emtansine (T-DM1) vs trastuzumab plus docetaxel (H + T) in previously untreated HER2-positive metastatic breast cancer (MBC): primary results of a randomized, multicenter, open-label phase II study (TDM4450g/B021976). *Eur. J. Cancer* **47**, Abstract 5001 (2011).

8. Junutula, J.R. *et al.* Site-specific conjugation of a cytotoxic drug to an antibody improves the therapeutic index. *Nat. Biotechnol.* **26**, 925-932 (2008).

9. Panowksi, S., Bhakta, S., Raab, H., Polakis, P. & Junutula, J. R. Site-specific antibody drug conjugates for cancer therapy. *mAbs* **6**, 34-45 (2014).

10. Shen, B.Q. *et al.* Conjugation site modulates the in vivo stability and therapeutic activity of antibody-drug conjugates. *Nature Biotech.* **30**, 184-189 (2012).

11. Hamblett, K.J. *et al.* Effects of drug loading on the antitumor activity of a monoclonal antibody drug conjugate. *Clinical Cancer Res.* **10**, 7063-7070 (2004).

12. McDonagh, C. F. *et al.* Engineered antibody-drug conjugates with defined sites and stoichiometries of drug attachment. *Prot. Eng. Des. Sel.* **19**, 299-307 (2006).

13. Sun, M.M. *et al.* Reduction-alkylation strategies for the modification of specific monoclonal antibody disulfides. *Bioconjugate Chem.* **16**, 1282-1290 (2005).

14. Strop, P. *et al.* Location matters: site of conjugation modulates stability and pharmacokinetics of antibody drug conjugates. *Chem. Biol.* **20**, 161-167 (2013).

15. Axup, J.Y. *et al.* Synthesis of site-specific antibody-drug conjugates using unnatural amino acids. *Proc. Natl. Acad. Sci. U.S.A.* **109**, 16101-16106 (2012).

16. Boeggeman, E. *et al.* Site specific conjugation of fluoroprobes to the remodeled Fc N-glycans of monoclonal antibodies using mutant glycosyltransferases: application for cell surface antigen detection. *Bioconjugate Chem.* **20**, 1228-1236 (2009).

17. de Graaf, A.J., Kooijman, M., Hennink, W.E. & Mastrobattista, E. Nonnatural amino acids for site-specific protein conjugation. *Bioconjugate Chem.* **20**, 1281-1295 (2009).

18. Wootton, S. K. & Yoo, D. Homo-oligomerization of the porcine reproductive and respiratory syndrome virus nucleocapsid protein and the role of disulfide linkages. *J. Virol.* **77**, 4546-4557 (2003).

19. Woo, H.J., Lotz, M.M., Jung, J.U. & Mercurio, A.M. Carbohydrate-binding protein 35 (Mac-2), a laminin-binding lectin, forms functional dimers using cysteine 186. *J Biol Chem.* **266**, 18419-18422 (1991).

20. Gomez, N. *et al.* Triple light chain antibodies: factors that influence its formation in cell culture. *Biotechnol. Bioeng.* **105**, 748-760 (2010).

21. Gomez, N. *et al.* Effect of temperature, pH, dissolved oxygen, and hydrolysate on the formation of triple light chain antibodies in cell culture. *Biotechnol. Progr.* **26**, 1438-1445 (2010).

22. Chumsae, C., Gaza-Bulseco, G. & Liu, H. Identification and localization of unpaired cysteine residues in monoclonal antibodies by fluorescence labeling and mass spectrometry. *Anal. Chem.* **81**, 6449-6457 (2009).

23. Deiters, A., Cropp, T.A., Summerer, D., Mukherji, M. & Schultz, P.G. Site-specific PEGylation of proteins containing unnatural amino acids. *Bioorg. Med. Chem. Lett.* **14**, 5743-5745 (2004).

24. Frei, E., 3rd. Combination cancer therapy: Presidential address. *Cancer Res.* **32**, 2593-2607 (1972).

25. DeVita, V.T., Jr., Young, R.C. & Canellos, G.P. Combination versus single agent chemotherapy: a review of the basis for selection of drug treatment of cancer. *Cancer* **35**, 98-110 (1975).

26. Mayer, L.D. & Janoff, A.S. Optimizing combination chemotherapy by controlling drug ratios. *Mol. Interventions* **7**, 216-223 (2007).

27. Mootz, H.D., Schorgendorfer, K. & Marahiel, M.A. Functional characterization of 4'-phosphopantetheinyl transferase genes of bacterial and fungal origin by complementation of Saccharomyces cerevisiae lys5. *FEMS Microbiol. Lett.* **213**, 51-57 (2002).

28. Lambalot, R.H. *et al.* A new enzyme superfamily - the phosphopantetheinyl transferases. *Chem. Biol.* **3**, 923-936 (1996).

29. Ton-That, H., Mazmanian, S.K., Faull, K.F. & Schneewind, O. Anchoring of surface proteins to the cell wall of Staphylococcus aureus. Sortase catalyzed in

vitro transpeptidation reaction using LPXTG peptide and NH(2)-Gly(3) substrates. *J. Biol. Chem.* **275**, 9876-9881 (2000).

30. Spirig, T., Weiner, E.M. & Clubb, R.T. Sortase enzymes in Gram-positive bacteria. *Mol. Microbiol.* **82**, 1044-1059 (2011).

31. 179. Rottig, A. & Steinbuchel, A. Acyltransferases in bacteria. *Microbiol. Mol. Biol. Rev.* **77**, 277-321 (2013).

32. Yin, J. *et al.* Genetically encoded short peptide tag for versatile protein labeling by Sfp phosphopantetheinyl transferase. *Proc. Natl. Acad. Sci. U.S.A.* **102**, 15815-15820 (2005).

33. Wong, L.S., Thirlway, J. & Micklefield, J. Direct site-selective covalent protein immobilization catalyzed by a phosphopantetheinyl transferase. *J. Am. Chem. Soc.* **130**, 12456-12464 (2008).

34. Quadri, L. E. *et al.* Characterization of Sfp, a Bacillus subtilis phosphopantetheinyl transferase for peptidyl carrier protein domains in peptide synthetases. *Biochemistry* **37**, 1585-1595 (1998).

35. Reuter, K., Mofid, M. R., Marahiel, M. A. & Ficner, R. Crystal structure of the surfactin synthetase-activating enzyme sfp: a prototype of the 4'-phosphopantetheinyl transferase superfamily. *EMBO J.* **18**, 6823-6831 (1999).

36. Zhou, Z. *et al.* Genetically encoded short peptide tags for orthogonal protein labeling by Sfp and AcpS phosphopantetheinyl transferases. *ACS Chem. Biol.* **2**, 337-346 (2007).

37. Owen, S.C. *et al.* Targeting HER2+ breast cancer cells: lysosomal accumulation of anti-HER2 antibodies is influenced by antibody binding site and conjugation to polymeric nanoparticles. *J. Controlled Release* **172**, 395-404 (2013).

38. Lee, K.K., Da Silva, N.A. & Kealey, J.T. Determination of the extent of phosphopantetheinylation of polyketide synthases expressed in *Escherichia coli* and *Saccharomyces cerevisiae*. *Anal. Biochem.* **394**, 75-80 (2009).

39. Fellouse, F.A. & Sidhu, S.S. Making antibodies in bacteria. In *Making and Using Antibodies: A Practical Handbook.* Edn. 2 (eds. Howard, G.C. & Kaser, M.R.) 151-172 (CRC Press, Boca Raton, Florida, USA, 2013).

40. Annunziato, M.E., Patel, U.S., Ranade, M. & Palumbo, P.S. p-maleimidophenyl isocyanate: a novel heterobifunctional linker for hydroxyl to thiol coupling. *Bioconjugate Chem.* **4**, 212-218 (1993).

41. Kabalka, G. W., Varma, M. & Varma, R. S. Tosylation of Alcohols. *J. Org. Chem.* **51** (1986).

42. Yin, J., Lin, A. J., Golan, D.E. & Walsh, C.T. Site-specific protein labeling by Sfp phosphopantetheinyl transferase. *Nat. Protoc.* **1**, 280-285 (2006).

43. Slamon, D.J. *et al.* Human breast cancer: correlation of relapse and survival with amplification of the HER-2/neu oncogene. *Science* **235**, 177-182 (1987).

44. Molina, M.A. *et al.* Trastuzumab (herceptin), a humanized anti-Her2 receptor monoclonal antibody, inhibits basal and activated Her2 ectodomain cleavage in breast cancer cells. *Cancer Res.* **61**, 4744-4749 (2001).

45. Baselga, J. & Albanell, J. Mechanism of action of anti-HER2 monoclonal antibodies. *Ann. Oncol.* **12 Suppl 1**, S35-41 (2001).

46. Canel, C., Moraes, R.M., Dayan, F.E. & Ferreira, D. Podophyllotoxin. *Phytochemistry* **54**, 115-120 (2000).

47. Ma, Y. *et al.* Biological evaluation and molecular modelling study of podophyllotoxin derivatives as potent inhibitors of tubulin polymerization. *Chem. Biol. Drug Des.* **82**, 12-21 (2013).

48. Desbene, S. & Giorgi-Renault, S. Drugs that inhibit tubulin polymerization: the particular case of podophyllotoxin and analogues. *Curr. Med. Chem. Anticancer Agents* **2**, 71-90 (2002).

49. Utsugi, T. *et al.* Antitumor activity of a novel podophyllotoxin derivative (TOP-53) against lung cancer and lung metastatic cancer. *Cancer Res.* **56**, 2809-2814 (1996).

50. Hande, K.R. Etoposide: four decades of development of a topoisomerase II inhibitor. *Eur. J. Cancer* **34**, 1514-1521 (1998).

51. Chang, J.Y. *et al.* Effect of 4 beta-arylamino derivatives of 4'-O-demethylepipodophyllotoxin on human DNA topoisomerase II, tubulin polymerization, KB cells, and their resistant variants. *Cancer Res.* **51**, 1755-1759 (1991).

3.7 Supplemental Tables

J PPTM Fab Light Chain	MKKNIAFLLASMFVFSIATNAYASDIQMTQSPSSLSASVGDRVTIT CRASQSVSSAVAWYQQKPGKAPKLLIYSASSLYSGVPSRFSGSRS GTDFTLTISSLQPEDFATYYCQQGYYYPFTFGQGTKVEIKRTVAAP SVFIFPPSDSQLKSGTASVVCLLNNFYPREAKVQWKVDNALQSGN SQESVTEQDSKDSTYSLSSTLTLSKADYEKHKVYACEVTHQGLSS PVTKSFNRGECGGSGGGGGGGGGGDSLSWLLRLLNGGGGGGG GGGDYKDDDDK
J S6A1 Fab Light Chain	MKKNIAFLLASMFVFSIATNAYASDIQMTQSPSSLSASVGDRVTIT CRASQSVSSAVAWYQQKPGKAPKLLIYSASSLYSGVPSRFSGSRS GTDFTLTISSLQPEDFATYYCQQGYYYPFTFGQGTKVEIKGDSLSW LLRLLNRTVAAPSVFIFPPSDSQLKSGTASVVCLLNNFYPREAKVQ WKVDNALQSGNSQESVTEQDSKDSTYSLSSTLTLSKADYEKHKV YACEVTHQGLSSPVTKSFNRGECGGSDYKDDDDK
J S6A1 Fab Heavy Chain	MKKNIAFLLASMFVFSIATNAYAEISEVQLVESGGGLVQPGGSLRL SCAASGFNLYSSYIHWVRQAPGKGLEWVASIYPYSSYTSYADSVK GRFTISADTSKNTAYLQMNSLRAEDTAVYYCARYYGFAMDYWG QGTLVTVSSGDSLDMLEWSLMASTKGPSVFPLAPSSKSTSGGTAA LGCLVKDYFPEPVTVSWNSGALTSGVHTFPAVLQSSGLYSLSSVV TVPSSSLGTQTYICNVNHKPSNTKVDKKVEPKSCDKTHTSRHHHH HH

Supplemental Table 3.1 *Amino acid sequences for phosphopantetheinyl transferase tagged modified J Fabs, J PPTM Fab and J S6A1 Fab. Blue highlights secretion factor, black highlights original J Fab sequence, purple highlights the S6 sequence, teal highlights the A1 sequence, pink highlights the glycine linker and green highlights the FLAG tag.*

3.8 Supplemental Figures

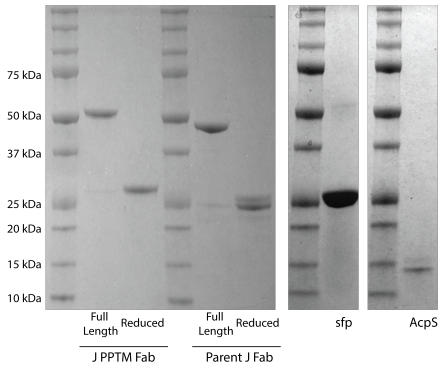

Supplemental Fig. 3.1 *SDS-PAGE of purified proteins. Fabs were run with non-reducing and reducing (5% ß-mercaptoethanol) loading buffers to visualize full length and reduced forms. Gel was stained using Coomasie blue and expected protein weights were confirmed, J PPTM Fab full length 52.095 kDa, Parent J Fab full length 49.585, sfp 26.882 kDa, and AcpS 14.875 kDa.*

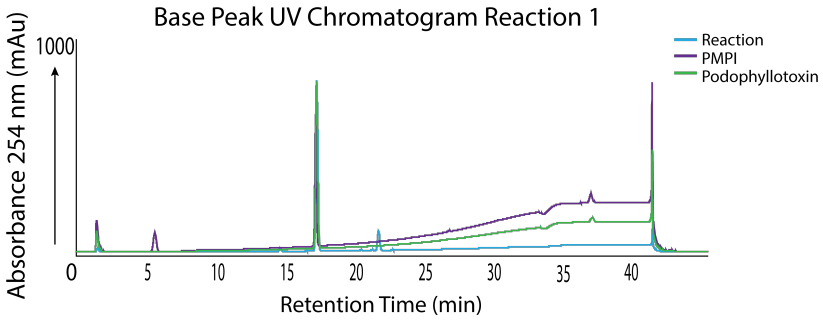

Supplemental Fig. 3.2 *Base peak UV chromatograms of podophyllotoxin standard, PMPI and reaction 1 stacked for comparison. It is evident that a new peak at retention time 21.5 minutes has arisen that was not present in either of the two standards, suggesting that the reaction has formed a unique product (podophyllotoxin-PMPI).*

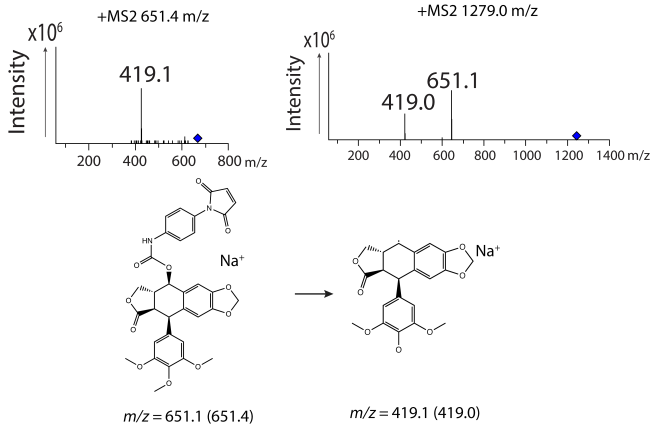

Supplemental Fig. 3.3 *The MS2 spectra and structural fragmentation pattern of the parent MS peaks of podophyllotoxin-PMPI.*

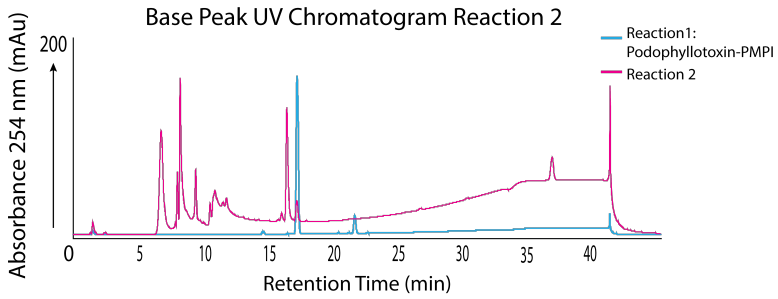

Supplemental Fig. 3.4 *Base peak UV chromatograms of reaction 1 (blue) and reaction 2 (pink) stacked for comparison. It is evident the peak at 21.5 minutes has disappeared, suggesting that podophyllotoxin-PMPI (blue) has been consumed during the formation of podophyllotoxin-PMPI-CoA (pink).*

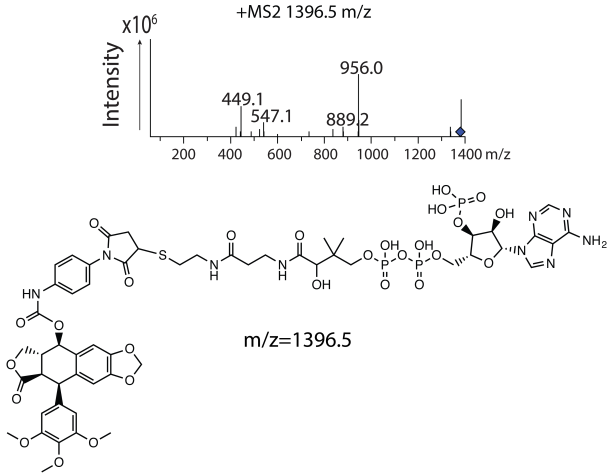

Supplemental Fig. 3.5 *The MS2 spectra showing the fragmentation pattern of the parent MS peak of podophyllotoxin-PMPI-CoA.*

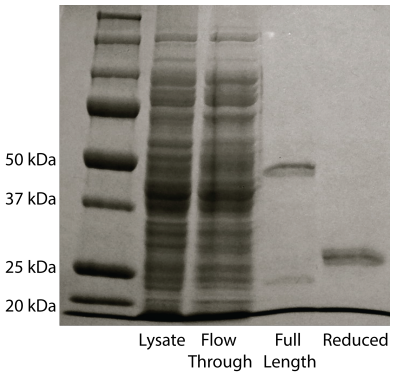

Supplemental Fig. 3.6 *SDS-PAGE analysis of protein A (eluted with pH 2.8 Buffer) purified J Fab S6A1. Sample was run in a non-reducing and reducing (5% ß-mercaptoethanol) loading buffer. Gel was stained using Coomassie blue and appropriate bands were visualized at 52.3 kDa full length and ~25 kDa for reduced heavy and light chain species. Gel was not run to full separation, therefore proteins between 10 and 15 kDa are not resolved.*

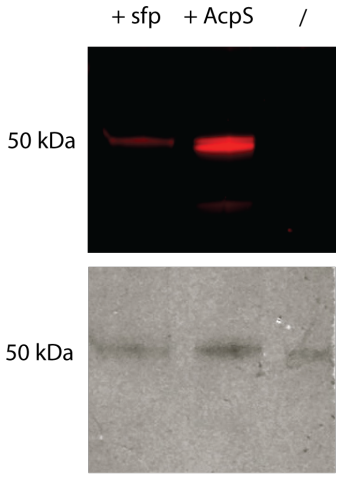

Supplemental Fig. 3.7 *SDS-PAGE gel and fluorescence scan of J S6A1 Fab + phosphopantetheinyl transferase + Texas red-CoA reactions. Both sfp and AcpS successfully conjugated Texas-red CoA to the Fab, however AcpS appears to do so with greater efficiency than sfp.*

Chapter 4. Future Directions and Significance

4.1 Work in Progress for The Site-Selective Generation of Antibody-Drug Conjugates Using Phosphopantetheinyl Transferases

There are additional components to this work that are not entirely completed, but have advanced to a preliminary stage. These steps are noteworthy because they are integral for the culmination of this work. They are as follows: the synthesis of podophyllotoxin-tosylate without a PMPI linker, optimization and further verification of the tandem S6A1 loading, and elongation and humanization of the J PPTM Fab into a humanized full length IgG. Here, the progress to date on these pursuits and the next experimental steps required to take them to completion are outlined.

4.1.1 Podophyllotoxin-Tosylate Synthesis

I was interested in generating a variety of podophyllotoxin chemical derivatives for CoA addition in order to maintain optimal bioactivity and attain the most stable ADC linking chemistry. I successfully generated a podophyllotoxin-CoA species that was bound with the PMPI linker, but for comparison I wanted to synthesize a "pure" species, composed only of CoA directly linked to podophyllotoxin through a stable thiother bond. In order to generate this compound, there was a need to modify the C4 hydroxyl of podophyllotoxin to a good leaving group. The podophyllotoxin alcohol was converted to a tosylate through a reaction with *p*-toluenesulfonyl chloride.[155] Product formation, 568.14 Da, was confirmed using LC-MS/MS with a peak at 23.8 minutes corresponding to parent *m/z*=569.1 $[M+H]^+$ (Fig. 4.1). The fragmentation pattern further confirmed the product with an *m/z*=401.0 corresponding to loss of the 3,4,5-trimethoxyphenyl group (Fig. 4.2).

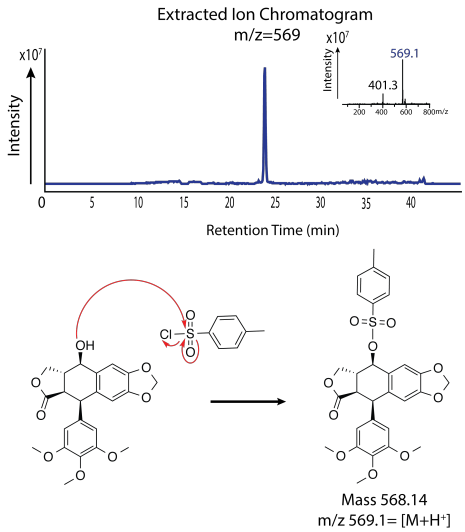

Fig. 4.1 *Synthetic route used for podphyllotoxin-tosylate generation and LC/MS extracted ion chromatogram (m/z=569.1) confirming product formation.*

Having confirmed product formation, further studies are needed to scale up the reaction. With sufficient product, the podophyllotoxin-tosylate can be purified using Flash chromatography. Coenzyme A may then be reacted with the podophyllotoxin-tosylate by adapting previously established methods involving thiol nucleophilic attack of a tosylate. For instance, a reaction may be performed with equimolar concentrations of the podophyllotoxin-tosylate and CoA in water and ethanol. The reaction would be refluxed for 3 hours and subsequently refluxed for another several hours after the addition of NaOH – a verified protocol (with other thiol and tosylate reagents) with 80% yield.[156]

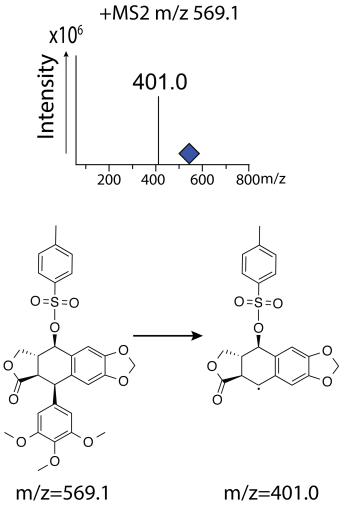

Fig. 4.2 *The MS2 spectra and structural fragmentation pattern of the parent MS peak of the podophylltoxin-tosylate.*

4.1.2 Tandem Loading J S6A1 Fab

As previously mentioned, the loading assay of unique small molecules using AcpS and sfp onto J S6A1 Fab requires optimization to gain a full understanding of the degree of site-selectivity provided by these enzymes. The experiment was repeated in reverse

order using sfp with Texas red-CoA first to occupy all S6 sites, followed by Acps (1), no enzyme (2), or sfp (3) with BODIPY-CoA to observe how conjugation occurred on the A1 site (data not shown). It was encouraging to note that in the second reaction step there appeared significant loading of BODIPY-CoA in the reaction with AcpS, no loading in the reaction containing only left over sfp, and minimal loading in the reaction with additional sfp, once again suggesting that these enzymes in tandem confer selectivity. However, the scan of the first reaction, used to confirm all S6 site occupation, did not show uniform loading of Texas red, rather there was greater red fluorescence observed in the reaction with sfp followed by AcpS (1). This is likely due to the fact that excess Texas red-CoA was not entirely washed away before the addition of the second enzyme, allowing AcpS to load both remaining Texas red-CoA and newly added BODIPY-CoA. However, because of this inconsistency it is necessary to repeat this reaction. Additionally, in future it will be important to perform mass spectrometry upon the product of J S6A1 Fab tandem orthogonally loaded using sfp and Texas red-CoA followed by AcpS and BODIPY-CoA. Gel-filtration chromatography or protein A resin purification will be used between the two enzymatic steps to ensure that all BODIPY-CoA loading in the second step is attributed to AcpS alone and not residual sfp. The product will then be trypsin digested for mass spectrometry. If the reaction is totally selective, mass peaks should only be identified for the phosphopantetheine arm-Texas red + S6 fragment and the phosphopantetheine arm-BODIPY + A1 fragment. If this is not the case, one can determine the degree of selectivity of this technique by comparing the proportions of the mass peaks for phosphopantetheine arm-Texas red + S6 fragment,

phosphopantetheine arm-Texas red + A1 fragment, the phosphopantetheine arm-BODIPY + A1 fragment and the phosphopantetheine arm-BODIPY + S6. Ultimately, this investigation will determine the full potential of the tandem phosphopantetheinyl transferase technique for site-specific ADC generation. Additionally, downstream one might gain insight into the clinical applicability of ADCs selectively loaded with uniquely function toxins to discern if they indeed provide a more effective treatment option than traditional ADCs.

4.1.3 Humanization and Elongation of Constructs

I initially utilized Fabs for ease of verification to establish that phosphopantetheinyl transferases act site-specifically in the context of antibodies. Moving forward, full length humanized IgGs are required to generate true phosphopantetheinyl transferase conjugated ADCs for *in vivo* cytotoxicity testing and evaluating pharmacokinetic properties. The JIgG construct has been provided by the Sidhu labratory, the variable heavy chain in a pFUSEss-HIgG1-Fc vector (Fc-fusion protein expression plasmid - Human IgG1 with IL2 signal sequence from Invivogen) and the variable light chain in a pFUSE2ss-CLIg-hK vector (constant region of the human Ig kappa light chain with IL2 signal sequence from Invivogen).[157] In collaboration with the Sidhu laboratory further studies are required to integrate the S6 tag into the C' terminus of the light chain. Two methods are in use to accomplish this task, cloning and site-based mutagenesis. An insert has been designed containing the sequence for the pFUSE2ss-CLIg-hK between two single cut restriction sites where the end of the light chain orf falls. At the end of the light chain nucleotide sequence the S6 sequence was integrated (Table 4.1). The sequence

can be ordered from DNA 2.0 and upon arrival can be digested, ligated to the vector and cloned. Alternatively, members of the Sidhu group are working to integrate the tag using PCR site-directed mutagenesis. Upon successful generation of the S6 tagged IgG with one of these techniques, the heavy and light chain vectors can be co-transfected into mammalian cells for humanized JIgG production with a phosphopantetheinyl transferase tag.

Nucleotide sequence containing LC C' terminus S6 tag and pFUSE2ss-CLJIg-hK vector sequence	GTCTACGCCTGCGAAGTCACCCATCAGGGCCTGA GCTCGCCCGTCACAAAGAGCTTCAACAGGGGAGA GTGTGGAGATAGTCTCAGTTGGCTACTGAGGCTTC TAAACTAGAGGGAGCTAGC

Table 4.1 *Synthetic design for cloning S6 Tag into C' terminus of full length humanized J antibody light chain. Teal highlights the onetime restriction site AccI and blue highlights the onetime restriction site NheI present in the vector that are amenable to cloning. Red highlights the S6 sequence and the original pFUSE2ss-CLJIg-hK sequence is in black.*

4.2 Future Directions for The Site-Selective Generation of Antibody-Drug Conjugates Using Phosphopantetheinyl Transferases

The groundwork has been established for the use of phosphopantetheinyl transferases to site-specifically load natural product toxins onto antibodies. However, further experimentation and development would enhance the potential of this technique and reveal its clinical value. It is important to further validate the homogeneity and site-selectivity of this technique, purify and load both toxin-CoA and toxin-PMPI-CoA onto an antibody, and then evaluate the efficacy of the ADC. The following sections include the proposed experiments required to achieve these final aims.

4.2.1 Further Verification of Homogeneity and Site-Selectivity

Additional quantitative experiments to verify the site-specificity and homogeneity of the phosphopantetheinyl transferase technique beyond the fluorescence loading assay would be beneficial. Hydrophobic interaction chromatography (HIC) has been extensively used to separate varying DAR species.[23,24,133] Therefore, HIC will separate 0 and 1 DAR J PPTM+TR-CoA Fab species, allowing integration of the peaks and quantification of the phosphopantetheinyl transferase loading efficiency. The J PPTM IgG + Texas red-CoA species will have two S6 sites, therefore creating more opportunities for heterogeneity. Upon generating this construct, HIC will separate 0, 1, and 2 DAR species, giving further information regarding homogeneity. Site-selectivity can also be verified by trypsin digesting the J PPTM+TR-CoA Fab species and performing mass spectrometry to accurately establish that the fluorophore has been conjugated to the S6 site.

4.2.2 Purification of Toxin and Generation of J PPTM IgG ADC

The podophyllotoxin-PMPI-CoA synthesis needs to be scaled up and purified using Flash chromatography. Once this product and podophyllotoxin-CoA (from tosylate synthesis route) are purified, the structures should be verified using the CMCB's High Resolution LC-MS/MS Orbitrap and NMR. Subsequently, using sfp, the podophyllotoxin-CoA derivatives will both be loaded onto the J PPTM IgG. The conjugation of the toxin species to the IgG can be confirmed using MALDI-TOF mass spectrometry. This will yield two podophyllotoxin ADC species with different linking

chemistries, a factor that may affect their stability profiles and consequently dose-limiting toxicity.

4.2.3 Cytotoxicity Testing

Assessing the efficacy of the phosphopantetheinyl transferase generated ADCs is critical to the advancement of this technique. *In vitro* efficacy assays can be performed using HER2+, SkBr3, and HER2-, MCF-7, cell lines. Unconjugated J PPTM IgG, free podophyllotoxin-PMPI-CoA, free podophyllotoxin-CoA, and the two podophyllotoxin ADC species of J PPTM IgG will be applied to the cell lines. Cell viability can be measured using a CellTiter-Glo Luminescent Cell Viability Assay 96.[122]

In vivo efficacy can subsequently be established using mouse models. KPL-4 (HER2 +) human breast tumor cells can be implanted into SCID mice and allowed to grow.[122,158] At a certain growth point the unconjugated J PPTM IgG, free podophyllotoxin-PMPI-CoA, free podophyllotoxin-CoA, and the two podophyllotoxin ADC species of J PPTM IgG will be given to the mice and the decrease in tumor size monitored. By comparing the efficacy of the phosphopantetheinyl transferase generated ADC to the free IgG and toxins *in vitro* and *in vivo*, one can determine if this enzymatic technique is a feasible and effective method for ADC generation, yielding therapies that are more potent than either component alone.

4.3 Significance and Concluding Remarks

This thesis highlighted that nature is a prolific source of chemistries with defined activities toward discrete cellular targets that happen to be up-regulated or overactive in cancer. The separate biosynthetic assemblies of these anticancer natural products are also

appreciated in depth. However, despite understanding the underlying biosynthetic logic, synthetic recombinations of biosynthetic components to yield hybrid assembly lines that produce molecules with unique or multiple activities are often ineffective. This is due to uncertainty regarding the mechanisms by which nature itself undergoes combinatorialization. There has been a lack of inquiry into the evolutionary principles that govern nature's rearrangements to yield molecules with distinct targets to inform these studies. This knowledge would provide insight into the assembly line sites that are amenable to modification and facilitate future combinatorial efforts. Furthermore, nature's sophisticated generation of natural products with unique activity remains to be improved through the use of cancer-specific delivery tools. Antibodies have provided a means to take these molecules to sites of disease, forming the class of therapy known as antibody-drug conjugates. This therapeutic class faced difficulties, specifically with methods to generate stoichiometrically and structurally uniform antibody-drug conjugates. This thesis illuminates some of the fundamental evolutionary changes to biosynthetic assembly lines that drive the observed shifts in natural products' targeted activity and additionally identifies a novel enzymatic method to site-selectively generate antibody-drug conjugates.

In **Chapter 2**, the antimycin-type family of depsipeptides was explored in depth to elucidate the evolutionary principles governing the diversification of the molecules' target cellular proteins, yet retained structural similarity. It was revealed that the starting enzymatic domains were highly genetically conserved across the four biosynthetic assembly lines, which has contributed to the maintenance of the structural relationship

between the four classes with each containing 3-formamido-2-hydroxybenzoic acid and threonine units. Divergence in structure was, as hypothesized, attributed to the incorporation or reduction of modular units, with the insertion or deletion of one, two, and three modules accounting for the change from 9 to 12 to 15 to 18-membered ring sizes. Therefore, it was identified that nature's evolutionary assembly line combinatorializations to create new molecules occurs through defined splicing and integration or deletion of enzymatic modules. It was difficult to conclude exactly how and where these are being inserted, but to broadly probe this matter a sequence alignment tool, Mauve analysis, was utilized that considers large-scale genetic evolutionary changes. This analysis showed sequence delineations occurring primarily around C domains rather than after T domains (the end of a module). This suggests genetic drift or perhaps repair occurs after modular insertions or deletions, making it complex to define exact genetic splice sites.

It was additionally identified that the PKS units imbue an important point of structural variation across and within the four depsipeptide classes. The 9-membered antimycin assembly line incorporates longer fatty acid tail units in comparison to the malonyl/methylmalonyl-CoA substrates of the other PKS units. Furthermore, the antimycin PKS unit appears to be highly flexible, incorporating a variety of fatty acid tail lengths as indicated by natural analogue isolation. This is particularly significant because we demonstrated that only the 9-membered antimycins have inhibitory activity toward Bcl-xL and that the alkyl tail, and particularly the length of the alkyl tail, plays a role in influencing Bcl-xL activity. Therefore, the antimycin PKS unit may be an interesting unit

to further probe and characterize in the future, in addition to transplant into more complex systems.

The role of docking domains to establish connections between modular units was also highlighted, and a potential conserved NRPS-PKS docking region in the PKS modules across the 4 assembly lines was identified. This lends support to the theory that docking domains are likely an intrinsically consistent component of evolutionary assembly line rearrangements and by gaining further understanding of these connections it may facilitate combinatorial biosynthetic efforts.[7] This work exposed some of the evolutionary principles involved in the modification of assembly lines to generate molecules with unique anticancer activities, particularly by modular insertions or deletions. Additionally, a list-parts of antimycin-type depsipeptide biosynthetic machinery was generated that is primed for manipulation. With this information in hand and future studies such as these, combinatorial biosynthetic efforts to yield natural products with activity toward a unique cellular target up-regulated in cancer or hybrid natural products that hit multiple targets may be more successful.

In order to further refine the targeting ability of natural products toward cancer cells, in **Chapter 3** a novel technique to generate site-specific antibody-drug conjugates was developed. Current methods for linking small molecules to antibodies are problematic, causing structural compromise, species heterogeneity leading to varied pharmacokinetic and efficacy profiles and creating the potential for immunogenicity and scalability issues. Moreover, these techniques cannot load multiple small molecules that hit different cellular targets onto an antibody with any degree of selectivity. In response to

this, engineered anti-HER2 J Fabs, J PPTM Fab and J S6A1 Fab, were designed and it was shown that biosynthetic group transfer enzymes, specifically of the phosphopantetheinyl transferase class, can site-specifically load small molecules onto the introduced enzymatic tags in the J PPTM Fab. To validate the activity of the J PPTM Fab, a binding study was performed and demonstrated that it still recognized and bound to its target antigen. Additionally, preliminary data showed that two unique small molecules can be loaded onto J S6A1 Fabs with a previously unattainable degree of stoichiometric and site-selectivity using two distinct phosphopantetheinyl transferases. This is particularly significant because to date ADCs have been loaded with extremely potent toxins in order to eradicate the cancerous cells, but premature release of these drugs leads to serious negative side effects. Thus, it would be beneficial to deliver multiple molecular species that hit unique targets up-regulated in cancer and have less generalized toxicity to tumor beds. For instance, it would be valuable to pursue the generation of an ADC loaded with antimycin and JBIR-06/neoantimycin to induce apoptosis in cancerous cells through the simultaneous inhibition of Bcl-xL and down-regulation of GRP78. Further, optimization of the J S6A1 Fab loading methodology will facilitate the realization of this concept. This work has therefore established the foundation for a totally novel approach to ADC generation that yields homogeneous drugs and potentially polytherapy ADCs with greater therapeutic indices.

This thesis expanded upon key aspects of enhancing natural products' targeting to cancerous cells by illuminating how molecules with activity toward diverse cellular targets that happen to be dysregulated in cancer are produced in nature, and further how

these molecules can then be selectively delivered to cancerous cells using antibodies. Collectively, this research has the potential to facilitate the development of hybrid natural products with dual activity toward cancerous cells and optimized antibody-drug conjugates that hit numerous cellular targets, providing more efficacious targeted cancer therapies and thus ultimately affecting the way that we treat cancer.

References

1. Canadian Cancer Society's Advisory Committee on Cancer Statistics. *Canadian Cancer Statistics 2013*. Toronto, ON: Canadian Cancer Society; 2013.
2. Mann, J. Natural products in cancer chemotherapy: past, present and future. *Nat. Rev. Cancer* **2**, 143-148 (2002).
3. Nagle, A., Hur, W. & Gray, N.S. Antimitotic agents of natural origin. *Curr. Drug Targets* **7**, 305-326 (2006).
4. Newman, D.J., Cragg, G.M. & Snader, K.M. The influence of natural products upon drug discovery. *Nat. Prod. Rep.* **17**, 215-234 (2000).
5. Newman, D.J. & Cragg, G. M. Natural products as sources of new drugs over the last 25 years. *J. Nat. Prod.* **70**, 461-477 (2007).
6. da Rocha, A.B., Lopes, R.M. & Schwartsmann, G. Natural products in anticancer therapy. *Curr. Opin. Pharmacol.* **1**, 364-369 (2001).
7. Fischbach, M.A. & Walsh, C.T. Assembly-line enzymology for polyketide and nonribosomal peptide antibiotics: logic, machinery, and mechanisms. *Chem. Rev.* **106**, 3468-3496 (2006).
8. Zerikly, M. & Challis, G.L. Strategies for the discovery of new natural products by genome mining. *Chembiochem* **10**, 625-633 (2009).
9. Corre, C. & Challis, G.L. New natural product biosynthetic chemistry discovered by genome mining. *Nat. Prod. Rep.* **26**, 977-986, (2009).
10. Lam, K.S. New aspects of natural products in drug discovery. *Trends Microbiol.* **15**, 279-289 (2007).

11. Magarvey, N.A. *et al.* Biosynthetic characterization and chemoenzymatic assembly of the cryptophycins. Potent anticancer agents from cyanobionts. *ACS Chem. Biol.* **1**, 766-779 (2006).

12. Cragg, G.M., Newman, D.J. & Snader, K.M. Natural products in drug discovery and development. *J. Nat. Prod.* **60**, 52-60 (1997).

13. Over, B. *et al.* Natural-product-derived fragments for fragment-based ligand discovery. *Nat. Chem.* **5**, 21-28 (2013).

14. Kotake, Y. *et al.* Splicing factor SF3b as a target of the antitumor natural product pladienolide. *Nat. Chem. Biol.* **3**, 570-575 (2007).

15. Issell, B.F. & Crooke, S.T. Maytansine. *Cancer Treat. Rev.* **5**, 199-207 (1978).

16. Franke, J., Eichner, S., Zeilinger, C. & Kirschning, A. Targeting heat-shock-protein 90 (Hsp90) by natural products: geldanamycin, a show case in cancer therapy. *Nat. Prod. Rep.* **30**, 1299-1323 (2013).

17. Ueda, J. Y. *et al.* A novel antimycin-like compound, JBIR-06, from Streptomyces sp. ML55. *J. Antibiot. (Tokyo)* **61**, 241-244 (2008).

18. Tzung, S. P. *et al.* Antimycin A mimics a cell-death-inducing Bcl-2 homology domain 3. *Nat. Cell Biol.* **3**, 183-191 (2001).

19. VanderMolen, K.M., McCulloch, W., Pearce, C.J. & Oberlies, N.H. Romidepsin (Istodax, NSC 630176, FR901228, FK228, depsipeptide): a natural product recently approved for cutaneous T-cell lymphoma. *J. Antibiot.* **64**, 525-531 (2011).

20. Gerber, H.P., Koehn, F.E. & Abraham, R.T. The antibody-drug conjugate: an enabling modality for natural product-based cancer therapeutics. *Nat. Prod. Rep.* **30**, 625-639 (2013).

21. Chari, R.V. Targeted cancer therapy: conferring specificity to cytotoxic drugs. *Acc. Chem. Res.* **41**, 98-107 (2008).

22. Ducry, L. & Stump, B. Antibody-drug conjugates: linking cytotoxic payloads to monoclonal antibodies. *Bioconjugate Chem.* **21**, 5-13 (2010).

23. Junutula, J.R. *et al.* Site-specific conjugation of a cytotoxic drug to an antibody improves the therapeutic index. *Nat. Biotechnol.* **26**, 925-932 (2008).

24. Sun, M.M. *et al.* Reduction-alkylation strategies for the modification of specific monoclonal antibody disulfides. *Bioconjugate Chem.* **16**, 1282-1290 (2005).

25. Zimmerman, E.S. *et al.* Production of site-specific antibody-drug conjugates using optimized non-natural amino acids in a cell-free expression system. *Bioconjugate Chem.* **25**, 351-361 (2014).

26. Strop, P. *et al.* Location matters: site of conjugation modulates stability and pharmacokinetics of antibody drug conjugates. *Chem. Biol.* **20**, 161-167 (2013).

27. Axup, J.Y. *et al.* Synthesis of site-specific antibody-drug conjugates using unnatural amino acids. *Proc. Natl. Acad. Sci. U.S.A.* **109**, 16101-16106 (2012).

28. Frei, E., 3rd. Combination cancer therapy: Presidential address. *Cancer Res.* **32**, 2593-2607 (1972).

29. Papac, R. J. Origins of cancer therapy. *Yale J. Biol. Med.* **74**, 391-398 (2001).

30. Inaba, M. & Sakurai, Y. Mechanism of resistance of Yoshida sarcoma to nitrogen mustard. *Int. J. Cancer* **7**, 430-435 (1971).

31. Fischer, G.A. Detective transport of amethopterin (methotrexate) as a mechanism of resistance to the antimetabolite in L5178Y leukemic cells. *Biochem. Pharmacol.* **11**, 1233-1234 (1962).

32. Brockman, R.W. A mechanism of resistance to 6-mercaptopurine: metabolism of hypoxanthine and 6-mercaptopurine by sensitive and resistant neoplasms. *Cancer Res.* **20**, 643-653 (1960).

33. Johnson, I.S., Armstrong, J.G., Gorman, M. & Burnett, J.P., Jr. The Vinca Alkaloids: A New Class of Oncolytic Agents. *Cancer Res.* **23**, 1390-1427 (1963).

34. Bensch, K.G. & Malawista, S.E. Microtubule crystals: a new biophysical phenomenon induced by Vinca alkaloids. *Nature* **218**, 1176-1177 (1968).

35. Chabner, B.A. & Roberts, T.G., Jr. Timeline: Chemotherapy and the war on cancer. *Nat. Rev. Cancer* **5**, 65-72 (2005).

36. Gordaliza, M. Natural products as leads to anticancer drugs. *Clin. Transl. Oncol.* **9**, 767-776 (2007).

37. Wani, M.C., Taylor, H.L., Wall, M.E., Coggon, P. & McPhail, A.T. Plant antitumor agents. VI. The isolation and structure of taxol, a novel antileukemic and antitumor agent from Taxus brevifolia. *J. Am. Chem. Soc.* **93**, 2325-2327 (1971).

38. Schiff, P.B., Fant, J. & Horwitz, S.B. Promotion of microtubule assembly in vitro by taxol. *Nature* **277**, 665-667 (1979).

39. Bollag, D.M. *et al.* Epothilones, a new class of microtubule-stabilizing agents with a taxol-like mechanism of action. *Cancer Res.* **55**, 2325-2333 (1995).

40. Amar, S., Roy, V. & Perez, E.A. Treatment of metastatic breast cancer: looking towards the future. *Breast Cancer Res. Treat.* **114**, 413-422 (2009).

41. McGuire, W. P. *et al.* Taxol: a unique antineoplastic agent with significant activity in advanced ovarian epithelial neoplasms. *Ann. Int. Med.* **111**, 273-279 (1989).

42. Rivera, E. & Gomez, H. Chemotherapy resistance in metastatic breast cancer: the evolving role of ixabepilone. *Breast Cancer Res.* **12 Suppl 2**, S2 (2010).

43. Preston, J.N. & Trivedi, M.V. Eribulin: a novel cytotoxic chemotherapy agent. *Ann. Pharmacother.* **46**, 802-811 (2012).

44. Cummings, J. & Smyth, J.F. DNA topoisomerase I and II as targets for rational design of new anticancer drugs. *Ann. Oncol.* **4**, 533-543 (1993).

45. Canel, C., Moraes, R.M., Dayan, F.E. & Ferreira, D. Podophyllotoxin. *Phytochemistry* **54**, 115-120 (2000).

46. Arcamone, F., Franceschi, G., Penco, S. & Selva, A. Adriamycin (14-hydroxydaunomycin), a novel antitumor antibiotic. *Tetrahedron Lett.*, 1007-1010 (1969).

47. Dimarco, A., Gaetani, M., Dorigotti, L., Soldati, M. & Bellini, O. Daunomycin: A New Antibiotic with antitumor activity. *Cancer Chemoth. Rep. Par. 1* **38**, 31-38 (1964).

48. Yang, F., Teves, S.S., Kemp, C.J. & Henikoff, S. Doxorubicin, DNA torsion, and chromatin dynamics. *Biochim. Biophys. Acta* **1845**, 84-89 (2014).

49. Teuffel, O. *et al.* Anthracyclines during induction therapy in acute myeloid leukaemia: a systematic review and meta-analysis. *Br. J. Haematol.* **161**, 192-203 (2013).

50. Kaklamani, V.G. & Gradishar, W.J. Epirubicin versus doxorubicin: which is the anthracycline of choice for the treatment of breast cancer? *Clin. Breast Cancer* **4 Suppl 1**, S26-33 (2003).

51. Judson, I. *et al.* Doxorubicin alone versus intensified doxorubicin plus ifosfamide for first-line treatment of advanced or metastatic soft-tissue sarcoma: a randomised controlled phase 3 trial. *Lancet Oncol.* **15**, 415-423 (2014).

52. Umezawa, H., Maeda, K., Takeuchi, T. & Okami, Y. New antibiotics, bleomycin A and B. *J. Antibiot.* **19**, 200-209 (1966).

53. Suzuki, H., Nagai, K., Yamaki, H., Tanaka, N. & Umezawa, H. On the mechanism of action of bleomycin: scission of DNA strands in vitro and in vivo. *J. Antibiot.* **22**, 446-448 (1969).

54. van Luijk, I.F. *et al.* Phase II study of bleomycin, vindesine, mitomycin C and cisplatin (BEMP) in recurrent or disseminated squamous cell carcinoma of the uterine cervix. *Ann. Oncol.* **18**, 275-281 (2007).

55. Bauer, K., Skoetz, N., Monsef, I., Engert, A. & Brillant, C. Comparison of chemotherapy including escalated BEACOPP versus chemotherapy including ABVD for patients with early unfavourable or advanced stage Hodgkin lymphoma. *Cochrane Db. Syst. Rev.*, CD007941 (2011).

56. D'Angio, G.J. *et al.* The treatment of Wilms' tumor: Results of the national Wilms' tumor study. *Cancer* **38**, 633-646 (1976).

57. Reich, E. Biochemistry of Actinomycins. *Cancer Res.* **23**, 1428-1441 (1963).

58. Miranda, M.B. *et al.* Mitomycin C and capecitabine in pretreated patients with metastatic gastric cancer: a multicenter phase II study. *J. Cancer Res. Clin. Oncol.* **140**, 829-837 (2014).

59. Tomasz, M. Mitomycin C: small, fast and deadly (but very selective). *Chem. Biol.* **2**, 575-579 (1995).

60. Ueda, H. *et al.* FR901228, a novel antitumor bicyclic depsipeptide produced by Chromobacterium violaceum No. 968. I. Taxonomy, fermentation, isolation, physico-chemical and biological properties, and antitumor activity. *J. Antibiot.* **47**, 301-310 (1994).

61. Insinga, A. *et al.* Inhibitors of histone deacetylases induce tumor-selective apoptosis through activation of the death receptor pathway. *Nat. Med.* **11**, 71-76 (2005).

62. Andersson, M., Daugaard, S., von der Maase, H. & Mouridsen, H.T. Doxorubicin versus mitomycin versus doxorubicin plus mitomycin in advanced breast cancer: a randomized study. *Cancer Treat. Rep.* **70**, 1181-1186 (1986).

63. Shuhendler, A.J. *et al.* A novel doxorubicin-mitomycin C co-encapsulated nanoparticle formulation exhibits anti-cancer synergy in multidrug resistant human breast cancer cells. *Breast Cancer Res. Tr.* **119**, 255-269 (2010).

64. Cheung, R.Y., Rauth, A.M., Ronaldson, P.T., Bendayan, R. & Wu, X.Y. In vitro toxicity to breast cancer cells of microsphere-delivered mitomycin C and its combination with doxorubicin. *Eur. J. Pharm. Biopharm.* **62**, 321-331 (2006).

65. Duong, H.H. & Yung, L.Y. Synergistic co-delivery of doxorubicin and paclitaxel using multi-functional micelles for cancer treatment. *Int. J. Pharm.* **454**, 486-495 (2013).

66. Kim, J.E. *et al.* Paclitaxel-exposed ovarian cancer cells induce cancerspecific CD4+ T cells after doxorubicin exposure through regulation of MyD88 expression. *Int. J. Oncol.* **44**, 1716-1726 (2014).

67. Brambilla, L. *et al.* Combination of vinblastine and bleomycin as first line therapy in advanced classic Kaposi's sarcoma. *J. Eur. Acad. Dermatol. Venereol.* **20**, 1090-1094 (2006).

68. Barlow, J. & Lele, S. Etoposide (VP-16) plus cisplatin (DDP) a new active cominvation in patients with ovarian adenocarcinoma. *Proc. Am. Soc. Clin. Oncol.* **4** (1985).

69. Evans, W.K. *et al.* VP-16 and cisplatin as first-line therapy for small-cell lung cancer. *J. Clin. Oncol.* **3**, 1471-1477 (1985).

70. Evans, W.K. *et al.* Etoposide (VP-16) and cisplatin: an effective treatment for relapse in small-cell lung cancer. *J. Clin Oncol.* **3**, 65-71 (1985).

71. Wong, F.T. & Khosla, C. Combinatorial biosynthesis of polyketides–a perspective. *Curr. Opin. Chem. Biol.* **16**, 117-123 (2012).

72. Wilkinson, B. & Micklefield, J. Mining and engineering natural-product biosynthetic pathways. *Nat. Chem. Biol.* **3**, 379-386 (2007).

73. Kong, D. *et al.* Echinomycin, a small-molecule inhibitor of hypoxia-inducible factor-1 DNA-binding activity. *Cancer Res.* **65**, 9047-9055 (2005).

74. Watanabe, K. *et al.* Total biosynthesis of antitumor nonribosomal peptides in Escherichia coli. *Nat. Chem. Biol.* **2**, 423-428 (2006).

75. Machida, K. *et al.* Organization of the biosynthetic gene cluster for the polyketide antitumor macrolide, pladienolide, in Streptomyces platensis Mer-11107. *Biosci. Biotechnol., Biochem.* **72**, 2946-2952 (2008).

76. Bai, R.L. *et al.* Halichondrin B and homohalichondrin B, marine natural products binding in the vinca domain of tubulin. Discovery of tubulin-based mechanism of action by analysis of differential cytotoxicity data. *J. Biol. Chem.* **266**, 15882-15889 (1991).

77. Marco, A. & Arcamone, F. DNA complexing antibiotics: daunomycin, adriamycin and their derivatives. *Arzneim.-Forsch.* **25**, 368-374 (1975).

78. ter Haar, E. *et al.* Discodermolide, a cytotoxic marine agent that stabilizes microtubules more potently than taxol. *Biochemistry* **35**, 243-250, (1996).

79. Mortison, J.D. & Sherman, D.H. Frontiers and opportunities in chemoenzymatic synthesis. *J. Org. Chem.* **75**, 7041-7051 (2010).

80. Sherman, D.H. The Lego-ization of polyketide biosynthesis. *Nat. Biotechnol.* **23**, 1083-1084 (2005).

81. Altschul, S.F., Gish, W., Miller, W., Myers, E.W. & Lipman, D.J. Basic local alignment search tool. *J. Molec. Biol.* **215**, 403-410 (1990).

82. Blin, K. *et al.* antiSMASH 2.0--a versatile platform for genome mining of secondary metabolite producers. *Nuc. Acid. Res.* **41**, W204-212 (2013).

83. Challis, G.L. Genome mining for novel natural product discovery. *J. Med. Chem.* **51**, 2618-2628 (2008).

84. Liu, X. & Cheng, Y.Q. Genome-guided discovery of diverse natural products from Burkholderia sp. *J. Ind. Microbiol. Biotech.* **41**, 275-284 (2014).

85. Laureti, L. *et al.* Identification of a bioactive 51-membered macrolide complex by activation of a silent polyketide synthase in Streptomyces ambofaciens. *Proc. Natl. Acad. Sci. U.S.A*. **108**, 6258-6263 (2011).

86. Nguyen, T. *et al.* Exploiting the mosaic structure of trans-acyltransferase polyketide synthases for natural product discovery and pathway dissection. *Nature Biotech.* **26**, 225-233 (2008).

87. Biggins, J.B., Gleber, C.D. & Brady, S.F. Acyldepsipeptide HDAC inhibitor production induced in Burkholderia thailandensis. *Org. Lett.* **13**, 1536-1539 (2011).

88. Wang, C. *et al.* Thailandepsins: bacterial products with potent histone deacetylase inhibitory activities and broad-spectrum antiproliferative activities. *J. Nat. Prod.* **74**, 2031-2038 (2011).

89. Menzella, H.G. *et al.* Combinatorial polyketide biosynthesis by de novo design and rearrangement of modular polyketide synthase genes. *Nat. Biotechnol.* **23**, 1171-1176 (2005).

90. Behrens, C.R. & Liu, B. Methods for site-specific drug conjugation to antibodies. *mAbs* **6**, 46-53 (2014).

91. Billingham, M.E., Mason, J. W., Bristow, M. R. & Daniels, J. R. Anthracycline cardiomyopathy monitored by morphologic changes. *Cancer Treat. Rep.* **62**, 865-872 (1978).

92. Myers, C.E. *et al.* Adriamycin: the role of lipid peroxidation in cardiac toxicity and tumor response. *Science* **197**, 165-167 (1977).

93. Yared, J.A. & Tkaczuk, K.H. Update on taxane development: new analogs and new formulations. *Drug Des. Dev. Ther.* **6**, 371-384 (2012).

94. Valero, V. Managing ixabepilone adverse events with dose reduction. *Clin. BreastCcancer* **13**, 1-6 (2013).

95. Cheung-Ong, K., Giaever, G. & Nislow, C. DNA-damaging agents in cancer chemotherapy: serendipity and chemical biology. *Chem. Biol.* **20**, 648-659 (2013).

96. Elting, L.S. *et al.* The burdens of cancer therapy. Clinical and economic outcomes of chemotherapy-induced mucositis. *Cancer* **98**, 1531-1539 (2003).

97. Beijers, A.J., Jongen, J.L. & Vreugdenhil, G. Chemotherapy-induced neurotoxicity: the value of neuroprotective strategies. *Neth. J. Med.* **70**, 18-25 (2012).

98. Goren, M.P., Wright, R.K., Horowitz, M.E. & Pratt, C.B. Cancer chemotherapy-induced tubular nephrotoxicity evaluated by immunochemical determination of urinary adenosine deaminase binding protein. *Am. J. Clin. Pathol.* **86**, 780-783 (1986).

99. Piekarz, R.L. *et al.* Phase II multi-institutional trial of the histone deacetylase inhibitor romidepsin as monotherapy for patients with cutaneous T-cell lymphoma. *J. Clin. Oncol.* **27**, 5410-5417 (2009).

100. Klimek, V.M. *et al.* Tolerability, pharmacodynamics, and pharmacokinetics studies of depsipeptide (romidepsin) in patients with acute myelogenous leukemia or advanced myelodysplastic syndromes. *Clin. Cancer Rese.***14**, 826-832 (2008).

101. Longley, R. E., Caddigan, D., Harmody, D., Gunasekera, M. & Gunasekera, S. P. Discodermolide--a new, marine-derived immunosuppressive compound. I. In vitro studies. *Transplantation* **52**, 650-656 (1991).

102. Molinski, T.F., Dalisay, D. S., Lievens, S. L. & Saludes, J. P. Drug development from marine natural products. *Nat. Rev. Drug Discovery* **8**, 69-85 (2009).

103. Widdison, W.C. *et al.* Semisynthetic maytansine analogues for the targeted treatment of cancer. *J. Med. Chem.* **49**, 4392-4408 (2006).

104. Shamma, M. & St. Georgiev, V. Camptothecin. *J. Pharm. Sci.* **63**, 163-183 (1974).

105. Hsiang, Y.H., Hertzberg, R., Hecht, S. & Liu, L.F. Camptothecin induces protein-linked DNA breaks via mammalian DNA topoisomerase I. *J Biol. Chem.* **260**, 14873-14878 (1985).

106. Cragg, G.M. & Newman, D.J. Plants as a course of anti-cancer agents. *J. Ethnopharmacol.* **100**, 72-79 (2005).

107. Wu, A.M. & Senter, P.D. Arming antibodies: prospects and challenges for immunoconjugates. *Nat. Biotechnol.* **23**, 1137-1146 (2005).

108. Chari, R.V., Miller, M.L. & Widdison, W.C. Antibody-drug conjugates: an emerging concept in cancer therapy. *Angew. Chem. Int. Ed.* **53**, 3796-3827 (2014).

109. Oldham, R.K. & Dillman, R.O. Monoclonal antibodies in cancer therapy: 25 years of progress. *J. Clin. Oncol.* **26**, 1774-1777 (2008).

110. Alley, S.C., Okeley, N.M. & Senter, P.D. Antibody-drug conjugates: targeted drug delivery for cancer. *Curr. Opin. Chem. Biol.* **14**, 529-537 (2010).

111. Senter, P.D. & Sievers, E.L. The discovery and development of brentuximab vedotin for use in relapsed Hodgkin lymphoma and systemic anaplastic large cell lymphoma. *Nat. Biotechnol.* **30**, 631-637 (2012).

112. Sievers, E.L. & Linenberger, M. Mylotarg: antibody-targeted chemotherapy comes of age. *Curr. Opin. Oncol.* **13**, 522-527 (2001).

113. Burnett, A.K. *et al.* Addition of gemtuzumab ozogamicin to induction chemotherapy improves survival in older patients with acute myeloid leukemia. *J. Clin. Oncol.* **30**, 3924-3931 (2012).

114. Vasu, S. & Blum, W. Emerging immunotherapies in older adults with acute myeloid leukemia. *Curr. Opin. Hematol.* **20**, 107-114, (2013).

115. Pro, B. *et al.* Brentuximab vedotin (SGN-35) in patients with relapsed or refractory systemic anaplastic large-cell lymphoma: results of a phase II study. *Jour. Clin. Oncol.* **30**, 2190-2196 (2012).

116. Younes, A. *et al.* Results of a pivotal phase II study of brentuximab vedotin for patients with relapsed or refractory Hodgkin's lymphoma. *J. Clin. Oncol.* **30**, 2183-2189 (2012).

117. Duvic, M., Tetzlaff, M., Clos, A.L., Gangar, P. & Talpur, R. Phase II trial of brentuximab vedotin for CD30+ cutaneous T-cell lymphomas and lymphoproliferative disorders. *Blood* **122**, 367 (2013).

118. Bartlett, N.L. *et al.* A phase 2 study of brentuximab vedotin in patients with relapsed or refractory CD30-positive non-hodgkin lymphomas: Interim results in patients with DLBCL and other B-cell lymphomas. *Blood* **15**, 848 (2013).

119. Wang, L., Amphlett, G., Blattler, W.A., Lambert, J.M. & Zhang, W. Structural characterization of the maytansinoid-monoclonal antibody immunoconjugate, huN901-DM1, by mass spectrometry. *Protein Sci.* **14**, 2436-2446 (2005).

120. Traynor, K. Ado-trastuzumab emtansine approved for advanced breast cancer. *Am, J. Health-Syst. Pharm.* **70**, 562 (2013).

121. Boyraz, B. *et al.* Trastuzumab emtansine (T-DM1) for HER2-positive breast cancer. *Curr. Med. Res. Opin.* **29**, 405-414 (2013).

122. Lewis Phillips, G.D. *et al.* Targeting HER2-positive breast cancer with trastuzumab-DM1, an antibody-cytotoxic drug conjugate. *Cancer Res.* **68**, 9280-9290 (2008).

123. Junttila, T.T., Li, G., Parsons, K., Phillips, G.L. & Sliwkowski, M.X. Trastuzumab-DM1 (T-DM1) retains all the mechanisms of action of trastuzumab

and efficiently inhibits growth of lapatinib insensitive breast cancer. *Breast Cancer Res. Treat.* **128**, 347-356 (2011).

124. Krop, I.E. *et al.* Phase I study of trastuzumab-DM1, an HER2 antibody-drug conjugate, given every 3 weeks to patients with HER2-positive metastatic breast cancer. *J. Clin. Oncol.* **28**, 2698-2704 (2010).

125. Hurvitz, S. *et al.* Trastuzumab emtansine (T-DM1) vs trastuzumab plus docetaxel (H + T) in previously untreated HER2-positive metastatic breast cancer (MBC): primary results of a randomized, multicenter, open-label phase II study (TDM4450g/B021976). *Eur. J. Cancer* **47**, Abstract 5001 (2011).

126. Okeley, N.M., Alley, S.C. & Senter, P.D. Advancing antibody drug conjugation: from the laboratory to a clinically approved anticancer drug. *Hematol. Oncol. Clin. North Am.* **28**, 13-25 (2014).

127. Govindan, S.V., Cardillo, T.M., Moon, S.J., Hansen, H.J. & Goldenberg, D.M. CEACAM5-targeted therapy of human colonic and pancreatic cancer xenografts with potent labetuzumab-SN-38 immunoconjugates. *Clin. Cancer Res.* **15**, 6052-6061 (2009).

128. Starodub, A.N. *et al.* Abstract C67: Safety, efficacy and pharmacokinetics of a new humanized anti-Trop-2 antibody-SN-38 conjugate (IMMU-132) from the treatment of diverse epithelial cancers: Phase I clinical experience. *Mol. Cancer Ther.* **12**, C67 (2013).

129. Sapra, P. *et al.* Anti-CD74 antibody-doxorubicin conjugate, IMMU-110, in a human multiple myeloma xenograft and in monkeys. *Clinical Cancer Res.* **11**, 5257-5264 (2005).

130. Thevanayagam, L. *et al.* Novel detection of DNA-alkylated adducts of antibody-drug conjugates with potentially unique preclinical and biomarker applications. *Bioanalysis* **5**, 1073-1081 (2013).

131. Lazar, A C. *et al.* Analysis of the composition of immunoconjugates using size-exclusion chromatography coupled to mass spectrometry. *Rapid Commun. Mass Spectrom.* **19**, 1806-1814 (2005).

132. Panowksi, S., Bhakta, S., Raab, H., Polakis, P. & Junutula, J. R. Site-specific antibody drug conjugates for cancer therapy. *mAbs* **6**, 34-45 (2014).

133. Hamblett, K.J. *et al.* Effects of drug loading on the antitumor activity of a monoclonal antibody drug conjugate. *Clinical Cancer Res.* **10**, 7063-7070 (2004).

134. Shen, B.Q. *et al.* Conjugation site modulates the in vivo stability and therapeutic activity of antibody-drug conjugates. *Nature Biotech.* **30**, 184-189 (2012).

135. Hofer, T., Skeffington, L.R., Chapman, C.M. & Rader, C. Molecularly defined antibody conjugation through a selenocysteine interface. *Biochemistry* **48**, 12047-12057 (2009).

136. Boeggeman, E. *et al.* Site specific conjugation of fluoroprobes to the remodeled Fc N-glycans of monoclonal antibodies using mutant glycosyltransferases: application for cell surface antigen detection. *Bioconjugate Chem.* **20**, 1228-1236 (2009).

137. McDonagh, C. F. *et al.* Engineered antibody-drug conjugates with defined sites and stoichiometries of drug attachment. *Prot. Eng. Des. Sel.* **19**, 299-307 (2006).

138. Junutula, J. R. *et al.* Engineered thio-trastuzumab-DM1 conjugate with an improved therapeutic index to target human epidermal growth factor receptor 2-positive breast cancer. *Clin. Cancer Res.* **16**, 4769-4778 (2010).

139. Gomez, N. *et al.* Triple light chain antibodies: factors that influence its formation in cell culture. *Biotechnol. Bioeng.* **105**, 748-760 (2010).

140. Gomez, N. *et al.* Effect of temperature, pH, dissolved oxygen, and hydrolysate on the formation of triple light chain antibodies in cell culture. *Biotechnol. Progr.* **26**, 1438-1445 (2010).

141. Woo, H.J., Lotz, M.M., Jung, J.U. & Mercurio, A.M. Carbohydrate-binding protein 35 (Mac-2), a laminin-binding lectin, forms functional dimers using cysteine 186. *J Biol. Chem.* **266**, 18419-18422 (1991).

142. Wootton, S. K. & Yoo, D. Homo-oligomerization of the porcine reproductive and respiratory syndrome virus nucleocapsid protein and the role of disulfide linkages. *J. Virol.* **77**, 4546-4557 (2003).

143. Michaelsen, T.E. *et al.* One disulfide bond in front of the second heavy chain constant region is necessary and sufficient for effector functions of human IgG3 without a genetic hinge. *Proc. Natl. Acad. Sci. U.S.A.* **91**, 9243-9247 (1994).

144. Romans, D.G., Tilley, C.A., Crookston, M.C., Falk, R.E. & Dorrington, K.J. Conversion of incomplete antibodies to direct agglutinins by mild reduction:

evidence for segmental flexibility within the Fc fragment of immunoglobulin G. *Proc. Natl. Acad. Sci. U.S.A.* **74**, 2531-2535 (1977).

145. Seegan, G. W., Smith, C. A. & Schumaker, V. N. Changes in quaternary structure of IgG upon reduction of the interheavy-chain disulfide bond. *Proc. Natl. Acad. Sci. U.S.A.* **76**, 907-911 (1979).

146. Chumsae, C., Gaza-Bulseco, G. & Liu, H. Identification and localization of unpaired cysteine residues in monoclonal antibodies by fluorescence labeling and mass spectrometry. *Anal. Chem.* **81**, 6449-6457 (2009).

147. Deiters, A., Cropp, T.A., Summerer, D., Mukherji, M. & Schultz, P.G. Site-specific PEGylation of proteins containing unnatural amino acids. *Bioorg. Med. Chem. Lett.* **14**, 5743-5745 (2004).

148. de Graaf, A.J., Kooijman, M., Hennink, W.E. & Mastrobattista, E. Nonnatural amino acids for site-specific protein conjugation. *Bioconjugate Chem.* **20**, 1281-1295 (2009).

149. DeVita, V.T., Jr., Young, R.C. & Canellos, G.P. Combination versus single agent chemotherapy: a review of the basis for selection of drug treatment of cancer. *Cancer* **35**, 98-110 (1975).

150. Mayer, L.D. & Janoff, A.S. Optimizing combination chemotherapy by controlling drug ratios. *Mol. Interventions* **7**, 216-223 (2007).

151. Umeda, Y. *et al.* Prunustatin A, a novel GRP78 molecular chaperone down-regulator isolated from Streptomyces violaceoniger. *J Antibiot. (Tokyo)* **58**, 206-209 (2005).

152. Caglioti, L. *et al.* The structure of neoantimycin. *Tetrahedron* **25**, 2193-2221 (1969).

153. Urushibata, I., Isogai, A., Matsumoto, S. & Suzuki, A. Respirantin, a novel insecticidal cyclodepsipeptide from Streptomyces. *J. Antibiot. (Tokyo)* **46**, 701-703 (1993).

154. Pettit, G.R. *et al.* Antineoplastic agents. 561. Total synthesis of respirantin. *J. Nat. Prod.* **70**, 1073-1083 (2007).

155. Kabalka, G. W., Varma, M. & Varma, R. S. Tosylation of Alcohols. *J. Org. Chem.* **51** (1986).

156. Snow, A.W. & Foos, E.E. Conversion of alcohols to thiols via tosylate intermediates. *Synthesis* **4**, 509-512 (2003).

157. Owen, S.C. *et al.* Targeting HER2+ breast cancer cells: lysosomal accumulation of anti-HER2 antibodies is influenced by antibody binding site and conjugation to polymeric nanoparticles. *J. Control. Release* **172**, 395-404 (2013).

158. Scheuer, W. *et al.* Strongly enhanced antitumor activity of trastuzumab and pertuzumab combination treatment on HER2-positive human xenograft tumor models. *Cancer Res.* **69**, 9330-9336 (2009).